

ERRATA CORRIGE

RESULTS

p. 37, eighth line from the top, replace sb 3015 with sb 3025,

p. 37, Fig. 3.7, structure of sb 4025 was erroneously replaced with the one of sb 3025.



UNIVERSITÀ
DEGLI STUDI
FIRENZE

DOTTORATO DI RICERCA IN SCIENZE FARMACEUTICHE
XXVII CICLO

COORDINATORE: Prof.ssa Elisabetta Teodori

SYNTHETIC PATHWAYS OF TSPO LIGANDS
AS THERANOSTIC TOOLS

Settore Scientifico Disciplinare CHIM/08

Dottorando

Dott.ssa Cecilia Bartoli

Tutor

Prof.ssa Silvia Selleri

Co-Tutor

Prof. Paolo Rovero

Coordinatore

Prof.ssa Elisabetta Teodori

Anni 2012 / 2014

“If we play without objectives, in the long run our decisions will become exclusively reactive and we will be made to play our opponents game, and not ours”.

(Gary Kasparov)

INDEX

1. INTRODUCTION	1
1.1 An overview on Neurosteroids	1
1.2 Translocator protein: discovery and characterization	5
1.3 TSPO: the mitochondrial “jack of all trades”	9
1.4 The raise of pharmaceutical interest	12
1.5 Pyrazolo[1,5- <i>a</i>]pyrimidineacetamides: a breakthrough in developing TSPO ligands	15
1.6 TSPO and imaging: the odd (but successful) couple	17
2. AIM OF THE THESIS	22
3. RESULTS	26
3.1 Optimization of the classical synthetic pathway	26
3.2 Direct synthesis of PBR 136 and a small series of analogues	30
3.3 Binding tests and steroidogenesis assay: the biological challenge	33
3.4 The imaging target	41
3.5 To bind or not to bind?	45
3.6 Deep in the labeling matter	46
3.6.1 ¹¹¹ In	46
3.6.2 ⁶⁸ Ga	49
4. DISCUSSION	53
5. CONCLUSIONS	56
6. EXPERIMENTAL	58
6.1 Data analysis	58
6.1.1 Chemical data	58
6.1.2 Biological data	58
6.1.3 Radiochemical data	59

Index

6.2	Chemistry of PBR 136 analogues	60
6.2.1	General procedure for the synthesis of compounds 8-9; 8F-12F	63
6.3	General procedure for DPA ether analogues (Prof. Michael Kassiou, University of Sydney, Australia)	65
6.4	Membrane preparation and binding assay	66
6.5	Cell culture	66
6.6	Steroids biosynthesis	67
6.7	Chemistry of PBR 127-DOTA conjugates	68
6.8	Membrane preparation and binding assay	71
6.9	Labeling procedure of compound f (Department of Nuclear Medicine, Azienda Ospedaliera di Careggi, Firenze, Italy)	71
6.10	General procedure for the labeling of compound f with ⁶⁸ Ga (IEO, European Institute of Oncology, Milan)	74
7.	REFERENCES	75

1. INTRODUCTION

1.1 An overview on Neurosteroids

In 1981, the french physiologist Etienne Baulieu coined the term “neurosteroids”¹ to describe steroids whose accumulation occurs in the nervous system independently, at least in part, of supply by the steroidogenic endocrine glands^{2, 3}. This term, widely accepted by scientific community, is today commonly used to identify a class of steroids which can be synthesized *de novo*^{2, 4} in the CNS (central nervous system), especially within glia, from sterol precursors, involved in the modulation of neuronal excitability by non-rapid genomic actions. Precursors for their synthesis, which is performed locally in the hippocampus and other brain structures⁵, are progesterone, deoxycorticosterone and testosterone, steroid hormones mainly synthesized in the gonads, adrenal gland and feto-placental unit. The major pathways in steroids biosynthesis is shown in Figure 1.1.

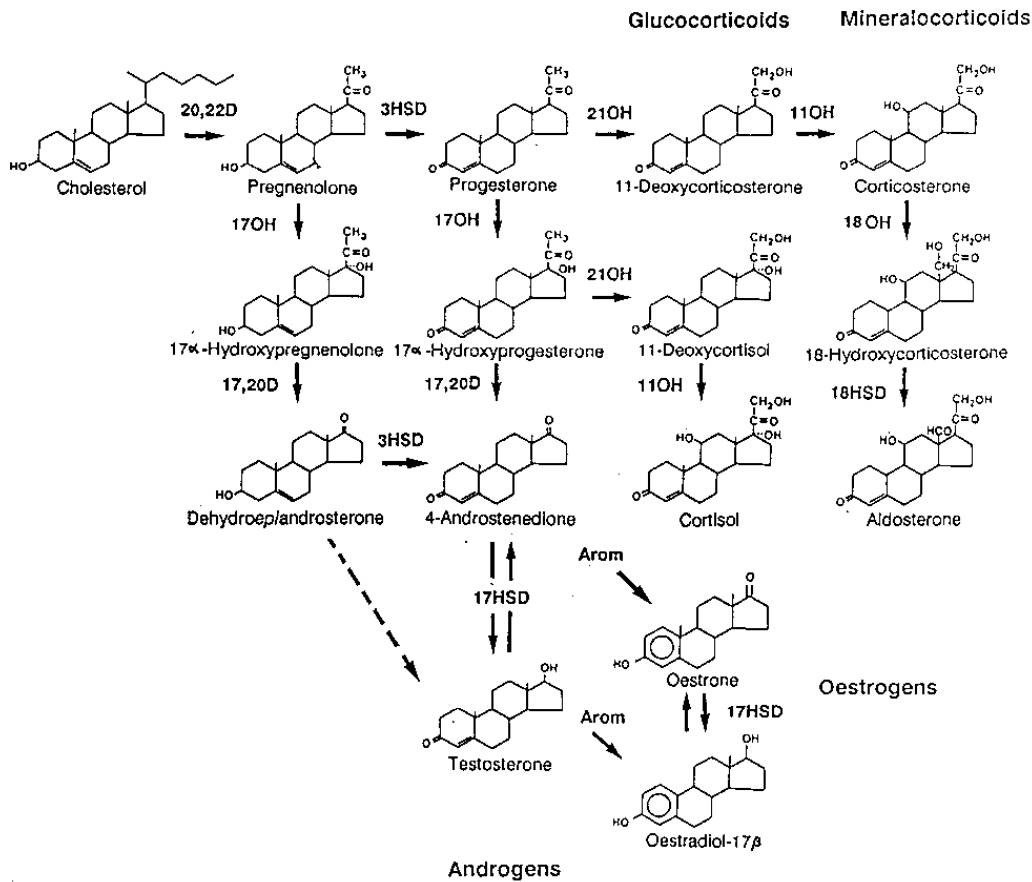


Figure 1.1 Schematic representation of the metabolic pathways of cholesterol in steroid biosynthesis.

INTRODUCTION

These hormones derive from pregnenolone, the first product of cholesterol metabolism, found in the brain⁶ at concentrations about one order of magnitude larger than those of its other derivatives, as might be expected from a precursor-to-product relationship⁷.

The derivatives neurosteroids are basically A-ring reduced metabolites of these steroids and, based on structural features, neurosteroids can be classified as pregnane neurosteroids, such as allopregnanolone and THDOC (allotetrahydrodeoxycorticosterone), androstane neurosteroids, such as androstanediol and etiocholanone, and sulfated neurosteroids, such as PS (pregnenolone sulfate), and DHEAS (dehydroepiandrosterone sulfate). Studies during the past two decades have uncovered that progesterone and deoxycorticosterone serve as precursors for the endogenous neurosteroids allopregnanolone, 5 α -pregnane-3 α -ol-20-one, and THDOC, 5 α -pregnane-3 α ,21-diol-20-one, respectively. Testosterone-derived androgens such as androstanediol, 5 α -androstane-3 α ,17 β -diol, and estradiol can either be considered as neurosteroids.

The conversion of parent steroids into the corresponding neurosteroids mostly consists in sequential reduction, mediated by 5 α -reductase and 3 α -HSOR (3 α -hydroxysteroid oxidoreductase). These reductions occur in peripheral tissues, such as reproductive endocrine, liver and skin⁸. Anyway, it's an evidence that neurosteroids biosynthetic enzymes are operating in human brain too⁹; as a matter of fact, 5 α -reductase has been identified in both neurons and glial cells¹⁰. 5 α -reductase and 3 α -HSOR have been found in human neocortex and subcortical white matter, as well as in hippocampal tissues^{8, 10}, thus we can assume that steroid precursor, peripherally synthesized, enter the brain and here are available for enzymatic pool to biosynthesize neurosteroids. At the same time, in brain region such as cortex, hippocampus and amygdala, are located enzymes required to convert cholesterol to pregnenolone, CYP450sc (cytochrome P450 cholesterol side-chain cleavage enzyme), and to sequently convert pregnenolone to progesterone, 3 β -hydroxysteroid dehydrogenase, so it is possible for these brain regions to synthesize neurosteroids directly *in situ*.

On the other hand, glial cells and principal neurons produce neurosteroids *de novo*^{9, 11} from their steroid precursors. In this regard can be mentioned the fact that allopregnanolone persists in the brain after adrenalectomy and gonadectomy or after pharmacological suppression of adrenal and gonadal secretions¹², indicating that

allopregnanolone can be synthesized *de novo* in brain via 5α -reduction of progesterone, thus some regulatory mechanisms of neurosteroids biosynthesis in brain still remain unclear.

Since neurosteroids are highly lipophilic, they can easily pass the blood-brain barrier and so, from the peripheral tissues where they've been synthesized, they can accumulate in the brain and modulate their interaction with transmembrane receptors and ion channels¹³. Neurosteroids are endogenous regulators of neuronal excitability, since their major target is the GABA_A receptor¹⁴, a subtype of receptor of the GABA (γ -aminobutyric acid), mediating the bulk of synaptic inhibition in the CNS.

Structurally, GABA_A receptors are heteropentamers with five protein subunits that form the chloride ion channels¹⁵ (common structure of the receptor complex is shown in Figure 1.2).

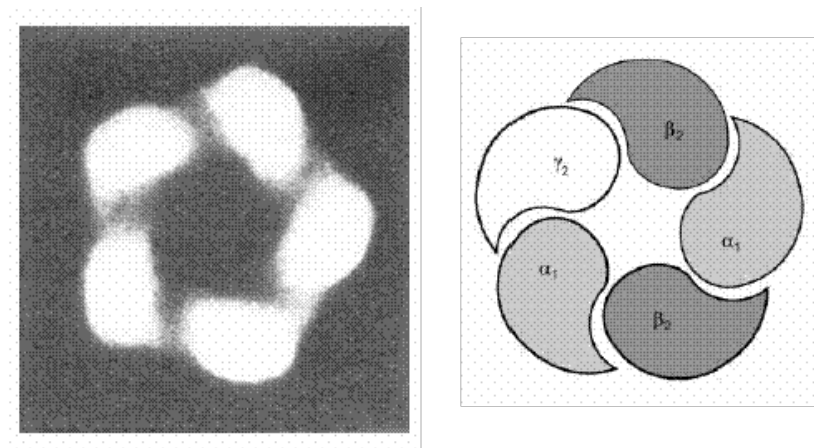


Figure 1.2 GABA_A receptor complex visualized by electron microscopy and, on the right, the common α_1 , β_2 , γ_2 GABA_A structure.

There are seven different classes of subunits, some of which have multiple homologous variants (α_{1-6} , β_{1-3} , γ_{1-3} , σ_{1-3} , δ , ϵ , θ); most GABA_A receptors are composed of α , β and γ or δ subunits¹⁶. GABA activates the opening of chloride ion channels, permitting chloride ion influx and, ultimately, hyperpolarization. GABA_A receptors action prevents potential generation by short-circuiting the depolarization produced by excitatory neurotransmission¹⁷.

Depending on their chemical structure, neurosteroids can be positive or negative modulators of the GABA-ergic system^{13, 18}; for example, allopregnanolone, THDOC

and androstenediol are potent positive allosteric modulators of GABA_A receptors^{19, 20}. The binding site for neurosteroids is proposed to be distinct from that of the GABA, benzodiazepine and barbiturate sites. Although the exact location of neurosteroids binding site is currently unknown, it has been shown that a highly conserved glutamine at position 241 in the M1 domain of the α -subunit plays a key role in neurosteroids modulation²¹.

Basically, exposure to neurosteroids enhances the open probability of the GABA_A receptor chloride channel, so that the mean open time is increased and the mean closed time is decreased. This increases the chloride current through the channel, ultimately resulting in a reduction of neuronal excitability^{22, 23}.

Neurosteroids mechanism of interaction shows both acute and chronic effects. Regarding the acute effects, it's an evidence that they are not due to interactions with steroid hormone receptors, that usually regulate genes transcription; we can state that the genomic effects of neurosteroids are mainly related to their metabolic interconversion to traditional steroids²⁴. On the other side, their chronic effects are due both to genomic (intracellular steroid receptors) and non-genomic rapid actions (ion channels and membrane receptors) in the brain. This is supported by the observation that the effects of neurosteroids raise quickly, while steroid hormone actions mediated by intracellular receptors take more time to occur and have prolonged duration²⁵, and also that neurosteroids don't exhibit high affinity towards nuclear steroid hormone receptors^{24, 26}. Moreover, studies in PR (progesterone receptor), knockout mice have conclusively demonstrated that the classical steroid receptor is not required for the sedative, anxiolytic, and anticonvulsant activity of progesterone and related neurosteroids²⁷, and neurosteroids have been demonstrated to directly modulate the activity of ligand-gated ion channels, most notably GABA_A receptors, as previously mentioned^{22, 23}.

The physiological and pharmacological profile of major neurosteroids has been widely investigated; in general, neurosteroids that are 3 α -hydroxy-pregnane derivatives such as allopregnanolone, pregnanolone, and THDOC elicit sedative, anxiolytic, and anticonvulsant actions while PS and DHEAS are excitatory and produce memory enhancing and anxiogenic effects.

To mention but a few more in details, neurosteroids are broad spectrum anticonvulsant agents, as demonstrated for epilepsy^{28, 29}, are released during physiological stress^{13, 30},

have a crucial role in depression³¹ (e.g. allopregnanolone, that both alleviates depressive behavior in animal models of depression and mediates the antidepressant action of drugs like fluoxetine³²), have been widely recognized to modulate learning and memory processes in young, aged and in pharmacological models of amnesia.

Another aspect strongly highlighted by evidences, though the precise mechanism underlying is not well defined, is the role of neurosteroids in sex differences in susceptibility to brain disorders³³. For instance, anxiety and depression affect more women than men, such as sex differences have been confirmed in the dynamics of tobacco smoking and cessation in humans. These differences have been attributed to acute and chronic effects of ovarian steroid hormones on nicotinic receptors, although findings have not been conclusive.

In conclusion, experimental and clinical evidences suggest an endogenous role for neurosteroids in several neurological and psychiatric conditions such as epilepsy, anxiety and depression, with different trends depending on the gender related differences, and, indeed, treatment of these neurological diseases and stress-sensitive conditions are among the clinical situations in which synthetic neurosteroid analogues may have clinical applications.

The biosynthesis of neurosteroids is controlled by the translocator protein.

1.2 Translocator protein: discovery and characterization

The translocator protein TSPO³⁴, formerly known as peripheral or mitochondrial benzodiazepine receptor³⁵, is a 18 kDa protein, consisting in a 169 amino acid sequence, mainly located in the outer mitochondrial membrane. First identified in 1977 as a new binding site for benzodiazepine diazepam, TSPO has been subsequently studied for its ability to bind different molecules, like cholesterol, porphyrins and drugs with various affinities.

TSPO represents an evolutionarily well-conserved family of ubiquitous proteins^{36, 37}; although its expression has its higher levels in tissues with steroid synthesizing cells, like gonads and ovary, as it is an ubiquitous protein, it has been reported in several tissues, like the renal and myocardial, and in hemopoietic and lymphatic cells; is poorly expressed in liver. Within the CNS, it is found limited to glia, microglia, the main CNS

immune defense, reactive astrocytes and in some neuronal cell types too³⁵. As a singular evidence, a small amount of TSPO is also found in the plasma membrane and in the cell nucleus³⁴, suggesting potential implications for this receptor in the regulation of specific genes expression.

TSPO plays a crucial role in cells physiology, as remarked by its high sequence conservation from bacteria to humans, typical for housekeeping gene, and the evidence that a genetic ablation of this receptor results in an embryonic lethal^{38, 39} suggests it to be critically involved in early embryonic developmental functions.

Since it is a component of the mitochondrial permeability transition pore MPTP, it interacts with various proteins, including the 32 kDa voltage-dependent anion channel VDAC and the 30 kDa adenine nucleotide translocase ANT⁴⁰, both essential for the complex to work as a functional unit. Moreover, TSPO action is often closely related to the activity of steroidogenic acute regulatory protein, StAR⁴¹, whose presence seems to be needful for steroidogenic cells to move large amounts of cholesterol from the outer mitochondrial membrane to the first steroidogenic enzyme, which lies on the matrix side of the inner membrane. In summary, the demonstrated TSPO interactions with several cytosolic proteins suggests the receptor as a transducer of intracellular signals to mitochondria.

Though a lot of implications regarding the exact physiological role of TSPO have not been defined yet, it is currently known its involvement in cholesterol metabolism, regulation of steroid biosynthesis⁴², mitochondrial respiration⁴³, cells apoptosis and proliferation^{40, 44}, reactive oxygen species ROS generation⁴⁵, porphyrins transport and biosynthesis of heme group (Fe-protoporphyrin IX)⁴⁶.

Being a membrane-bound protein have hindered the X-ray determination of TSPO crystal structure, and difficulties are also in expression, purification and stabilization of the native structure⁴⁷. Nevertheless, because of the high homology shown by TSPO through different species, relevant investigations have been performed on different TSPO homologues, such as the receptor in yeast mitochondrial membranes and bacterial homologue tryptophan-rich sensory protein, TspO, of *Rhodobacter sphaeroides*, evaluated as a structural and functional model of the human receptor. *Rhodobacter sphaeroides* TspO primary structure shows 33,5% identity with the aligned amino acid sequence of human TSPO (Figure 1.2)⁴⁸ and this highly significant level of

homology makes the TspO a good candidate for biochemical and structural investigations.

```

rsTspO 1 MNMDWALFLTELAACGAPATTGALLKPDE---WYDNLNKEWNNPFRWVFP
hTSP0  1 MAPPVVPAMGETLAPSLGCFVGSRFVHGEGLRWYAGLQKESWHPHPHWVLG

rsTspO 48 LAWTSLSLYFLMSLAAMRVAQLEG-----SGQALAFYAAQLAFNTLWTEVFF
hTSP0  51 PVNGTLYSAMYGSYLVWKELGGFTEKAVVPLGLYTGOLALNWANPPIFF

rsTspO 93 GMKRMATALAVVMVMWLFVAATMWAFPLDWTAGVLEVPYLIWATAATGL
hTSP0  101 GAROMGVALVDLLLVSGAAAATTVWYQVSPLAARLLYPYLANLAFTTTL

rsTspO 143 NFEAMRLNWNRPEARA--- 158
hTSP0  151 NYCWWRDNDHGWRGGHRLPE 169
    
```

Figure 1.3 Comparison of sequence and topology of the human (hTSP0) and bacterial (rsTspO) receptor homologues.

Electron cryomicroscopy of TspO at 10 Å resolution⁴⁹ has highlighted a three-dimensional subunit arrangement composed of five transmembrane α helices forming a channel-like monomeric structure. Two monomers are tightly associated to form a symmetric dimer, which works as a functional unit (Figure 1.3). The arrangement of transmembrane domains of individual TspO subunits indicates the chance of two binding sites per dimer which, in turn, allows for the possibility of cooperation in substrate transport and potential allosteric modulation.

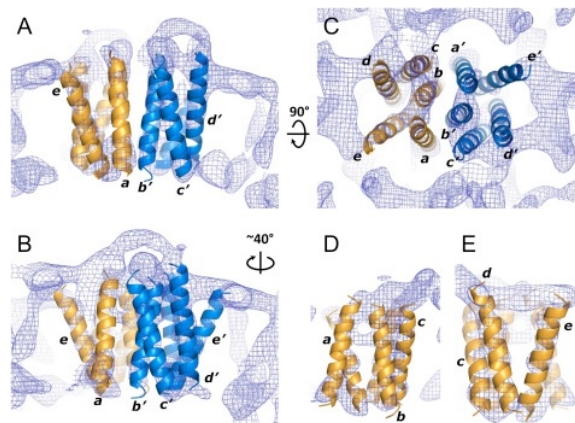


Figure 1.4 (A) A view perpendicular to the membrane plane of the TpsO dimer; (B) view parallel to the membrane plane of the TspO dimer and after a 40° rotation; (C) view perpendicular to the membrane plane; (D) TspO monomer viewed parallel to the membrane plane; (E) TspO monomer viewed from the lipid bilayer.

It's currently accepted that TSPO has multiple binding sites, but the nature and function of most of them still remain undiscovered. Anyway, the little that is known about this topic, has been characterized thanks to a couple of two different synthetic ligands: the benzodiazepine derivative Ro5-4864 (7-chloro-5-(4-chlorophenyl)-1,3-dihydro-1-methyl-2H-1,4-benzodiazepin-2-one)^{50, 51}, *in vivo* agonist⁵², and the isoquinoline carboxamide PK11195 (N-(sec-butyl)-1-(2-chlorophenyl)-N-methylisoquinoline-3-carboxamide)⁵³, *in vivo* antagonist⁵² (Figure 1.4).

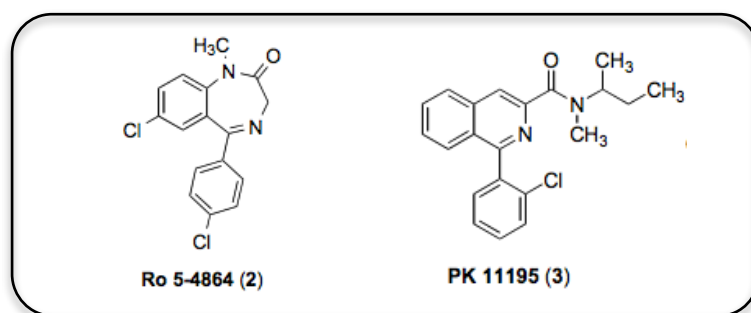


Figure 1.5 TSPO synthetic ligands Ro5-4864 (agonist) and PK11195 (antagonist).

It is noteworthy that although these ligands bind to TSPO in a specific manner, they have sometimes been shown to produce comparable results, depending upon the treatment conditions. More in details, both of these ligands display nano molar affinity for the receptor, but while PK11195 binds effectively on TSPO, the binding ability of Ro5-4864 requires the cooperation of other mitochondrial components to be completely achieved. Especially important, PK11195 behaves as nano molar ligands in both rat (K_i of 3.0 nM) and human (K_i of 4.5 nM). Studies of site-directed mutagenesis have suggested some particular residues in the first putative loop of TSPO to be essential for the binding of Ro5-4864 but not for PK11195; this evidence leads to the consequence that the two ligands bind to heterogeneous sites at TSPO, either overlapping or allosterically coupled⁵⁴.

Although the early observations on PK11195 seemed to indicate a single population of saturable sites for this ligand, further studies, performed with [³H]PK11195 on Ehrlich tumor cells, revealed two independent binding sites⁵⁵.

Recently, studies performed using different TSPO radioligands for PET imaging have

highlighted the variability of TSPO binding sites across individuals and tissue type. For instance, whereas PBR28 (N-(2-methoxybenzyl)-N-(4-phenoxy pyridin-3-yl)acetamide), a well known compound with high affinity towards TSPO, radiolabeled with ^3H for PET analysis, binds competitively to the [^3H]PK11195 site in the brains of rhesus monkeys, it binds to multiple sites in *post mortem* human brains, with different affinities across a range of patients⁵⁶. Differences between patients have been measured also for [^3H]PK11195 in some peripheral tissue, as heart and lungs, correlating to the changes in the binding of PBR28 in brain, and this leads to the hypothesis that the variability of binding profiles shown by several ligands across patients could derive from differences in microglial activation levels, or instead from the concentration at which TSPO ligands are evaluated.

1.3 TSPO: the mitochondrial “jack of all trades”

The principal and most characterized function of TSPO is the translocation of cholesterol from the cellular cytosol, through the mitochondrial membranes, into mitochondria, where it can follow its metabolic pathways. The binding site of cholesterol at TSPO is located on the carboxy-terminus region, containing a conserved cholesterol recognition amino acid consensus sequence [L/V-X₍₁₋₅₎-Y-X₍₁₋₅₎-R/K], called CRAC⁵⁷. Though a unique structural determinant for protein interaction with cholesterol has not yet been identified, the CRAC sequence is one of the most characterized protein domain playing this role, found e.g. in caveolin-1 and in other proteins targeted to lipid rafts⁵⁸, in addition to TSPO⁵⁹. Remarkably, all other drug ligands bind at the amino-terminus region, but also other overlapping binding sites have been identified.

The translocation of cholesterol into the mitochondria happens to be the rate-determining step in the biosynthesis of steroids³⁸, as the binding of this ligand to the receptor enables the start of steroidogenesis.

The first metabolic step, once cholesterol has been translocated in mitochondria, is the oxidative cleavage of its side chain, performed by CYP450_{sc}, converting cholesterol into pregnenolone; from this intermediate all the other steroids and, as a consequence, neurosteroids are originated by several enzymatic reactions, as previously mentioned.

Though translocation of cholesterol is the main function of TSPO, this is far to be the

last. For instance, other endogenous ligands, endowed with high affinity for this receptor, are porphyrins and endozepines⁶⁰, a family of neuropeptides, deriving from proteolytic degradation of a same polypeptide precursor, able to displace benzodiazepines from their binding at the GABA_A receptor.

Most generally, being part of the MPTP implicates the involvement of TSPO receptor in a series of crucial events, as the regulation of apoptosis and necrosis, modulation of cells proliferation, immune regulation⁶¹, neuroprotection, injury and inflammatory processes. For instance, it has been demonstrated that some TSPO ligands can inhibit proliferation in cancer cell lines, showing an accumulation of cells in G₁/G₀ phase of the cell cycle without the possibility to progress to the duplicative phase S and G₂/M⁶². It has been suggested that effect on proliferation may be related to the small amount of TSPO located inside the cell nucleus, anyway the most interesting point is the correlation between concentration of TSPO ligands and the consequent effect on cells proliferations: at micro molar concentrations dominates the anti proliferative and proapoptotic action, while at nano molar the prevalence is proliferative and antiapoptotic effects, through stimulation of mitosis⁶³. Regarding the role of TSPO on immune regulation, as it is expressed in microglia and other immune cells⁶⁴, binding of specific ligands on this receptor enables the modulation of cytokine production, generating relevant neuroprotective effects at micro molar concentration^{55, 64}.

Since TSPO has been admitted to play a key role in a variety of physiological and pathological conditions⁶⁵, several studies have been aimed at the willing to better understand the molecular mechanisms it is involved in. It's today an evidence that there is a strict correlation between the TSPO expression levels and the progression state of a number of diseases⁶⁶. More in detail, it results upregulated in a number of pathologies like particular type of cancers⁶⁷, brain injury and inflammation and several neurodegenerative disorders⁶⁸, such as Alzheimer's^{68, 69}, Huntington's⁷⁰ and Parkinson's⁷¹ disease, multiple and amyotrophic lateral sclerosis⁷², dementias⁷³. As a matter of fact, it had been widely demonstrated by a series of studies that TSPO is consistently overexpressed in highly invasive human breast cancer cells and that the strength of cancer cells in origin tumors is directly related to the amount of TSPO within these cells^{74, 75}. At the same time, evaluation of TSPO levels in human ovary⁷⁶, colon⁷⁷, prostate⁷⁷ and brain cancer cells, shows a consistent increase in concentration, comparing with healthy tissues. Notably, positive correlation between TSPO expression

levels and the metastatic potential of different human tumor, as breast cancer^{74, 75}, gliomas⁷⁸ and astrocytomas⁷⁹, has been demonstrated, reinforcing the hypothesis of a role for this receptor in carcinogenesis, though its specific involvement is far to be cleared up.

Concerning microglia, the mechanisms controlling TSPO expression still remain unclear. It is possible that the increase in its levels may be merely due to a general increase in the microglial cells number, or that TSPO increases within each microglial cell, as it becomes activated. As an instance, in Leydig cells, the activation by cytokines leads to the raising of TSPO mRNA levels, proving that the enhancement in TSPO concentration is linked to transcriptional events.

At the state of the art, several studies have shown evidences that cholesterol plays a certain role in the progression of a number of pathologies and cancers, as it is accumulated at intracellular level; in fact, in animal models, cholesterol synthesis inhibitors, such as statins⁸⁰, are selective for cancer cells, where they carry out the inhibition of cellular growth and motility. Another evidence is offered by numerous epidemiological studies which highlight the probability that a diet frequently rich in fats might promote cancer onset and growth. As TSPO is the intracellular receptor to whom cholesterol binds, this can explain at least its first implication in some pathological conditions.

As noticed before, the regulation of TSPO expression happens to be significantly increased also in neurological injury⁸¹, inflammation⁸² and degeneration. If in healthy central nervous system, TSPO is expressed in low concentration limited to glia and some type of neurons, its expression dramatically increase in pathological conditions. At the same time, in PNS (peripheral nervous system), TSPO levels result transiently increased in response to nerve injury, in dorsal root ganglia sensory neurons, in Schwann cells and in macrophages, right at the site of injury^{83, 84}.

The principal physiological effects of TSPO mediated neuroprotection and neurogenesis, assessed by different works, have been so far accounted for by the stimulation of steroids and neurosteroids biosynthesis and activity⁸⁵. As an instance, allopregnanolone has been recently studied for its ability to promote neuroregeneration in an Alzheimer's disease mouse model⁸⁶. This neurosteroid, administered in chronic exogenous treatment regimen, has been demonstrated to induce neurogenesis correlated with restoration of learning and memory function; its efficacy was comparable also

when administered in aged normal mice, as endogenous allopregnanolone declines with age, as well as in neurodegeneration.

The importance of TSPO in regenerative processes, concerning nervous system, is supported by the evidence that its strongly upregulated expression, saw after injury and inflammation, returns to low control values only when nerve regeneration is completed.

Moreover, sex steroids promote neural protection and repair; after neurotrauma, for example, locally produced estrogens reduce neurodegeneration in zebra finch cerebellum by suppressing different steps of the apoptotic pathways⁸⁷. Obviously, sex steroidogenesis is started thanks to TSPO translocation of cholesterol, as well as the involvement of the StAR protein, and once again this accounts for the strategic role played by the receptor in multiple CNS and PNS physiological and pathological events.

Finally, one more interesting point researchers are focusing on is TSPO involvement in the transport of protoporphyrins, which are needed as precursors in the biosynthetic pathway of heme group, carried out both in cytoplasm and mitochondria. A study on zebrafish *Tspo* has demonstrated that this protein modulates *in vivo* primitive erythropoiesis⁸⁸. Moreover, the lack of functionality of *Tspo*, both genetically and pharmacologically induced, resulted in embryos with specific erythropoietic cell depletion⁸⁸, which is not due to the invalidation of cholesterol binding site and such an evidence highlights that the essential *in vivo* role of this receptor is far to be only accounted for this, although important, function.

1.4 The raise of pharmaceutical interest

As far as told until now, the intense pharmaceutical interest, raised in the last two decades, in developing specific ligands for TSPO appears perfectly justified. The research of new potent and selective molecules able to bind the receptor has been guided through a number of compounds, belonging to various chemical classes, as pyrrolobenzodiazepines, phenoxyphenylacetamide derivatives, indole derivatives and imidazopyridines. Most of these ligands have been designed starting from selective CBR ligands, already deeply investigated in the previous years, which were structurally modified in order to shift their affinity towards TSPO.

Indeed, at first, the ligands chosen for the evaluation of the new receptor characteristics

were benzodiazepines themselves, not taking account of the lack of specificity of most of these compounds. As an example, Diazepam, which is able to bind, with different affinity, both GABA_A and TSPO; its ability to bind the two receptors, didn't allow to define the particular chemical properties required for the specific targeting of TSPO. Unlikely, Clonazepam, a Diazepam analogue with binding selectivity for GABA_A, didn't show any affinity for TSPO. Another remarkable benzodiazepine derivative was the already mentioned Ro5-4864, a ligand for both the peripheral and central nervous system benzodiazepine binding sites, acting as an *in vivo* TSPO agonist⁵². Afterwards, with the aim to develop new TSPO ligands, in 1983 were described a series of compounds called isoquinoline carboxamides which, although being structurally different from benzodiazepines, had greater specificity for the TSPO than for the GABA_A receptors⁸⁹. To this family belongs the PK11195⁵³, previously mentioned as *in vivo* TSPO antagonist⁵², deeply investigated in the past years with the aim to better understand the receptor structure and the physiological effects induced by its action. The PK11195 displaced [³H]Ro5-4864 from its binding sites in all the organs. Subsequently, in 2001 as an extension of the SAR (structure-activity relationship) on TSPO ligands structurally related to PK11195, Anzini et al.⁹⁰ performed the design, by means of computational approach, of a series of carboxamide derivatives bearing differently substituted planar aromatic or heteroaromatic systems. The main aim was to get further information on the topological requisites of the carbonyl and aromatic moieties for interaction with the TSPO.

More recently, several new synthetic ligands have been developed and carefully investigated for their binding selectivity for TSPO as, to name but a few, PK14105 (N-(sec-butyl)-1-(2-fluoro-5-nitrophenyl)-N-methylisoquinoline-3-carboxamide), FGIN-1-27 (2-hexyl-indole-3-acetamide), FEAC (N-benzyl-N-ethyl-2-(7,8-dihydro-7-(2-fluoroethyl)-8-oxo-2-phenyl-9H-purin-9-yl)acetamide), FEDAC (N-benzyl-N-methyl-2-(7,8-dihydro-7-(2-fluoroethyl)-8-oxo-2-phenyl-9H-purin-9-yl)acetamide), AC-5216 (N-benzyl-N-ethyl-2-(7,8-dihydro-7-methyl-8-oxo-2-phenyl-9H-purin-9-yl)acetamide) and DAC (N-benzyl-N-methyl-2-(7-methyl-8-oxo-2-phenyl-7,8-dihydro-9H-purin-9-yl)acetamide).

As a consequence of the number of TSPO ligands belonging to different chemical families, yielding results of high affinity and selectivity, several pharmacophore models have been proposed, depending on the different SAR (structure-activity relationship)

data, despite the topology of the TSPO binding cleft is still not completely defined. Notably, a pharmacophore model widely accepted is the one derived from the binding evaluation of imidazopyridine and pyrrolo[3,4-b]quinoline derivatives. Imidazopyridine derivatives are a family of compounds obtained by modifications of the progenitor Alpidem (6-chloro-2-(4-chloro-phenyl)-N,N-dipropylimidazo[1,2-a]pyridine-3-acetamide)⁹¹, an anxiolytic drug developed by Synthélabo, approved for marketing in France in 1991 and withdrawn from the French market by 1994 as a consequence of several cases of severe and even lethal side effects⁹². Alpidem was known to bind both CBR and TSPO with nanomolar affinity, with K_i respectively 1-28 nM and 0.5-7 nM. The anxiolytic and anticonvulsant effects of Alpidem were accounted to a double mechanism of action, one directly mediated by its interaction with CBR and the other elicited with neurosteroids production, obtained as an indirect consequence of the interaction with TSPO. A wide SAR study, performed in 1977, on Alpidem and a series of 2-phenyl-imidazo[1,2-a]pyridine derivatives, showing different degrees of affinity and selectivity for TSPO with respect to CBR, led to the proposal of a TSPO pharmacophore model whose schematic representation includes three regions: a freely rotating aromatic ring region (FRA), an electron rich zone ($\delta 1$), a planar aromatic region (PAR) and a lipophilic area (LA). The same model seems to be working for CBR too, with the exception of an out plane region (OPR) in place of the LA. The different zones were termed using the nomenclature proposed by Wermuth and Bourguignon in 1987⁹³. Hereafter, pursuing the goal to evaluate the effects of structural modifications on the amide nitrogen at both CBR and TSPO, Trapani and coworkers synthesized a new family of compounds, the imidazopyridineacetamides⁹⁴. Their research was taking advantage also of the recent results obtained by new SAR studies of different class of ligands and further informations deriving from molecular biology experiments⁹⁰. This relevant amount of data allowed to highlight three key structural features for the achievement of ligands with high affinity toward TSPO: a conveniently located and oriented C(=O)N functional group, the involvement of lipophilic substituents attached to this C(=O)N group and the presence of an aromatic or heteroaromatic system with a pendant phenyl ring. Moreover, a unique 3D model of interaction between endogenous and synthetic ligands and TSPO had been developed in 2000⁹⁵. This model, based on TSPO primary sequence, describes the presence of two lipophilic regions (L1 and L3),

one polar residue (H2), shown to be essential for the interaction with TSPO and one more lipophilic portion (L4) playing a direct modulation in receptor binding. Receptor mapping and receptor fitting approaches suggested in particular three amino acid residues Ser41, Trp107, and Trp161 as the key elements for ligand interaction, due to their involvement in a hydrogen bond with the amide carbonyl group (Ser41 residue) and in hydrophobic interactions with the groups bounded to this amide group (Trp107 and Trp161 residues).

1.5 Pyrazolo[1,5-*a*]pyrimidineacetamides: a breakthrough in developing TSPO ligands

Relating to the wide investigated family of imidazopyridines, in 2001 Selleri *et al.* developed a series of new compounds, shaped as azaisosters of Alpidem, based on the clear knowledge that introduction of proper substituents and opportune modifications on the acetamido[1,2-*a*]pyrimidine nucleus of Alpidem leads to compounds with improved TSPO affinity and selectivity *vs* CBR. These new molecules were formed on the basis of a N,N-diethyl-(2-aryl)pyrazolo [1,5-*a*]pyrimidin-3-ylacetamide⁹⁶.

At first, maintaining fixed the tertiary acetamide moiety at position 3, as previously state crucial for the formation of the hydrogen bond necessary to achieve the binding to the target protein, positions 5 and 7 of the central scaffold and *para*-substitution at the 2-phenyl ring were carefully investigated. From the corresponding SAR data it turned out that the presence of small lipophilic substituents (CH₃) in 5 or 7 didn't entail selectivity, suggesting a tolerance of these groups into both the lipophilic pockets of CBR and TSPO. On the other hand, substitutions at position 6, corresponding to position 7 in the imidazopyridine nucleus of Alpidem, as well as the contemporary presence of two or more substituents (CH₃ or more steric demanding phenyl group) on the fused pyrimidine ring, allowed the obtainment of derivatives with high affinity and selectivity for TSPO. Likewise, the choice of substituents such as Cl, F, CH₃, OCH₃ in *para* at the 2-phenyl ring results in a sensitive increase in TSPO affinity and selectivity.

In a further study of 2005, the same authors explore the position 3, on the fused aromatic rings, to clarify the role of the amide moiety and the principal structural features of the substituents on the amide nitrogen⁹⁷. Choosing the 2-(5,7-dimethyl-2-(*p*-

INTRODUCTION

tolyl)pyrazolo[1,5-*a*]pyrimidin-3-yl)-*N,N*-diethylacetamide as lead compound, the authors performed a series of further modifications to this scaffold, keeping fixed the 2-phenyl ring and the two methyl groups at positions 5 and 7, while switching the substituents on the amide nitrogen between different alkyl and aryl-alkyl chains (CBR, central benzodiazepine receptor, and TSPO affinity of different pyrazolopyrimidine derivatives are shown in Figure 1.6).

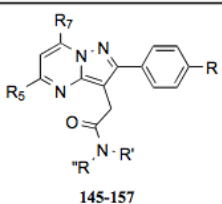
 145-157								
Compound	R ₅	R ₆	R ₇	R	R'	R''	K _i (nM) ^a CBR	K _i (nM) ^b TSPO
145 ^c	CH ₃	H	H	H	Et	Et	92	40
146 ^c	H	H	CH ₃	H	Et	Et	518	155
147 ^c	CH ₃	H	CH ₃	Cl	Et	Et	>10,00	2.4
148 ^c	CH ₃	H	CH ₃	F	Et	Et	>10,00	9.2
149 ^c	CH ₃	H	CH ₃	CH ₃	Et	Et	>10,00	0.8
150 ^c	CH ₃	H	CH ₃	OCH ₃	Et	Et	>10,00	4.7
151 ^d	CH ₃	H	CH ₃	H	<i>n</i> -Pr	<i>n</i> -Pr	>10,00	0.8
152 ^d	CH ₃	CH ₃	CH ₃	H	<i>i</i> -Pr	<i>i</i> -Pr	>10,00	89
153 ^d	CH ₃	H	CH ₃	H	Et	Ph	>10,00	0.8
154 ^d	CH ₃	H	CH ₃	H	Et	Bz	>10,00	7.3
155 ^d	CH ₃	H	CH ₃	H	Me	(<i>R</i>)-CHCH ₃ Ph	>10,00	22
156 ^d	CH ₃	H	CH ₃	H	Me	(<i>S</i>)-CHCH ₃ Ph	>10,00	156
157 ^d	CH ₃	H	CH ₃	H	-(CH ₂) ₄ -		>10,00	1154

Figure 1.6 CBR and TSPO affinity of pyrazolopyrimidine derivatives 145-157.

Analyzing data of binding tests, the presence of phenyl ring on the amide nitrogen emerged as a positive contribute in increasing the TSPO affinity, while the introduction of chains between the amide nitrogen and the aromatic ring involved in a moderate reduction of this parameter. Concerning the alkyl substituents on the amide nitrogen group, the most appealing observation resulted the importance of its length, with the three atoms linear chain performing the best affinity, with a K_i value of 0.8 nM. Otherwise, ramifications of the chain or introduction of cyclic amines on it worsened

the affinity of the compounds.

Notably, in the whole series of pyrazolo[1,5-*a*]pyrimidines, the high affinity and binding potency appeared to be assured by the methylene linker between the pyrazolopyrimidine nucleus. In fact, the removal of this methyl group from the chain, as well as the substitution of the amide group with the ester function, led to compounds with a substantial decrease in binding capability.

The most promising compounds, in terms of affinity and selectivity, were also tested for their ability in stimulating steroidogenesis. The tests were performed by radioimmunoassay in C6 rat glioma cells. Some of the compounds tested showed a capability in stimulating steroid biosynthesis comparable to that of Ro5-4864 and PK11195. At the same time, three molecules showing high affinity properties were not able at all to induce steroidogenesis, confirming the previous hypothesis that no correlation between affinity and steroidogenic activity can be declared for TSPO ligands and introducing the necessity to identify the specific features of TSPO agonists and antagonists.

1.6 TSPO and imaging: the odd (but successful) couple

As above mentioned, an elevated TSPO expression is found in several disease states, including neuroinflammation, neurologic disorders, such as Alzheimer's^{68, 69}, Huntington's⁷⁰ and Parkinson's⁷¹ disease, as well as cancers of the breast⁷⁴, prostate⁹⁸, oral cavity⁹⁹, colon rectal⁶⁷, liver¹⁰⁰ and brain^{78, 79}.

Given that most of these pathologies show poor prognosis, constantly increasing with their staging, it's obviously desirable to find specific biomarkers, whose presence or quantified concentration leads to an early and exact diagnosis. For these reasons, TSPO has become over the years a promising biological target for diagnostic purposes in the imaging of neurological disorders or cancer spread, and this relevance as a biomarker has been fueled mainly by PET (positron emission tomography) studies^{101, 102}.

With this aim, several compounds, previously tested for their binding ability against TSPO, have been radiolabeled and screened as PET radio tracers. The first to be synthesized was [¹¹C]PK11195¹⁰³, clinically used since 1986 (Figure 1.7).

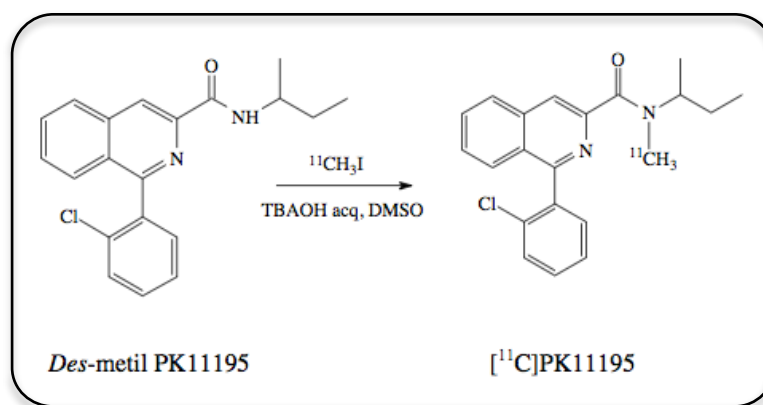


Figure 1.7 ^{11}C labeling of the PK11195 by means of a methylation reaction.

As for the non radiolabeled molecules, the isoquinoline carboxamide $[^{11}\text{C}]$ PK11195 still represents a standard for TSPO PET radioligands, but in fact it shows critical limitations for PET imaging, such as a poor signal-to-noise ratio and low brain penetration (not taking account of the short half life of ^{11}C , with a $t_{1/2}$ of 20.4 minutes). Such drawbacks have encouraged the development of new radiotracers, in the willing to improve these crucial parameters. For instance, in the phenoxyphenyl acetamide class, $[^{11}\text{C}]$ DAA1106 ($[^{11}\text{C}]$ -N-(2,5-dimethoxybenzyl)-N-(4-fluoro-2-phenoxyphenyl)-acetamide)¹⁰⁴ and its fluorinated analogue, $[^{18}\text{F}]$ FEDAA1106 ($[^{18}\text{F}]$ -N-(5-fluoro-2-phenoxyphenyl)-N-(2-(2-fluoroethoxy)-5-methoxybenzyl) acetamide)¹⁰⁵, the latter labeled with the longer half lived positron emitter ^{18}F ($t_{1/2}$ of 109.8 minutes), turned out as better radioligands compared to $[^{11}\text{C}]$ PK11195, with an improved signal-to-noise ratio and, indeed, showing better imaging results.

To the same chemical family of $[^{11}\text{C}]$ DAA1106 and $[^{18}\text{F}]$ FEDAA1106 belong $[^{18}\text{F}]$ PBR06 ($[^{18}\text{F}]$ -N-fluoroacetyl-N-(2,5-dimethoxybenzyl)-2-phenoxyaniline)¹⁰⁶, bearing the ^{18}F at the N-acyl function. This radiolabeled compound has been recently reported as high affinity tracer for both brain tumors visualization and TSPO quantification in tumor and healthy tissues¹⁰⁷.

Subsequently, from $[^{18}\text{F}]$ PBR06, new compounds were derived, featuring a pyridine motif. In particular, in 2007 was developed $[^{11}\text{C}]$ PBR28 ([methyl- ^{11}C]N-acetyl-N-(2-methoxybenzyl)-2-phenoxy-5-pyridinamine)¹⁰⁸, which gave promising imaging results in monkeys and rats and is still widely used, such as its fluorinated analogue 6- $[^{18}\text{F}]$ fluoro-PBR28.

As above described for TSPO non labeled ligands, bioisosteric derivatives of Alpidem have been projected as specific tracers to target the receptor. Within this class, [¹¹C]DPA-713 (N,N-diethyl-2-[2-(4-methoxyphenyl)-5,7-dimethylpyrazolo[1,5-a]pyrimidin-3-yl]acetamide)¹⁰⁹ is one of the most important and investigated compound. In 2007, Boutin *et al.* performed PET studies on a rat model of neuroinflammation, induced by α -amino-3-hydroxy-5-methyl-4-isoxazolepropionate (AMPA), using both [¹¹C]PK11195 and [¹¹C]DPA-713 and comparing the differences in terms of binding ability and image quality¹¹⁰. The AMPA lesion gave rise to a well defined TSPO rich lesion that could be easily and similarly visualized using appropriate TSPO tracers. The results proved [¹¹C]DPA-713 to have a higher signal-to-noise ratio than [¹¹C]PK11195 because of a lower level of unspecific binding, with high probability due to the lower lipophilicity of [¹¹C]DPA-713. The latter showed also to image better the contrast between healthy and damaged brain area, though in the ipsilateral side its uptake was significantly lower than [¹¹C]PK11195.

In 2008, as a result of a project led in collaboration with our group, James reported the synthesis, radiofluorination and pharmacologic evaluation of a new TSPO ligand, belonging to the same class of [¹¹C]DPA-713, [¹⁸F]DPA-714 (N,N-diethyl-2-(2-(4-(2-¹⁸F-fluoroethoxy)phenyl)-5,7-dimethylpyrazolo[1,5-a]pyrimidin-3-yl)acetamide)¹¹¹. PET studies in rats and baboons confirmed the view of this compound as a specific ligand of TSPO, endowed of high selectivity and good pharmacokinetics properties, as well as low toxicity. Even though [¹⁸F]DPA-714 has a slightly higher lipophilicity than [¹¹C]DPA-713 which, as seen, can lead to an increase of non specific binding, this compound allows longer imaging protocols and, as a consequence, can be considered as a more suitable radiotracer (structures of both cold and labeled [¹¹C]DPA-713 and [¹⁸F]DPA-714 are shown in Figure 1.8).

Afterwards, in 2009, Chauveau *et al.* related of a new comparative PET study, in the same AMPA neuroinflammation rat model above mentioned, between [¹¹C]PK11195, [¹¹C]DPA-713 and [¹⁸F]DPA-714, and this direct comparison proposed the [¹⁸F]DPA-714 as the overall most promising PET radiotracers for TSPO imaging for image definition, uptake and biodistribution¹¹², not to mention the ease of labeling with ¹⁸F.

INTRODUCTION

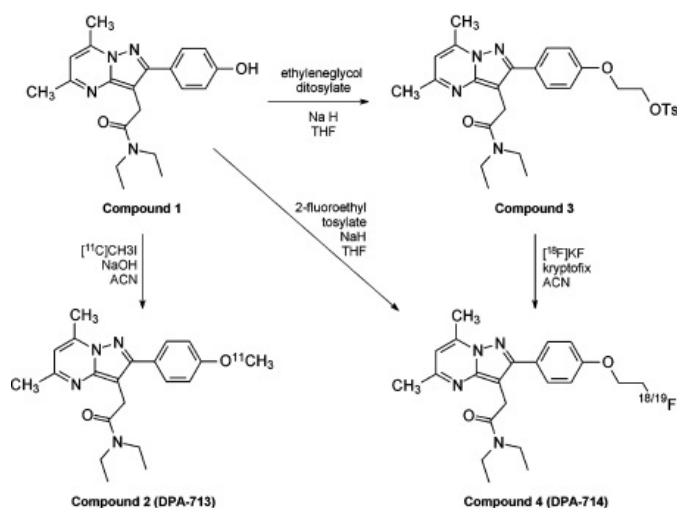


Figure 1.8 Labeling and structure of $[^{11}\text{C}]\text{DPA-713}$ and $[^{18}\text{F}]\text{DPA-714}$ radiotracers.

Since it has been demonstrated that $[^{18}\text{F}]\text{DPA-714}$ rapidly and extensively undergoes *in vivo* metabolism in animal models (rats and baboons), in particular for the cleavage of fluoroethoxy side chain which leads to the formation of small radio metabolites entering the brain and lowering PET imaging quality, a recent study (2014) has developed a DPA-714 analogue, CfO-DPA-714. This compound is obtained replacing the DPA-714 oxygen atom bridging the phenyl ring and the fluoroethyl motif with a methylene group. The corresponding ^{18}F labeled version $[^{18}\text{F}]\text{CfO-DPA-714}$ has been recently synthesized and is currently studied for *in vivo* evaluation¹¹³.

As a further advancement, in 2013 has been published an interesting article about the implementation of DPA-713 as part of a new probe for magnetic resonance imaging (MRI)¹¹⁴. This probe consists of two sections, linked by a six carbon atom chain: the TSPO ligand DPA-713 and a mono amide DOTA (1,4,7,10-tetraazacyclododecane-1,4,7,10-tetraacetic acid) cage. The gadolinium (Gd) dedicated DOTA chelator represents the magnetic resonance imaging reporter, while the DPA-713 is the part of the conjugate designated to target the TSPO receptor.

Indeed, such a conjugate shows different bioavailability and biodistribution properties than DPA-713; for instance, the good hydrophilicity of the metal chelate makes DPA- C_6 -(Gd)DOTAMA soluble in water, so the authors decided to load the probe to a large carrier, such as a liposome, with the aim to increase its lifetime in blood. Considering

INTRODUCTION

the promising availability of the whole complex, including the liposome it is loaded to, and the consequently increased half life in blood stream, the authors suggest future *in vivo* studies, encouraging the search of new slow releasing MRI targeting agents.

Though what it has been here written until now represents only a brief overview of the whole subject, it should be enough to deeply understand how important and desirable is the comprehension of the molecular mechanisms of TSPO function and regulation, as well as how challenging and appealing is, for medicinal chemistry, the fine tuning of specific ligands developed for both therapeutic and diagnostic purposes.

2. AIM OF THE THESIS

Considering the broad spectrum of actions demonstrated and suggested for TSPO, researchers interest has been focused both on the therapeutic and, more recently, with the spread of imaging techniques, the diagnostic goal.

In regard of the first purpose, we can characterize applications in three main paths, that is control of the inflammatory response after injury, cancer regression and axonal regeneration.

The latter aim appears especially appealing, as there is no currently efficient treatment for enhancing axonal regeneration, including elongation speed and functional reinnervation.

As local production of neurosteroids has been demonstrated to confer neuroprotection in CNS, the chance of modulating TSPO activity with pharmacological ligands, in order to start or enhance the production of neurosteroids locally in the injured CNS, should result in attenuating several neuroinflammation and neurodegeneration pathologies.

A recent paper from Daugherty D. and coworkers (2013) examined the effects of etifoxine, a clinically available anxiolytic drug, in the development and progression of mouse EAE (experimental autoimmune encephalomyelitis), a model for multiple sclerosis¹¹⁵. Results showed that etifoxine modulation of TSPO attenuated EAE severity when administered before the development of clinical signs and improved symptomatic recovery when administered at the peak of the disease, suggesting TSPO ligands to be a potential new therapeutic option for multiple sclerosis, avoiding the detrimental side effects of long term direct use of steroids, and leaving an open door for therapeutic approaches to other neurodegenerative diseases.

The first aim of this work was to synthesize a small number of compounds, belonging to the 2-arylpyrazolo[1,5-*a*]pyrimidin-3-yl acetamides series, to be investigated for their binding affinity towards TSPO and for their ability to induce the endogenous production of pregnenolone (the first steroid deriving from cholesterol metabolism) in C6 cells, a cellular line derived from rat glioma.

The lead compound that we chose as reference for the new series was the PBR 136, 4-(3-(2-(diethylamino)-2-oxoethyl)-5,7-dimethylpyrazolo[1,5-*a*]pyrimidin-2-yl)phenyl benzoate; this molecule was beforehand obtained, in high percentage (80%), as secondary product in the first synthesis of PBR 137, 2-(2-(4-

(difluoromethoxy)phenyl)-5,7-dimethylpyrazolo[1,5-*a*]pyrimidin-3-yl)-N,N-diethylacetamide, and, sent to the binding test, by surprise tuned out to have a very low K_i (0.02 nM). Despite its K_i , the steroidogenesis assay showed a pregnenolone increment of about + 25.55% vs controls.

Anyway, encouraged by the binding result of PBR 136 and by the will of trying to understand whether a compound can act as a TSPO agonist or antagonist, we decided first of all to obtain PBR 136 directly as the desired goal of the synthetic pathway, by the way performing an optimization of some critical reaction steps, and then to investigate its analogues, joint by the presence of ester group at the phenolic -OH of the aromatic ring in position 2 of the pyrazolo[1,5-*a*]pyrimidine nucleus.

Thanks to a collaboration with Prof. Michael Kassiou, University of Sidney, Australia, we were able to test two other series of TSPO ligands, the sb, to which belong analogues of our PBR 136 but with an ether, instead of an ester, group, and the Raj, composed of different structure bearing an indole-2-carboxamide core. The availability of a wide number of different compounds to screen both by binding test and pregnenolone assay, suggested us the idea to perform a future SAR study statistically sizable.

Regarding the other principal field of interest of this project, the developing of TSPO radiotracers as tools for the biomedical imaging, blasted in the last 10 years, boosted by the strong evidence of an increasing in TSPO expression levels, directly linked with a pathological event occurrence, as neuroinflammation or neurodegeneration, right at the site of injury. Since this correlation was demonstrated, the new researchers purpose has been to synthesize, label and test new molecules endowed not only with high affinity to TSPO but even low toxicity profile and proper bioavailability and distribution.

As previously said, within the class of bioisosteric derivatives of Alpidem previously synthesized in our laboratories, [^{11}C]DPA-713 and [^{18}F]DPA-714¹¹¹, were labeled and extensively tested as PET radiotracers on mouse and baboons by Prof. Kassiou staff, as a part of the above mentioned collaboration between the two groups, giving promising results. Due to their binding ability, image quality and lower level of unspecific binding, at the state of the art these two molecules have been both tested on human, showing good pharmacokinetic properties, and still clinical trials with [^{18}F]DPA-714 are in progress.

These strong results, both with new recent papers based on the use of DPA-713 as a part of magnetic resonance probe¹¹⁴, further reinforces our aim to promote TSPO ligands as carriers of radionuclides for diagnostic (and therapeutic) purposes. This time we decided to synthesize a radioconjugate of a 2-aryl substituted pyrazolo[1,5-*a*]pyrimidin-3-yl acetamides (already validated as TSPO ligand) linked by a PEG spacer to a chelating complex, to be subsequently labeled. At the first time we decided to perform the synthesis with two different PEG, one of intermediate molecular weight (3000) and the other of low molecular weight (149,19), attracted by the possibility to split them to different applications; hereafter, as we had to choose one for the labeling trials, we preferred to focus on the second one, which was the most simple to handle. Anyway, if all the tests on this conjugate will be successful, our aim will be to subsequently investigate the one of higher molecular weight as a diagnostic/therapeutic agent carried by the lymphatic system for the identification of metastasis (as TSPO has been assessed to be over expressed more and more with the malignancy spread in several cancer type). The chosen chelating group in both cases was DOTA (tetraazacyclododecane tetraacetic acid), even if, once optimized the synthesis, the radioconjugate could be obtained with a range of specific chelating groups tailored to the complexation properties of each radiometal and non-radiometal.

Back to the selected conjugate, we decided to perform the labeling trials with ¹¹¹In, as a first approach, to determine the best radiochemistry procedure. Once optimized the ¹¹¹In labeling, we thought that performing other trials, this time with the ⁶⁸Ga isotope, could give more completeness to our project. In fact, together with the better signal to noise ratio of ⁶⁸Ga with respect to ¹¹¹In, it is sometimes used as a surrogate of ⁹⁰Y, since they have a very similar radiochemistry. In this way it is possible to take advantage of the ease of using ⁶⁸Ga for preclinical and clinical studies, and eventually replace it with ⁹⁰Y if a therapeutic approach is requested.

It goes without saying that the ultimate target of this work was to test the radiolabeled compound in a wild type mouse and in a neurodegenerative mouse model, to take account of the possible metabolization, biodistribution and toxicity and the effective ability of the conjugate to be a novel, predictive imaging biomarker. The selected imaging technique for the study was PET, which is today widely used for the sensitivity and high quality results of images as they are better than those achievable by MRI and CT (computed tomography) as an example in brain tumors, like gliomas, reason why

Aim of the thesis

there is a considerable need to develop and validate selective radiotracers (wishing both with improved new imaging techniques).

Although the time required by the *in vivo* tests have not yet made it possible to achieve them, they will be performed before long.

3. RESULTS

3.1 Optimization of the classical synthetic pathway

As already known, the first aim of our work was to obtain compound PBR 136 (4-(3-(2-(diethylamino)-2-oxoethyl)-5,7-dimethylpyrazolo[1,5-*a*]pyrimidin-2-yl)phenyl)benzoate, Figure 3.1) as the final, desired, product of the synthetic pathway, since previously it had been obtained just as a side product during the synthesis of a different compound.

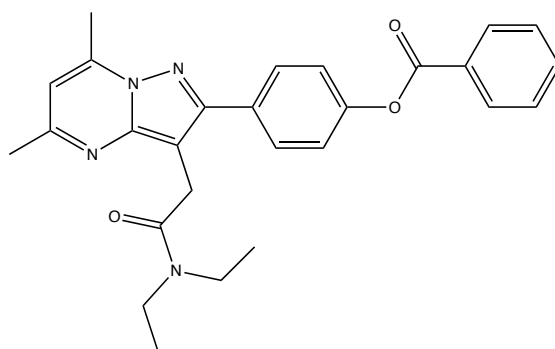


Figure 3.1 Chemical structure of the lead compound PBR 136.

To obtain the precursor of PBR 136, that is PBR 129 (N,N-diethyl-2-(2-(4-hydroxyphenyl)-5,7-dimethylpyrazolo[1,5-*a*]pyrimidin-3-yl)acetamide), we chose to follow the synthetic strategy (displayed in Figure 3.1) already described in earlier works from our group (Selleri et. al., 2001)⁹⁶. Concerning this point, we thought about the possibility to perform at least a slight optimization of some of the most critical steps of this synthetic strategy, without changing the nature and sequence of the reactions, but trying to influence their duration and yield. In addition, we decided to synthesize 5-(4-methoxyphenyl)isoxazole as the precursor to achieve, after opening of the isoxazole ring by means of a sodium alcoholate solution, the 3-(4-methoxyphenyl)-3-oxopropanenitrile (compound 3 in Figure 3.2 below), unlike the synthesis previously reported in the article. This intermediate step, which doesn't invalidate the obtainment in high percentage yield of the desired compound, was originally studied by Prof. Sarti

Results

Fantoni at the University of Florence, and turned out to be a valid option whether the commercial 3-(4-methoxyphenyl)-3-oxopropanenitrile is not available.

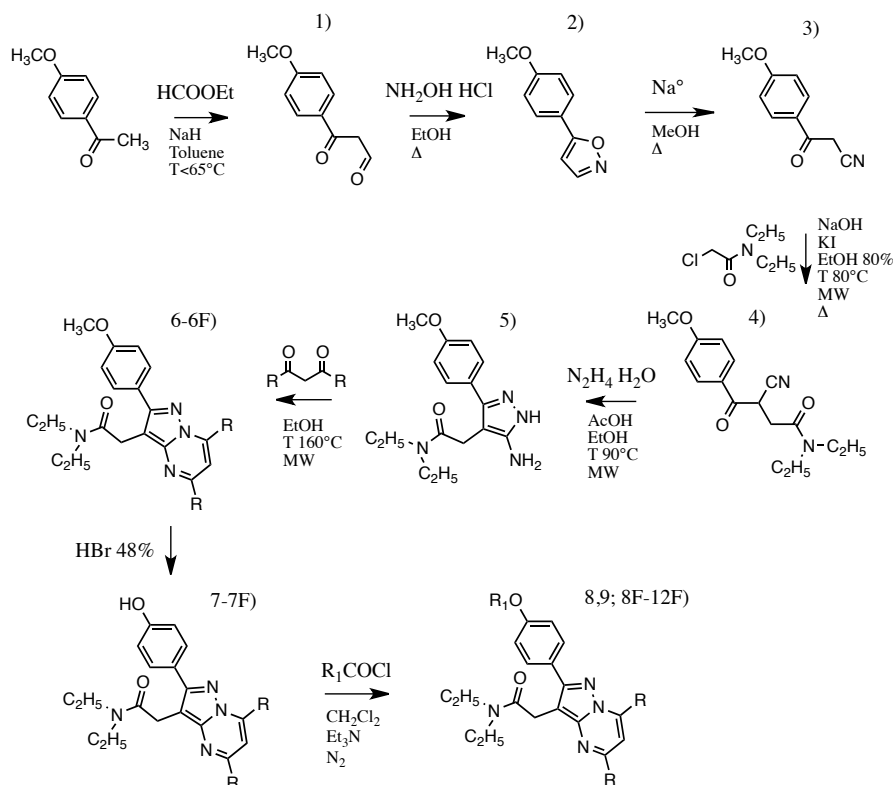


Figure 3.2 General synthetic procedure for the attainment of compounds 8,9; 8F-12F. The abbreviation MW indicates the microwave assisted steps.

Also, the direct attainment of the latter compound by reaction of the relative ester with CH_3CN and NaH was not possible, as the presence in *p*-position of the methoxy group led to a left shift in the reaction balance, as previously noticed by my research group. As sometime reported by literature, during the attainment of 5-(4-methoxyphenyl)isoxazole, we obtained, as side product in reasonable proportion, a precipitate not soluble in EtOH, which showed a NMR signal compatible with 2-(4-methoxyphenyl)-2,5-dihydroisoxazole; its formation, at first glance, seemed to be temperature-depending.

Concerning the functionalization of position 3 with the N,N-diethylacetamide chain, this one is the most critical step of the whole synthetic process. According to literature previously reported by my group⁹⁷, it is better to insert this chain before the closure that

leads to the aminopyrazole core; for this reason, in the article above mentioned, the proper aroylacetonitriles were reacted in alkaline medium with *N,N*-diethylchloroacetamide to afford the deriving *N,N*-diethylbutanamides. However, as reported, the desired product was obtained after two days of reflux and together with tars and impurities; this event, both with the fact that, in my case, the 3-cyano-*N,N*-diethyl-4-(4-methoxyphenyl)-4-oxobutanamide (compound 4) had an oily texture, complicated the final purification, making flash column chromatography mandatory.

Taking into account these difficulties, to the left of a classic synthetic approach, we chose to experiment a couple of new strategies in the willing to optimize the obtainment of 3-cyano-*N,N*-diethyl-4-(4-methoxyphenyl)-4-oxobutanamide, without overturning the whole synthetic pathway already developed.

The first attempt was to make 3-(4-methoxyphenyl)-3-oxopropanenitrile react with 2-iodoacetic acid, heating to reflux in EtOH with LiOH, to achieve the 3-cyano-4-(4-methoxyphenyl)-4-oxobutanoic acid, to be subsequently converted in the corresponding amide. This reaction happened to be more favorable than the one that led directly to the formation of 3-cyano-*N,N*-diethyl-4-(4-methoxyphenyl)-4-oxobutanamide, in terms of duration. Anyway, the yield after chromatography purification and closure with hydrazine monohydrate, to achieve 2-(5-amino-3-(4-methoxyphenyl)-1*H*-pyrazol-4-yl)acetic acid after a second purification on silica gel, led to a lack of pure compound, because of the amount of side products and impurities still taking origin from the reaction.

Considering the point, we decided to go back to the direct formation of the oxobutanamide, exploring the possibility to optimize the reaction yield and/or duration by means of microwave radiation. We followed this way encouraged by a paper of Tang¹¹⁶ (2010), discussing the implementation of microwave in the obtainment of similar products, so building on from this article we decided to work our way to the best matching of usable solvents and methods and timing of radiation.

At the beginning, we started with the formation of compound 4 by reaction of 3-(4-methoxyphenyl)-3-oxopropanenitrile and 2-chloro-*N,N*-diethylacetamide in 80% EtOH, KI and NaOH. We performed different tests, irradiating with microwave three different vessels respectively to a temperature of 65 °C for 60 min, 80 °C for 40 min, 100 °C for 25 min, taking only a fixed temperature value on the instrument (Explorer 48, CEM), without setting up the potency. As a first result, after the work up of the three reactions

Results

and their purification by flash chromatography, the two vessels with the higher temperature were the best in terms of yield (about 70%), but the reaction carried out at 100 °C seemed to have more impurities. So we prefer to choose the 80 °C for 40 min protocol (about 30 W of potency), even if it had to be carried out for more time.

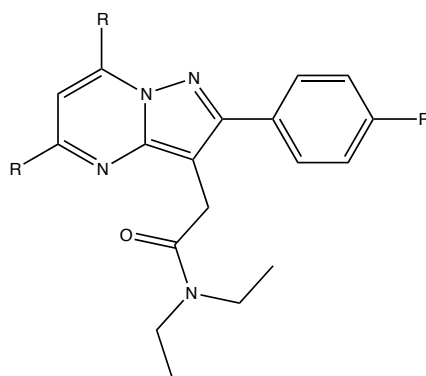
With the same approach of the three vessels, we investigate then the reaction of compound 4 in EtOH with hydrazine monohydrate and with a catalytic amount of acetic acid, same reagents as for the classic synthetic strategy. We performed the reaction at 70 °C for 60 min, 90 °C for 40 min and 110 °C for 20 min. As for the synthesis above, the best results in terms of final yield (42%) of compound 5 were achieved by the 90 °C for 40 min protocol still with no fixed potency (about 35 W), still confirming the key role of temperature.

Concerning the synthesis of compounds 6 and 6F, this step, involving in one case the reaction between compound 5 and 2,4-pentanedione and in the other with 1,1,1,5,5,5-hexafluoropentane-2,4-dione, usually carried out in EtOH heated to reflux, had an outcome rather satisfying in the classic synthetic strategy (about 80% yield for 6 and 60% yield for 6F). Anyway, we decided to try to achieve 6F performing a microwave assisted reaction, particularly to try to reduce the duration of the classic synthetic reaction (about 5 h). After several attempts, we found that carrying out the reaction in DMF with a power cycle protocol gave the best results. During the power cycle mode, the instrument perform a number of short cycle of irradiation and consecutive cooling of the reaction mixture. This protocol is sometime found in literature to promote cyclization or closure of organic molecules. In our case, we chose 300 cycles with a maximum potency of 300 W, with a range of temperature between 115 °C, lower limit, and 130 °C, upper limit. The duration of the whole protocol was less than 2 h and, after the work up and the purification via flash chromatography, the final yield was of 70% (instead of 60% mentioned above), so we reached a reasonable optimization in the synthesis of compound 6F.

The de-methylation of compounds 6 (to obtain PBR 129, 7 in reaction pathway) and 6F (to obtain PBR 127, 7F in reaction pathway) was carried out directly pouring HBr (48% in H₂O) in the flask containing the dry compound and well heating to reflux overnight in an oil bath. This reaction, even if it had to be carried out overnight, enabled after very simple work up to purify the mixture and to obtain the desired product with a good yield of about 65% in both cases.

3.2 Direct synthesis of PBR 136 and a small series of analogues

Once optimized the achievement of the two precursor PBR 129 and PBR 127, the next step was to synthesize directly the PBR 136, as previously said. For this reason, we chose at first to proceed in one of the most classic way, that is making the proper precursor react with the selected acyl chloride in dry pyridine, stirred at room temperature and under N_2 atmosphere. In the case of PBR 136, we made PBR 129 react with benzoyl chloride; unfortunately, even if the NMR spectrum of the mixture showed that the reaction was proceeding, the subsequent work up, involving the use of HCl (tested 6 M, 3 M and 1 M in three distinct attempts), brought principally back to the initial phenolic compound.



Compounds	R	R1
8	CH3	benzoyl ester
9	CH3	4-toluenesulfonyl ester
8F	CF3	benzoyl ester
9F	CF3	4-toluenesulfonyl ester
10F	CF3	4-Fbenzoyl ester
11F	CF3	2-Fbenzoyl ester
12F	CF3	2-furoylester

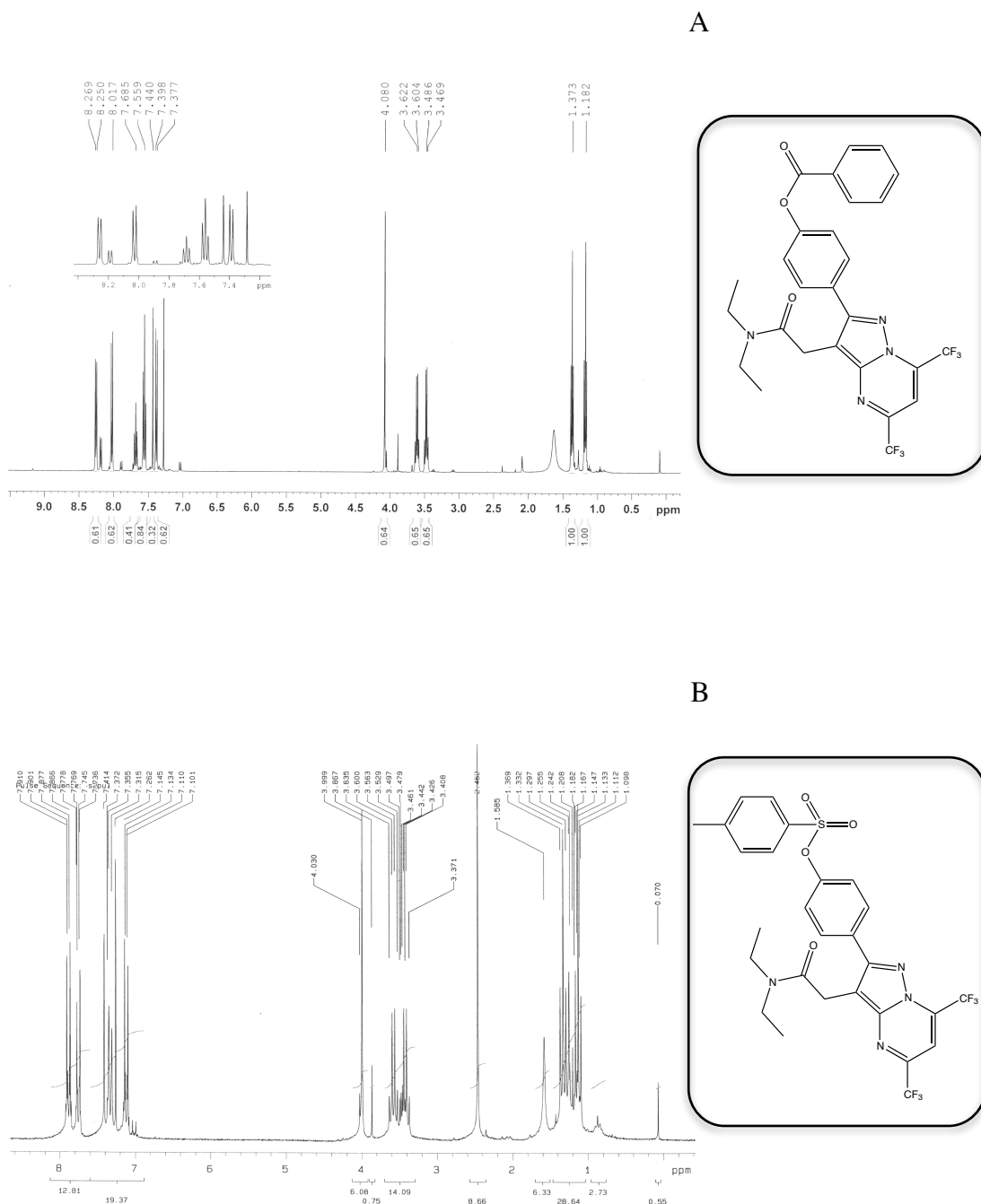
Figure 3.3 Ester derivatives of PBR 127 and 129.

The ester hydrolysis in presence of H^+ is usually due to the presence of H_2O , so as at a first time we used fresh pyridine dried on molecular sieves, we performed another synthesis with anhydrous pyridine (obtained after distillation), under N_2 atmosphere. However, after the new work up with fresh HCl, we found that the result was the same. So far, we decided to change the reaction conditions, as we were focused on the obtainment of the products to be subsequently tested, so we moved to the esterification of PBR 129 and benzoyl chloride with triethylamine in dry CH_2Cl_2 , under N_2 atmosphere, stirred at room temperature. This attempt happened to be successful; then, after filtering the solution, washing with a 1 m solution of KOH, extracting it in EtOAc and drying the organic phase under vacuum, we performed a purification via flash chromatography to obtain PBR 136, the desired product, as light brown crystals (about 50% yield).

Results

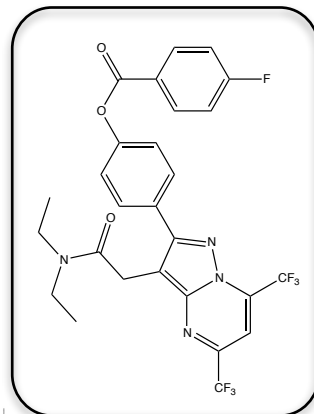
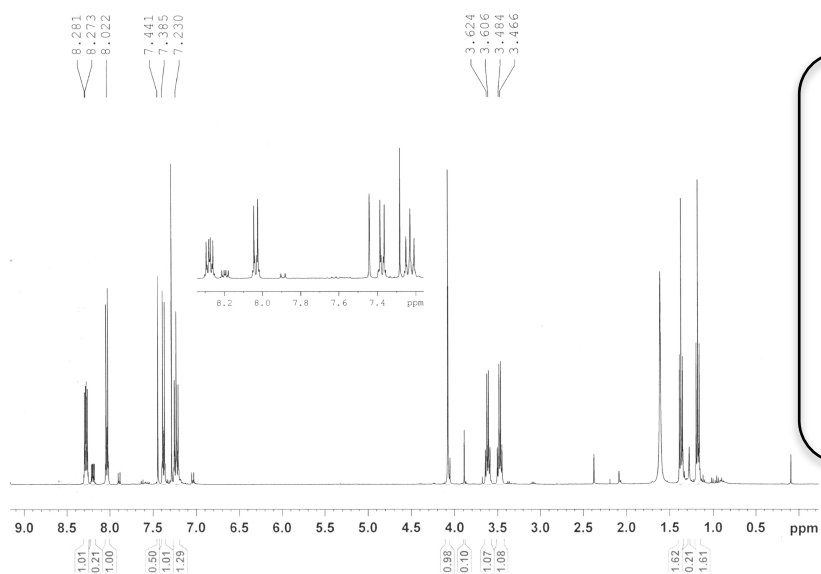
After the attainment of PBR 136, our following purpose was to synthesize a small series of ester analogues, so we prepared, with the same procedure already specified, the compounds reported in the grid above (Figure 3.3).

We built this small series with the aim to test these compounds for their affinity vs TSPO receptor and for their ability to provoke a biological response when interacting with it, so to analyze their pharmacological profile. Spectra of the compounds from 8F to 12F are shown below (A, B, C, D, E in Figure 3.4).

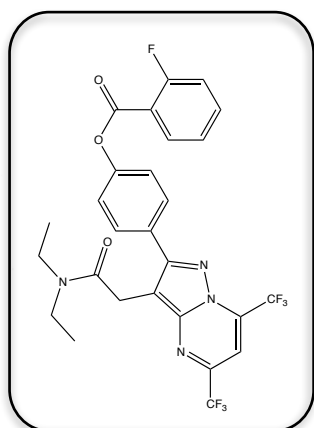
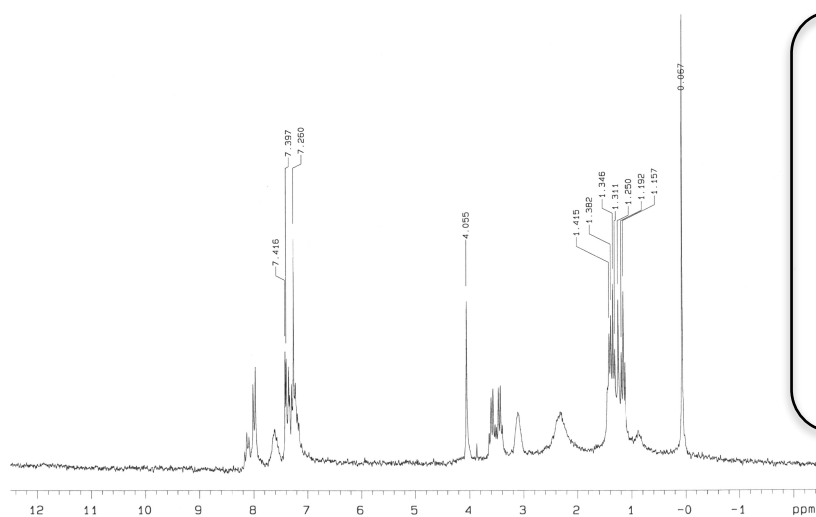


Results

C



D



E

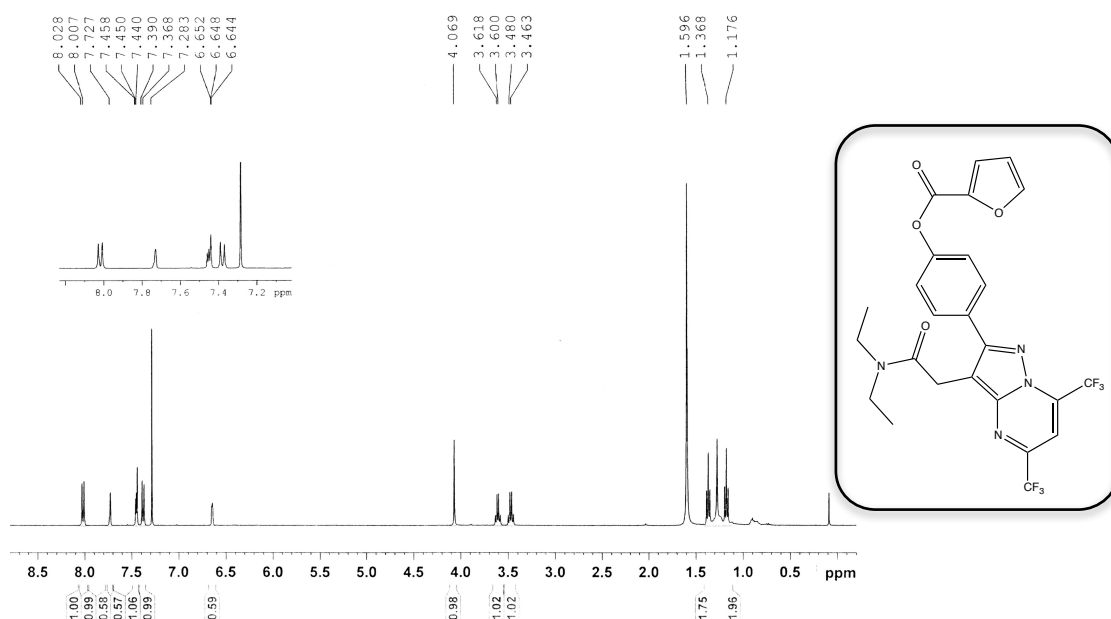


Figure 3.4 ¹H-NMR in CDCl₃ of compounds 8F-12F, respectively A-E. The structure of each analyzed compound is reported next to the related spectrum. Spectra A, C and E were obtained with a 400 MHz instrument; B and E with a 200 MHz instrument.

3.3 Binding tests and steroidogenesis assay: the biological challenge

To assess the affinity of a compound toward a receptor, it is necessary to test it with a binding assay. We went to Pisa, among the group of Prof.ssa C. Martini, to perform this for TSPO receptor.

During the test, a crude mitochondrial pellet, as the TSPO source, deriving from kidneys of male Wistar rats properly treated and diluted, after determination of its protein concentration, was incubated with 0.6 nM [³H]PK11195 (well known and studied TSPO specific ligand) in ice-cold buffer B (50 mM Tris-HCl, pH 7.4). Then, a range of concentration (from 0.1 nM to 10 μM), of every single compound from 8F to 12F was added, in a total volume of 0.5 mL. The overall time of incubation was 90 min at a

temperature of 4 °C. When finished, the incubation was stopped by dilution with ice-cold buffer B and then the suspension was filtered and the amount of radioactivity retained on the filters was determined. It is really important that all this procedure is carried out quickly and at low temperature, not to influence the dissociation rate of the complex. Then we derived the IC₅₀ for every compound and subsequently obtained the K_i values, according to the commonly used equation of Cheng and Prusoff.

To quantify the non specific binding activity, the incubation was performed both in the presence and in the absence of unlabeled 1 μM PK11195; the concentration of the unlabeled ligand has to be higher than that of the receptor, that we had determined first with the protein assay, to clearly evaluate the rate of radioligand bound to tissues or other structures.

The results for our compounds, expressed as K_i values derived from the [³H]PK11195 displacement plots, are illustrated below (Figure 3.5). It is worth mentioning that the displacement plot of compound 9 isn't shown as this molecule had serious solubility problems in DMSO, solvent commonly used for the test in standard practice, and it was not possible to perform the test. Similarly, compound 9F was only partially soluble in DMSO, but in this case we decided to evenly perform the test. Anyway, the results of binding could not be accepted because the [³H]PK11195 displacement curve didn't show a regular pattern, failing to reach the x-axis, that is the complete [³H]PK11195 displacement. For compound 8F, tested before of the other, the binding plot is not shown below, but the K_i value derived form [³H]PK11195 displacement was of 0.3 ± 0.02 nM.

It should be noted that, during these tests, sometimes we referred to the compounds with a different nomenclature than that used up to now, that is the P series. Here, both of them are reported, to better understand the following plot:

- P3 stays for 10F;
- P4 stays for 9F;
- P5 stays for 12F;
- P6 stays for 11F.

Results

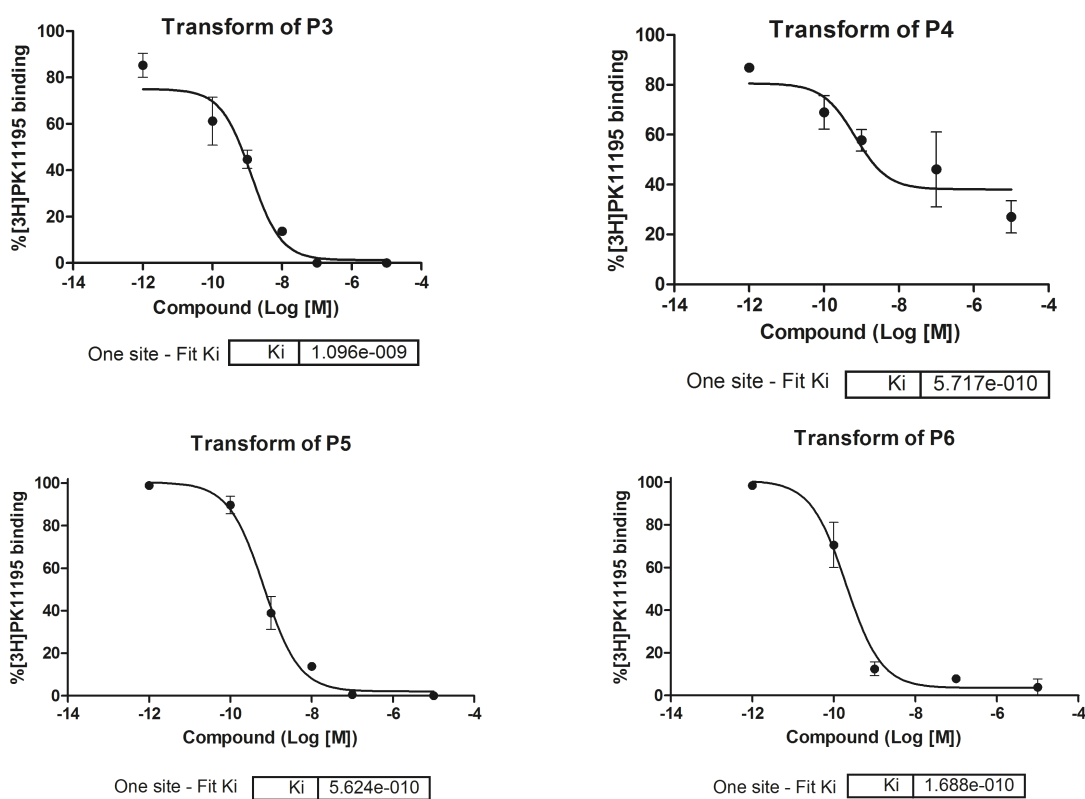


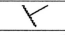
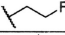
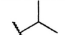
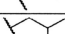
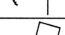
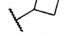
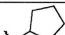
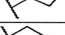

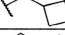
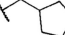

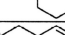
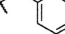
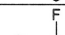
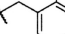
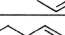
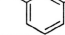
Figure 3.5 $[^3\text{H}]$ PK11195 displacement curve derived from the TSPO binding of compound 10F (P3), 9F (P4), 11F (P5) and 12F (P6). As already mentioned, the P4 plot shows an irregular trend, probably due to the poor solubility of 9F in DMSO, which results in a not derivability of its K_i real value.

Thanks to a long-standing partnership of my group with Prof. Michael Kassiou, of the Brain and Mind Research Institute of Sydney, Australia, it was possible to test for the binding assay a wide range of molecules, whose synthesis was performed by Prof. Kassiou's staff. This series, named sb, consists essentially of analogues of DPA-714 (N,N-diethyl-2-(2-(4-(2-fluoroethoxy)phenyl)-5,7-dimethylpyrazolo[1,5-a]pyrimidin-3-yl)acetamide), and it is comparable with our product, since the main difference is the ether vs ester functionalization. The synthetic strategy isn't shown in details, as this

Results

work is actually under publication. We performed with the same protocol already reported the binding assays for these compounds: their structures together with the respective K_i values are reported in the following table (Figure 3.6).

For both these analogues and our compounds, the selectivity for TSPO of their founders (PBR 136, DPA-713 and DPA-714) was previously verified by binding tests towards CBR, using [^3H]Ro15-1788 displacement in rat brain tissue.

Compound	R	TSPO K_i (nM)
1 (PK11195)	-	9.3 ± 0.5^b
5 (DPA-713)		4.7 ± 0.2^b
6 (DPA-714)		7.0 ± 0.4^b
12 (sb2097)		2.239 ± 0.2
14 (sb4023)		2.415 ± 0.2
15 (sb3105)		0.8639 ± 0.1
16 (sb3109)		1.533 ± 0.2
17 (sb3115)		3.023 ± 0.2
18 (sb4109)		1.404 ± 0.2
19 (sb4117)		2.150 ± 0.2
20 (sb4021)		3.582 ± 0.5
21 (sb3025)		0.9872 ± 0.1
22 (sb4001)		0.3131 ± 0.1
23 (sb4003)		0.4738 ± 0.1
24 (sb3089)		0.7720 ± 0.1
25 (sb4033)		1.394 ± 0.2
26 (sb4031)		0.6691 ± 0.1
27 (sb4035)		1.559 ± 0.2
28 (sb4025)		0.1256 ± 0.1

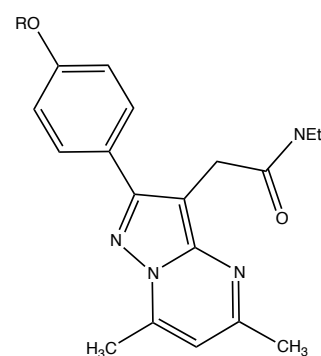


Figure 3.6 Table of sb series substituents, with K_i value of each compounds. On the right, the general structure is reported.

Once assessed the affinity and selectivity of all the compounds, since our goal was to select molecules potentially valid as therapeutic agents, we had to investigate whether they were also able to generate some biological response, in other words to determine

their pharmacological profile. So, as TSPO is primarily involved in the synthesis of steroids, we planned to carry out the steroidogenesis assay, which is widely accepted to predict the profile of a molecule interacting with this receptor. The first results of the pregnenolone assay for the analogues of our series and the sb seemed to be encouraging in terms of finding new TSPO agonists, but needed to be rearranged a second time, as expected by standard practice before being displayed as statistically relevant. As an instance, in the following graphic (Figure 3.7) we reported the percentage result in pregnenolone increase of compound sb 4025 which, together with sb 3015, can be considered a direct analogue of our lead compound PBR 136 (also referred to as 8 compound). At this regard, it is worth to note that this value is similar for both sb 4025 and PBR 136, near 24-25% more than that showed by controls (cells incubated with only EtOH and DMSO).

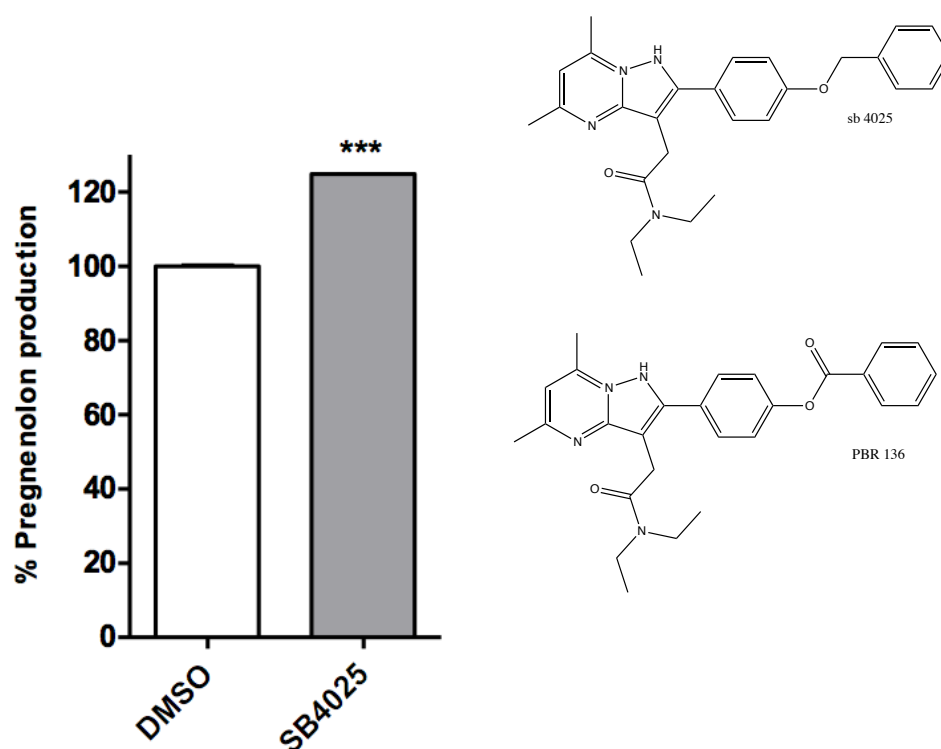


Figure 3.7 Histogram reporting the preliminary data of percentage increase in pregnenolone production of C6 cells after incubation with sb 4025. On the right, comparison between sb 4025 and PBR 136 structures.

Results

At the same time, in agreement with the Australian group, we performed the steroidogenesis assay on another set of compounds, previously tested for their binding affinity, referred to as Raj, still addressing TSPO receptor but belonging to the family of indole-2-carboxamide compounds. The products that gave back the best results in terms of affinity, were chosen to carry out the steroidogenesis assay, on rat glioma C6 cells. The cells were incubated with the simple salt medium, consisting of 140 mM NaCl, 5 mM KCl, 1.8 mM CaCl₂, 1 mM MgSO₄, 10 mM glucose, 10 mM HEPES/NaOH, pH 7.4, plus 0.1% BSA, with an addition of 25 μM Trilostane and 10 μM SU10603, specific inhibitors of 3β-hydroxysteroid dehydrogenase and 17α-hydroxylase, respectively, in order to block the further metabolism of pregnenolone. Then, 40 μM solutions of the new synthetic compounds and PK11195, as reference compound, were added, one at a time, to the 96 multiwell plate, and leaved for two hours. At the end of the incubation, the quantity of pregnenolone released by cells in the medium was quantified by an immunoenzymatic assay. Briefly, we poured a solution of pregnenolone conjugated with the HRP (horseradish peroxidase) enzyme into the wells, and then added the HRP substrate TMB (3,3',5,5'-tetramethylbenzidine); the colorimetric reactions developed were evaluated by measuring the absorbance at 450 nm. This is an indirect measurement, based on the evidence that the more pregnenolone cells are stimulated to produce, the less pregnenolone-HRP will be able to bind.

We screened compounds Raj 210, 211, 292, 297, 299, 300, 301 and 304, whose general or particular structure is reported below, together with the K_i values of some of them (Figure 3.8, 3.9, 3.10); the reference compound was still PK11195, but we took in account also the effect of EtOH and DMSO, solvents used during the assay. The test was performed in triplicate for each compound and the whole procedure was repeated two times. Results are shown in the following panel; the percentage of increasing in pregnenolone synthesis are high for some compounds, with respect to the EtOH and DMSO wells value while, referring to the PK11195 value, the buildup is about 20% maximum. As an instance, if we compare the K_i values in rats of PK11195 (3.0 nM) and Raj 300 (0.017 nM), a difference in pregnenolone increase of only 20% confirms what already known, namely that there is no forced correlation between these two parameters.

Results

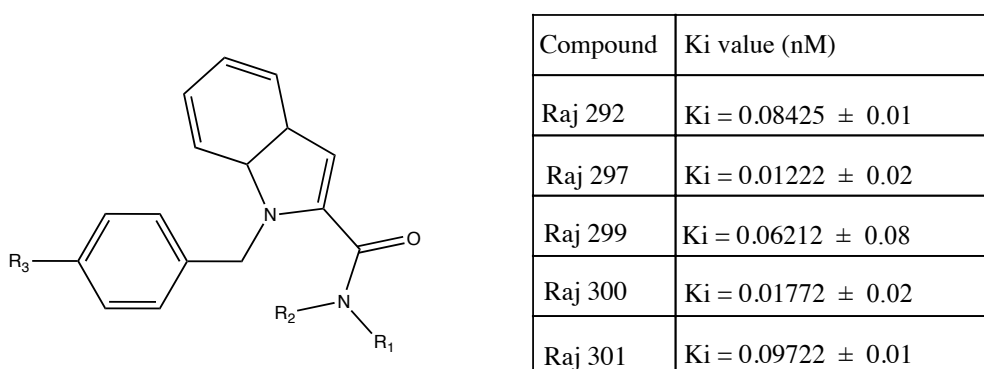
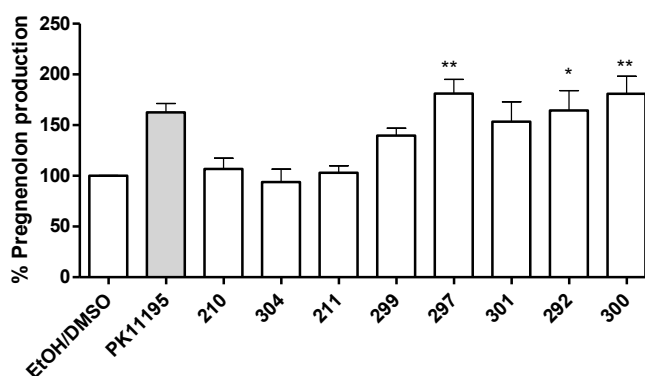


Figure 3.8 General structure of Raj series compounds; the grid on the right shows the Ki value of 5 of the 8 molecules subsequently tested with the pregnenolone assay.



EtOH/DMSOvs PK11195	-62.67	2.694
EtOH/DMSOvs 210	-6.676	0.2722
EtOH/DMSOvs 304	6.097	0.2486
EtOH/DMSOvs 211	-2.918	0.1342
EtOH/DMSOvs 299	-39.66	1.824
EtOH/DMSOvs 297	-81.12	3.731
EtOH/DMSOvs 301	-53.48	2.460
EtOH/DMSOvs 292	-64.44	2.878
EtOH/DMSOvs 300	-80.84	3.718

Figure 3.9 The above histogram reports the percentage increase in pregnenolone production of C6 cells after incubation with Raj compounds 210, 304, 211, 299, 297, 301, 292, 300, with PK11195 as reference compound. In the grid is shown the % difference in pregnenolone production of the non incubated (EtOH/DMSO) vs the incubated cells and, in the far right column, are reported the Dunnett's multiple comparison test value.

Results

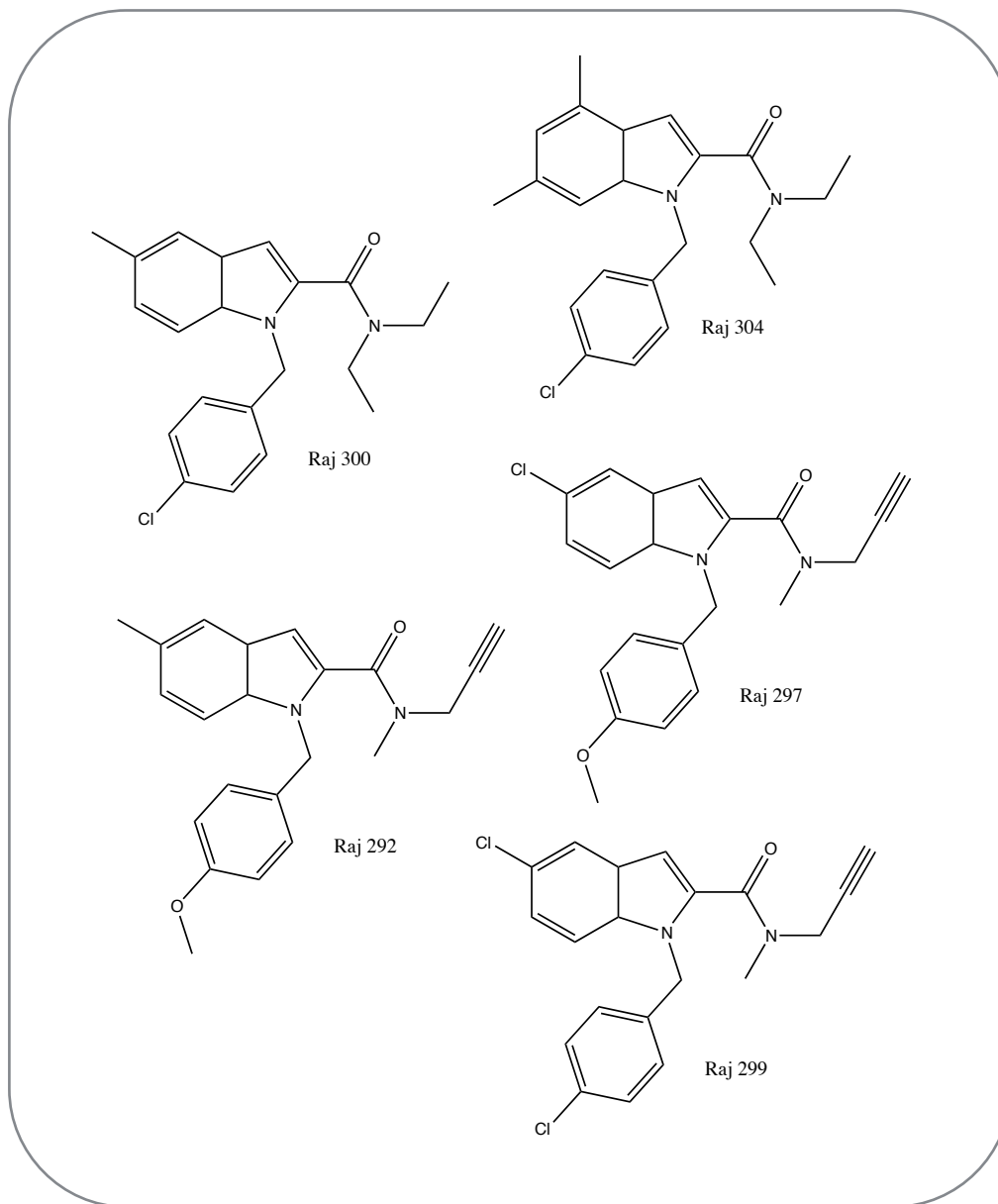


Figure 3.10 Structures of five of the eight compounds of Raj series tested with the pregnenolone assay, which results are shown above.

The availability of all these different chemical structures (PBR, sb and Raj) suggested us the idea to perform a SAR study among them. Although, as known, the structure of TSPO isn't already resolved, one of the most commonly accepted TSPO pharmacophore model can be represented with the presence of three regions: a freely rotating aromatic ring region (FRA), an electron rich zone ($\delta 1$), a planar aromatic region (PAR) and a lipophilic area (LA). We planned a future investigation of the interactions of these three class of compounds with the active site of the receptor, choosing the most active ligands for each of the three series to derive a pharmacophore, to be subsequently applied to the 21 molecules of the whole dataset. The in silico simulation should be carried out with the Molecular Discovery FLAP, a software that provides a common reference framework for comparing molecules, using molecular interaction fields.

3.4 The imaging target

The second main purpose of my PhD project was addressed to the interest, recently sprouted in the last decade, about the potential diagnostic applications of TSPO ligands. It goes without saying that the after all recent interest in this direction came with the expansion of the imaging techniques (as NMR, PET, SPECT), that highlighted the necessity of new selective and potent tracers to be availed.

As previously described, my research group had already worked at the synthesis of tracers deriving from DPA-713 and DPA-714, respectively labeled with ^{11}C and ^{18}F , successfully tested as PET tracers and actually used even in NMR and SPECT analysis. This time we decided to experiment something different, not labeling directly the molecule but using the specific TSPO ligand as a carrier of a radionuclide inserted inside a special cage.

The chosen ligand was PBR 127 ($K_i = 6.3 \text{ nM}$), so we synthesized it as previously explained in this section. Then, to join the ligand with the chosen basket to hold the proper radionuclide, we decided to insert a pegylated linker. In a previously reported paper by Cerutti *et al.* (2013)¹¹⁴ a similar conjugate was done using an alkyl spacer of 6 C atoms. So at the beginning we decided to maintain a similar distance between the ligand and the radionuclide and that was the reason why the choice was addressed on an heterobifunctional $\text{H}_2\text{N-PEG}_3\text{-OH}$. The nature of the terminal groups was determined by

Results

the will of join the linker to the TSPO ligand with a stable ether bound and the cage to the linker with a classic amide bound. Concerning the cage, we decided at first to use a DOTA chelator (commercially available as DOTA-tris(tBu)ester, 2-(4,7,10-tris(2-(*tert*-butoxy)-2-oxoethyl)-1,4,7,10-tetraazacyclododecan-1-yl)acetic acid), without prejudice to the possibility of subsequently choose between a range of specific chelating agents, tailored to the complexation properties of each radiometal and non-radiometal (the structure of the conjugate is shown in Figure 3.11).

The H₂N-PEG₃-OH was treated first to protect the amine group, leaving it react overnight with Boc₂O (di-*tert*-butyl dicarbonate) in CH₂Cl₂ with DIPEA (N,N-diisopropylethylamine). The reaction was monitored with TLC and diluted fluorescamine, to verify the presence or not of the free amine group.

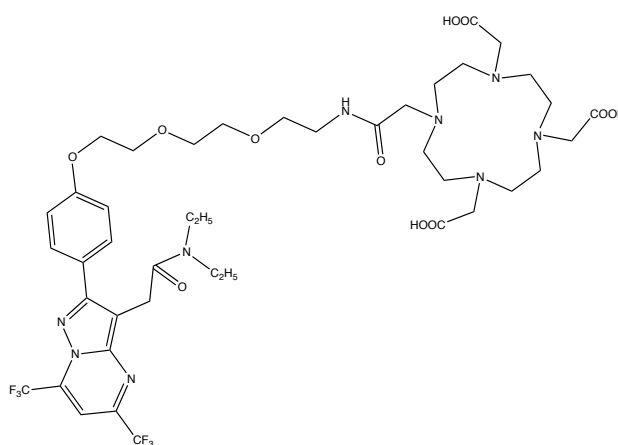


Figure 3.11 DOTA-PEG₃-PBR 127 conjugate structure.

After that, the hydroxy group was functionalized with tosyl chloride, in dry CH₂Cl₂ with TEA (triethylamine) and then, once this reaction was completed, the intermediate was left to react overnight with PBR 127 at 85 °C in DMF with K₂CO₃. The day after, demineralized H₂O was poured into the flask and the volume was extracted with EtOAc; then, the organic layer was collected and dried under vacuum, to obtain compound **c**. The following passage, deprotection of the amine, was a quick step (45 min) performed with 30% TFA (trifluoroacetic acid) in CH₂Cl₂ and the presence of free amine during the reaction was still detected in TLC by fluorescamine.

Once achieved the **d** compound, this had to react with DOTA-tris(tBu)ester in DMF, at room temperature, in the presence of both HATU (1-[bis(dimethylamino)methylene]-1H-1,2,3-triazolo[4,5-*b*]pyridinium 3-oxid hexafluorophosphate) and NMM (N-methylmorpholine), necessary to form the active

Results

ester of the carboxylic acid to force the reaction towards the formation of its products. The reaction was monitored by TLC and the solution of *p*-anisaldehyde as stain color for developing TLC plates. The last step, to obtain compound **f**, was the deprotection of the three tBu ester of DOTA carboxyl groups. At first, we proceeded as for the deprotection of the compound **c**; then, after 60 min, we evaporated all the volume in the flask, poured inside fresh TFA and left the solution stirring, monitoring every hour the progress of the reaction. When finished, compound **f** was obtained as a yellow solid, analyzed by means of NMR and UPLC/ESI-MS and subsequently purified by HPLC/ESI-MS system, Waters Symmetry 200 Å C18 reverse-phase column (in Figure 3.12 is reported in scheme the followed synthetic strategy; Figure 3.13: HPLC/ESI-MS of the DOTA-PEG₃-PBR 127 conjugate).

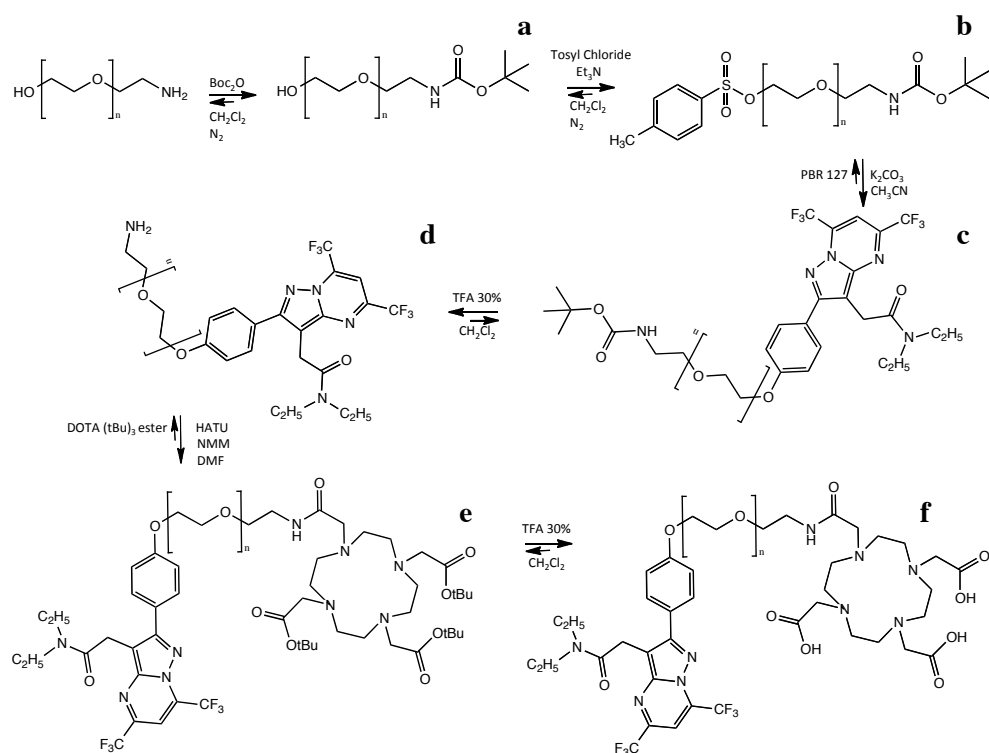


Figure 3.12 General synthetic pathway for the attainment of DOTA-PEG_n-PBR 127 conjugate.

Results

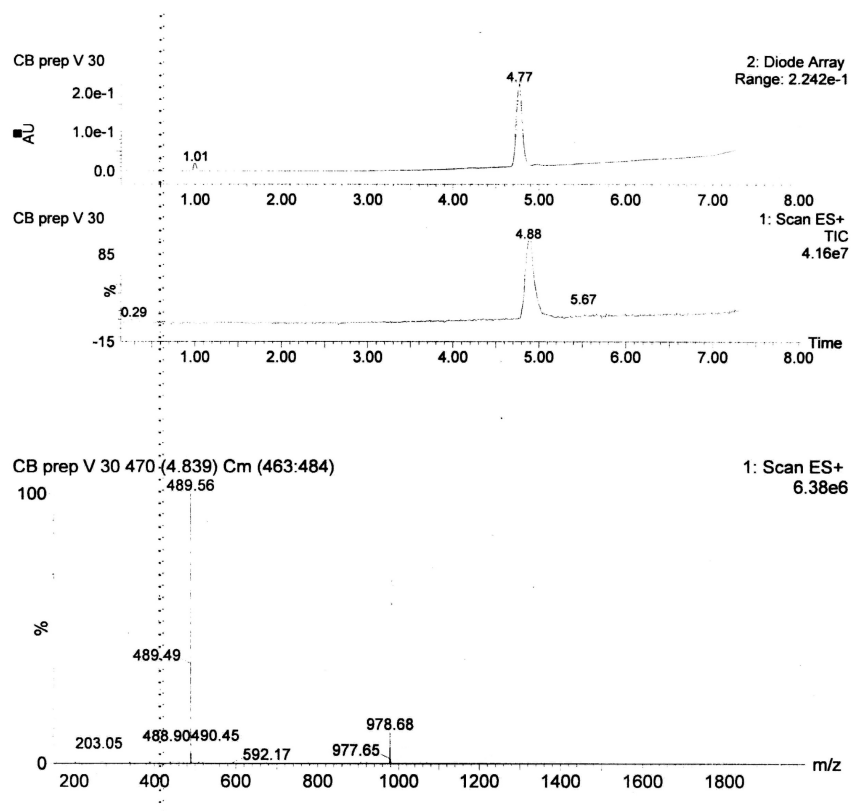


Figure 3.13 HPLC/ESI-MS of DOTA-PEG₃-PBR 127 conjugate; $t_R = 4.77$ min. (selected gradient 40700506, solvent A (H₂O milliQ and 0.1% of TFA), solvent B (CH₃CN 84% and 0.1% of TFA)); m/z 977 M^+ ; 978 $[M + 1]$, 489 $[(M + 2H)/2]^+$.

The same procedure already described was used to synthesize another conjugate, that differs from the previous one only for the length of the spacer. In fact, in this case we used a PEG still functionalized with a free amine end on one side and an hydroxy group on the other, but with a molecular weight of 3000. Because of the weight of this PEG, the work up of several reactions were more difficult as the compound tended to precipitate together with reactions impurities, forming some kind of skeins not easy to purify. The reason why we chose to synthesize this second conjugate was the chance to benefit of the presence of a PEG long enough to confer all the features that usually have the pegylated drugs, as the prolonged permanency in the biological system, the stealth effect and the ability to enhance the action of the radionuclide within the molecule, as for therapeutic purpose.

3.5 To bind or not to bind?

An especially critical point of this project was the prospect that the presence of a spacer and a cage, joint in the conjugate to the chosen TSPO ligand, could too much adversely affect its ability to bind the receptor. In fact this sort of tail, whatever its length, adds weight to the molecule, necessarily varying its tridimensional arrangement. That could seriously invalidate the ligand affinity towards TSPO, preventing the functional PBR 127 spatial conformation needed for the correct receptor interaction.

In this respect, we chose the PEG₃ conjugate to be tested for its ability to compete against [³H]PK11195 for the affinity toward TSPO. The test was performed in Pisa, as above described for the other compounds, with a range of concentration of the analyzed molecule, on mitochondrial pellet deriving from male rats kidneys.

The results, reported in the image below as [³H]PK11195 displacement curve (Figure 3.14), showed a binding affinity of the compound, expressed with a K_i value of 0.856 μM, still very significant, although to a lesser extent compared to that of the free ligand PBR 127 (K_i value of 6.3 nM).

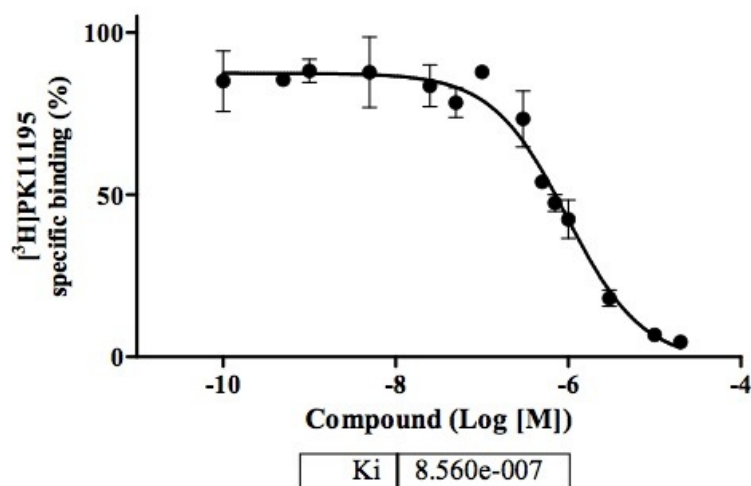


Figure 3.14 [³H]PK11195 displacement curve derived from the TSPO binding of DOTA-PEG₃ - PBR127 conjugate.

3.6 Deep in the labeling matter

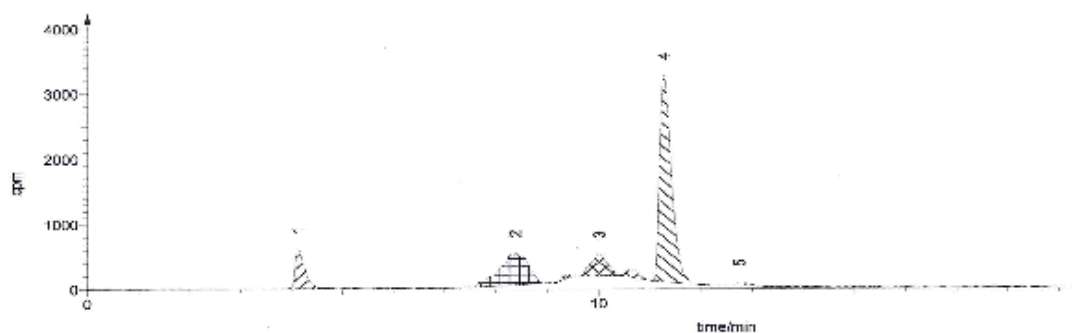
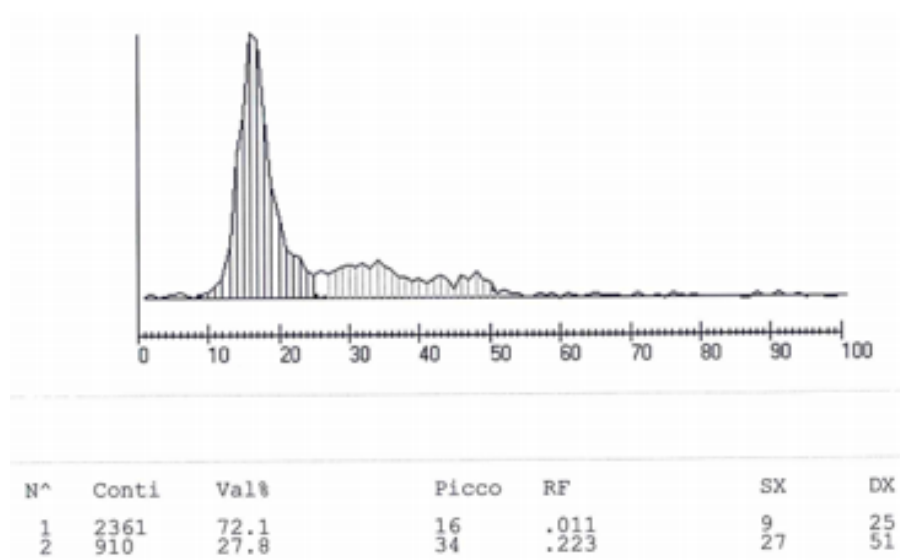
3.6.1 ¹¹¹In

Once assumed the favorable binding profile of the final compound, we chose to examine in depth the same conjugate with the labeling trials; regarding the latter perspective, we started a collaboration with the équipe of Prof. Alberto Pupi, section director of Nuclear Medicine at the AOU of Careggi, Florence. In particular, Doc. A. D'agata and Doc. S. Raspanti offered us the chance to perform together several labeling trials, with the benefit of their deep experience in this subject.

As labeling reagent, we decided to work at a first time with ¹¹¹In chloride, which is one of the key radionuclides in preliminary test, since it is readily available, not too much expensive and safe to handle.

For the first trial, a solution 2mg/ml of compound **f** in CH₃CN/H₂O 10:90, previously aliquoted, was diluted with the ammonium acetate buffer 0.2 M, pH 4-5, to obtain a solution 1mg/ml. Then, 10 µl of this solution were taken and added to 100 µl of the same ammonium acetate buffer 0.2 M, 90 µl of gentisic acid (10 mg/900 µl), commonly used as scavenger, and 100 µl of ¹¹¹In chloride, to a final volume of the solution of 200 µl. This mixture was incubated at 90 °C for 20 min. At the end of the reaction, the analysis of the quality control assessed the pH value, the TLC-determined radiochemical purity and the HPLC-determined radiochemical purity. Then, the mixture was purified on a C18 Sep-Pak column, to remove impurities such as unbounded ¹¹¹In, and on the eluted fraction (with an activity equal to a yield of labeling of about 21%) containing the ¹¹¹In-**f** was newly performed TLC and HPLC determination of radiochemical purity. The peak of ¹¹¹In-**f** was the most represented, with a total yield of 57.68% (see Figure 3.15).

Results



No	Name	Type	w _r [min]	t _R [min]	Calibrated []	Area [cpm]	Area Base [cpm]	% (Area-Base)
1			0.70	4.18	0.00	8463.05	7785.73	87.8
2			1.28	8.31	0.00	23365.28	18178.41	21.82
3			2.00	10.00	0.00	30438.74	8851.44	10.92
4			0.08	11.33	0.00	58841.11	51182.12	57.68
5			0.48	12.80	0.00	2608.43	358.54	1.00
-		Sum	0.45	--	0.00	121126.11	68725.73	100.00 *
-		TU	20.93	--	0.00	127183.62	80647.51	100.00

Figure 3.15 Radiochemical purity of the labeled conjugate evaluated by TLC and HPLC (respectively displayed on the upper and lower graph). The predominant peak in both cases is ascribed at the $^{111}\text{In-f}$ complex.

Following the same protocol, several trials were performed (reported in details in the Experimental section), varying the volumes of the reagent and, most of all, time and temperature of reaction. The best results, in term of percentage yield of radiochemical

Results

purity of the final product after purification, were achieved with an incubation at 60 °C for 30 min, in the absence of gentisic acid, that gave back a value of 76% (see TLC and HPLC chromatogram in Figure 3.16). Although most of the literature concerning DOTA radiochemistry relates of higher percentage values of labeling, our best value of 76% has really to be considered promising for performing animal trials, and especially considering that this yield was principally affected by the non extremely high purity of the cold **f** used in the reactions (75-80%).

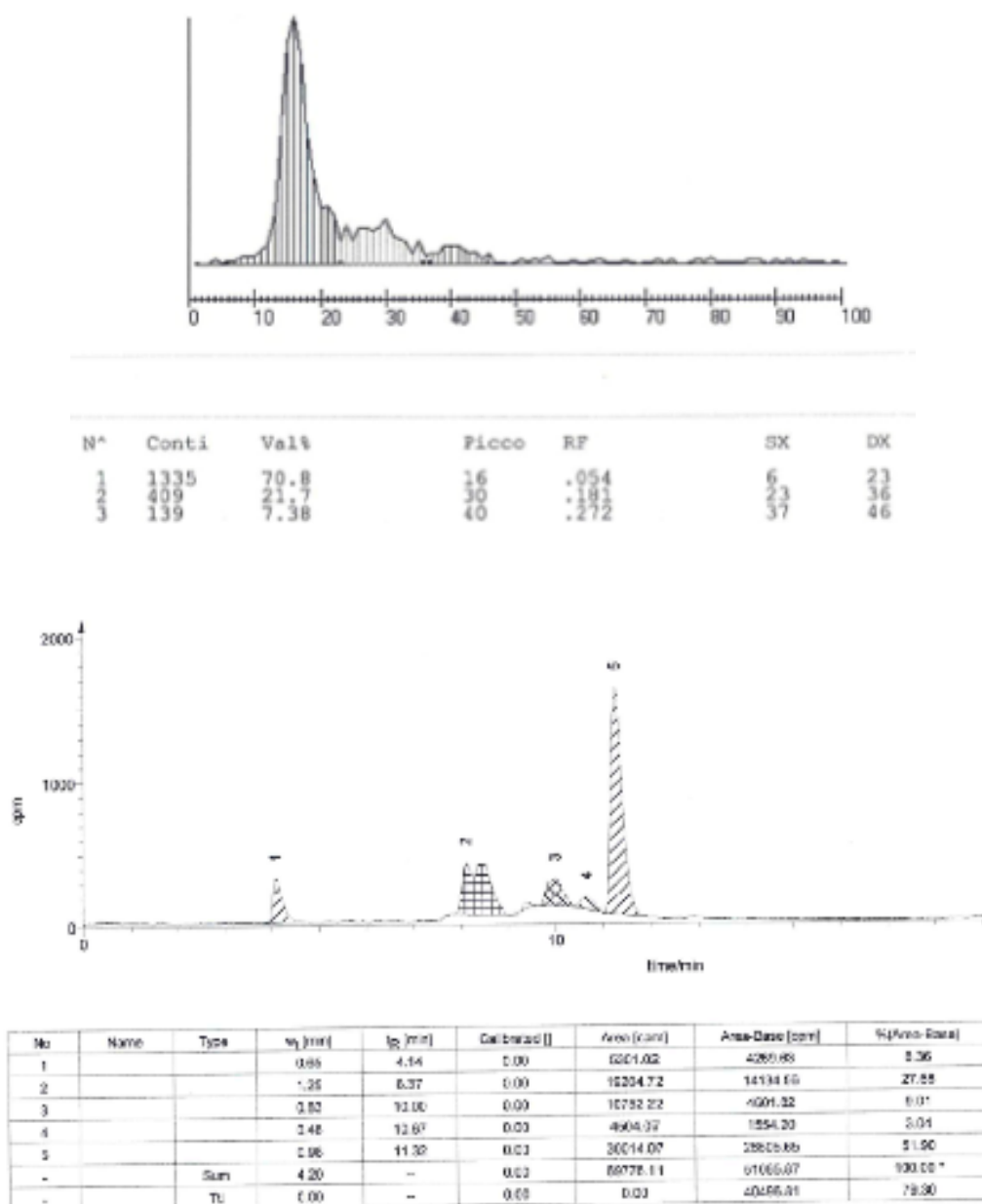


Figure 3.16 Radiochemical purity of the labeled conjugate after reaction carried out at 60 °C for 30 min, evaluated by TLC and HPLC.

3.6.2 ⁶⁸Ga

After the significant labeling results obtained with ¹¹¹In, we thought about the possibility to try other radionuclides, such as ⁶⁸Ga and ¹⁷⁷Lu, that display a similar reactivity and radiochemistry. ⁶⁸Ga and ¹⁷⁷Lu are, with ¹¹¹In, two of the most used metals routinely used as ⁹⁰Y surrogates in the labeling of diagnostic and therapeutic agents¹¹⁷. As a plus, ⁶⁸Ga has the advantage of being available in cyclotron independent way, via the ⁶⁸Ge/⁶⁸Ga generator system.

With respect to ⁶⁸Ga, a variety of radiopharmaceuticals were developed for the imaging of different organ functions, even if only few of them had successfully reached the clinical use. Though the imaging in clinical practice relies particularly on compounds labeled with cyclotron produced ¹⁸F and ¹¹C, ⁶⁸Ga has gained more importance, especially for peptide and non peptide probes developed with high tumor affinity (for instance, ⁶⁸Ga-DOTA-TOC¹¹⁸ and ⁶⁸Ga-DOTA-hEGF¹¹⁹, tracers for the visualization of neuroendocrine tumors and the EGFR over expression in tumors, respectively).

Considered this, we went to IEO (European Institute of Oncology, Milan), thanks to the helpfulness of Doc. Stefano Papi, to perform one preliminary ⁶⁸Ga labeling test in the Radiopharmacy laboratories.

As a first attempt, we decided to use the same protocol of the ⁶⁸GA-DOTA-TOC, as it represents one of the most well known and characterized labeling procedure, and because the macrocycle of the two molecules was the same.

At the moment of our test, the ⁶⁸Ge/⁶⁸Ga generator system was able to release an activity of 35/37 mCi, which is about 12 pM of pure ⁶⁸Ga, hence we chose to dilute 10 µl of the 2mg/ml solution of compound **f** in 30 µl of H₂O (water for injection) to obtain the best concentration values for the labeling trial. Then, we took 40 µl of this solution, which is 20 µg of cold **f**, and put it together with 200 µl of sodium acetate buffer 1 M and 1 ml of physiological saline in the reaction vessel of the synthesis module CEB 2R HE, Radiopharma. As the synthesis started, the generator was eluted with diluted HCl, to remove the ⁶⁸Ga within, and this flow was directed into the reaction vessel, heated to 95 °C. When all the ⁶⁸Ga was collected, the solution was heated up to 100 °C for 8 min. Then the mixture was pumped through a C18 Sep-Pak column, and physiologic saline was poured to remove the unbounded ⁶⁸Ga (and this flow-through was collected into the waste). After the physiologic saline, 50% EtOH in H₂O was fluxed through the C18

Results

Sep-Pak to elute the $^{68}\text{Ga-f}$ produced, and other side products within, to the final collecting flask. In Figure 3.17 below are shown the report modular-lab synthesis plots with the trends of activity, respectively measured in the reaction vessel and in the C18 Sep-Pak column, during the whole reaction time.

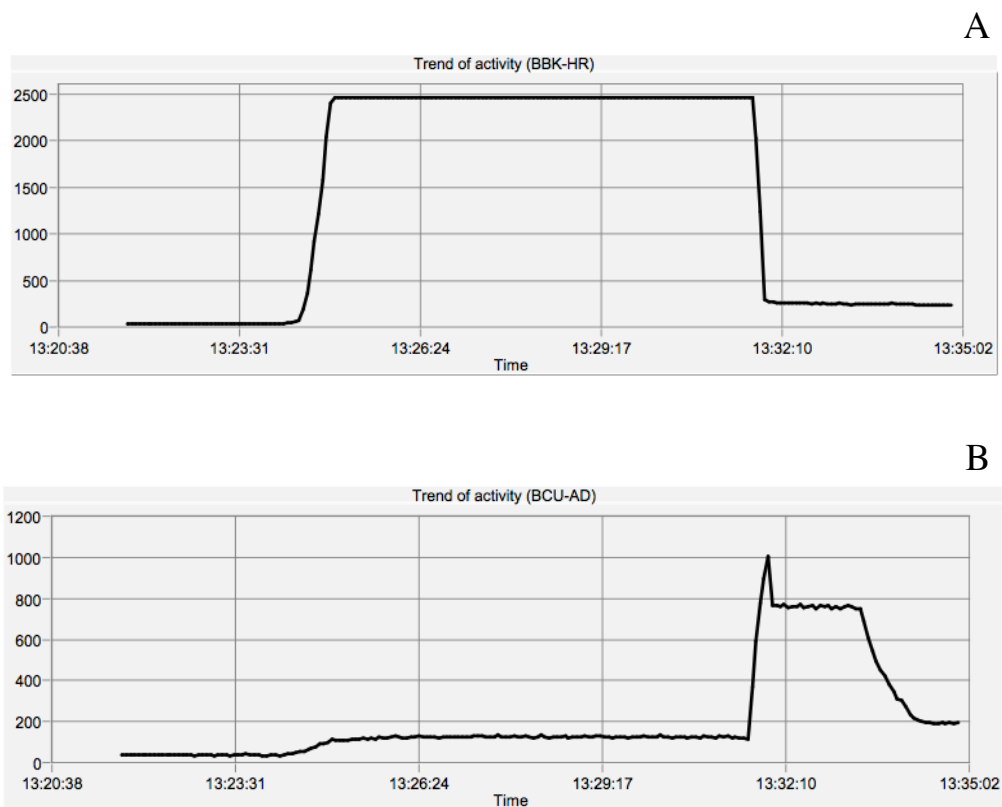
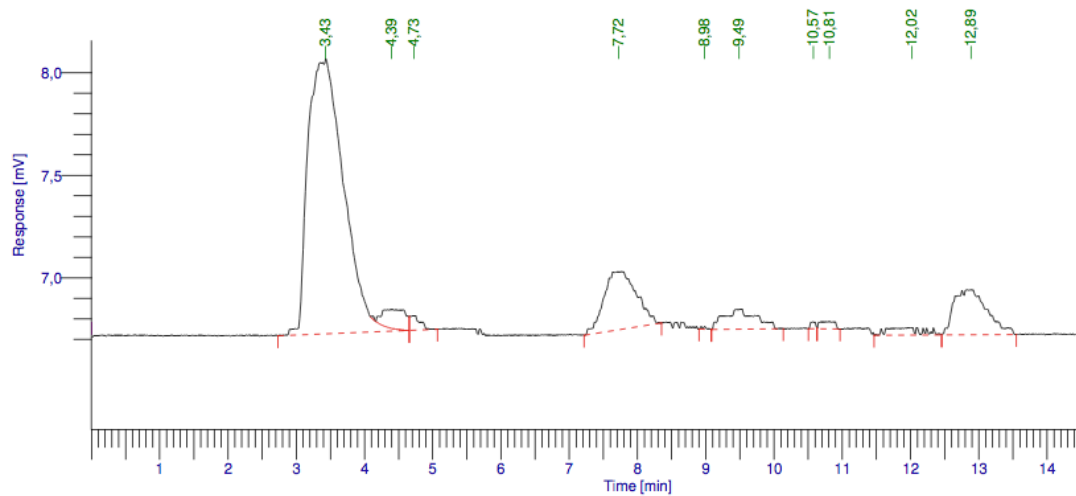


Figure 3.17 Trends of activity measured in the reaction vessel (A) and in the C18 Sep-Pak column (B), to monitor in progress the reaction. The end of activity in the reaction vessel matches the beginning of activity in the column, as these steps are one after another.

During the synthesis, to better estimate the percentage proportion between free and labeled ^{68}Ga , we paused for a moment the instrument before the purification step and collected 0.5 ml of the crude solution that came out from the reaction vessel. The pH measurement on this fraction was near 4.5, which is needed.

The activity measured at the end of the reaction was of about 5 mCi in 1.5 ml of the purified solution, and about 3.4 mCi in 0.5 ml of the crude solution sample. Both the sample were analyzed by means of HPLC-UV coupled to a flow scintillation analyzer, Radiomatic 150RT PerkinElmer (see Figure 3.18).

A



B

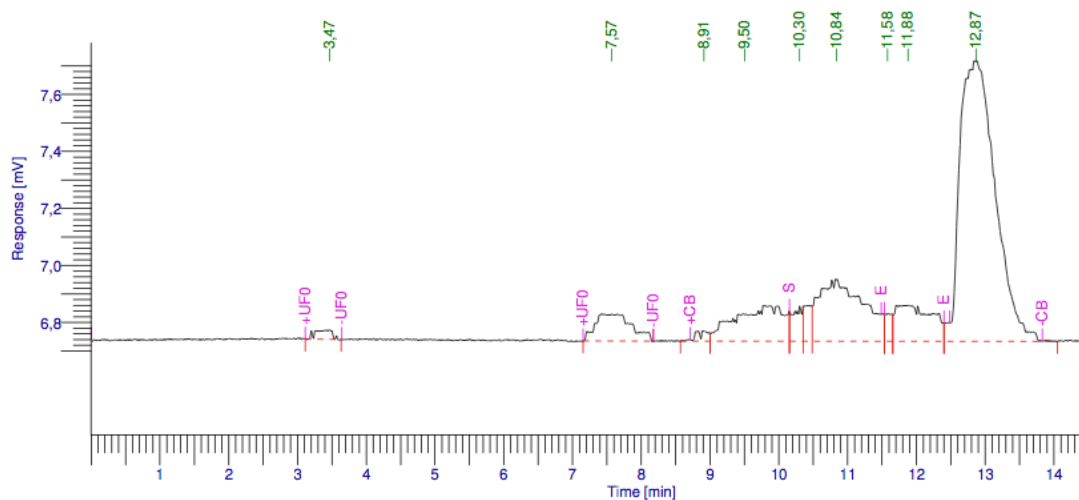


Figure 3.18 Chromatogram deriving from Radiomatic 150RT (radioactivity transformed in mV). In the crude sample (A), the main peak at 3.43 min is ascribable to free ^{68}Ga ; in the purified sample (B), the main peak at 12.87 min is due to $^{68}\text{Ga-f}$.

After this first ^{68}Ga labeling trial, we reached a final yield of $^{68}\text{Ga-f}$ of about 30%, referring to the total activity released by the generator. In the purified sample, the activity due to our labeled compound represented the 56% of the total activity, while the

Results

remaining activity was split between a minimal residue of free ^{68}Ga and at least two non characterized side products.

It's clear that the ^{68}Ga labeling of our compound have to be optimized, evaluating the best conditions to improve the percentage of final yield. Anyway, considering that the labeling of DOTA-TOC, whose purity as cold precursor is near 98%, gives back a yield of about 75%, our 30% of labeling yield obtained with a cold precursor at 75-80% of purity, without the aid of a tailored protocol, has to be considered very promising, and seems a good encouragement to proceed in these studies.

4. DISCUSSION

The stimulation of steroids and neurosteroids biosynthesis as the keystone in the process of axonal and neuronal regeneration has been extensively studied since the past years, in order to derive the causes of the onset and possible treatment of a large number of neurological diseases. It's already clear that the faster way for triggering this process is mediated by TSPO, whereby molecules targeting this receptor are deeply investigated for their possible neuroprotective action. At the same time, the direct association between TSPO concentration levels and the staging of various diseases, as several type of cancers, confirms the convenience of having available new powerful ligands, endowed with high affinity towards this receptor, as diagnostic tracers for modern imaging techniques.

The outcomes of this research project are aligned with these two topics.

On the therapeutic approach side, we have focused our interest on the study of new synthetic ligands, endowed of particular high affinity towards TSPO, and their ability in stimulating the endogenous production of steroid precursor pregnenolone (as proved in C6 rat glioma cells). We directly synthesized a small series of compounds, belonging to the class of *N,N*-diethyl-(2-aryl)pyrazolo[1,5-*a*]pyrimidin-3-ylacetamides, referred to also as P series, and then we evaluated their biological activity, together with that of two more classes of compounds, sb and Raj, respectively related to the chemical family of analogues of DPA-714 and indole-2-carboxamides.

With regard to the synthesis of the precursors of P products, we followed the classic synthetic pathway already reported by our group, while implementing certain critical steps by the use of microwave, most of all to remarkably reduce the reaction time and, in some cases, with a reasonable increase in terms of yield.

The first biological evaluation of series P, sb and Raj was to test their specific binding abilities. Concerning this aspect, we obtained a set of extremely interesting K_i values, many of which in the low micro, low nano and even high pico molar range, some of the lowest values currently available between the synthetic ligands currently studied or in trials.

Although SAR studies are still under development, in addition to the already clarified importance of presence and length of the amide chain at position 3 of the pyrazolopyrimidine scaffold and the key role of the substitutions on the pyrimidine

DISCUSSION

moiety in directing the selectivity towards TSPO (instead of CBR), it seems reasonable to assume that groups providing steric hindrance, bound at *para*- position of the 2-phenyl ring, promote a gain in affinity. As preliminary observation, we had the best affinity results with aromatic and cycloalkyl groups, compared to alkyl chains.

Despite the excellent affinity values found for most of the new synthetic ligands of the three series, only a part of them has shown likewise favorable pharmacological profile as TSPO agonist. Such a result didn't come unexpected, since, as highlighted by several studies, it is still not possible to ascertain a correlation between affinity and intrinsic activity of TSPO ligands (here measured as steroidogenic activity), despite the large number of structures synthesized and investigated to date. In general we can say that several of the tested molecules displayed functional effects which did not correlate to the binding trend observed in competition assay. These evidences further complicate the development of TSPO agonists for therapeutic purposes. In summary, some of the tested molecules showed a significant efficiency in inducing the cellular production of pregnenolone, in some cases with an increase of even more than 80% compared to controls. On the other side, several compounds that showed very promising K_i values, didn't significantly affect the steroids production or revealed pregnenolone percentage values even lower than that shown by controls.

Anyway, the molecules found to be the most efficient in significantly increasing the endogenous pregnenolone percentage in rat cells will be subsequently tested on human astrocytes and SH-SY5Y neuroblastoma cells for their ability in generating protective effects against neuroinflammation and neurodegeneration human models, as a further and more reliable evidence of their potential development for therapeutic use.

Concerning the diagnostic approach, as formerly reported, my research group had investigated (in a previous study of 2008)¹¹¹ the labeling and *in vivo* evaluation in rodents and baboons by micro-PET and PET imaging of TSPO ligands [¹¹C]DPA-713 and [¹⁸F]DPA-714, in collaboration with Prof. M. Kassiou's research group in Sidney. This time we decided to synthesize a new TSPO targeting conjugate, with an articulated structure composed of a TSPO ligand (PBR 127), a spacer and a DOTA cage (explained in details before) to be chosen as imaging tracers, but with the possibility to make it usable even as therapeutic radiopharmaceutical. The project provided for the synthesis of two conjugates, which diversified themselves for the length of the pegylated spacer,

DISCUSSION

so the followed synthetic strategy was the same in both cases, even if we had to adapt the work up of some reactions because the longer PEG gave problems of precipitation of the compound and complicate the purification steps. Given these problems, once attained the final conjugates we decided to use the one with the shorter PEG chain to perform binding test, as an initial evaluation parameter of its possible maintenance of affinity towards TSPO. The results were encouraging, with an obtained K_i value of 0.856 μM which, although less good than that of the free ligand PBR 127 (K_i of 6.3 nM), still remains significant and undoubtedly gives way to the idea of attempting the *in vivo* tests.

After this preliminary biological evaluation, we chose to perform the first labeling of the same conjugate **f** with ^{111}In radionuclide at the AOU of Careggi, Florence. In this respect, we carried out seven labeling tests, at first following the general instructions given by literature and in a second moment varying different parameters of reagents, time and temperature, with the aim to optimize the obtainment of the radiolabeled compound. Although the most common conditions for the charging of DOTA cage report high temperature values (usually near 90 °C) and longer reaction time, we found the best results, in terms of TLC and HPLC measured radiochemical purity of the final compound, in performing the reaction at 60 °C for 30 min, reaching a 75.9% yield. This percentage of radiochemical purity is already quite acceptable for preliminary *in vivo* tests, however can be further improved increasing the purity of the unlabeled conjugate as, for these preliminary tests, we used a 75-80% pure compound.

Concerning the ^{68}Ga labeling, even though we can rely only on one test, the same evaluations made for ^{111}In about the purity of the cold compound can be considered crucial for improving the final labeling yield. As the DOTA macrocycle is the same for the two molecules, we performed the labeling of compound **f** using the ^{68}Ga -DOTA-TOC protocol, which was optimized years ago and is by now well known and commonly applied. Anyway, both with the already mentioned limitations due to the purity of the cold compound, there may be different parameters to be set during the synthesis, more suitable for the best labeling conditions of our conjugate. Still, the final ^{68}Ga -**f** yield of 30% and its 56% radiochemical purity, was a remarkable result, consistent with what expected for the first attempt.

5. CONCLUSIONS

The interest in TSPO ligands as potential therapeutic agents or efficient tracers for imaging techniques stayed strong during these years. In particular, referring to molecules belonging to the pyrazolo[1,5-*a*]pyrimidines class, several studies have investigated DPA-714 and its fluorinated analogue, [¹⁸F]DPA-714; the latter has recently attained the clinical trials. As an instance, it is currently in progress, at the University Hospital of Tours, a pilot study of [¹⁸F]DPA-714 as biomarker of neuroinflammation in cognitive decline on healthy patients and two groups of volunteers affected by mild to moderate Alzheimer's disease and amnesic mild cognitive impairments (see references at clinicaltrials.gov). Such investigations seem even more desirable considering that, at the state of the art, there are no definitive procedures for the determination of the early onset of numerous neurodegenerative diseases such as Alzheimer's and dementia. This aspect goes together with the fact that several of these pathologies, at the beginning, cause cognitive changes, the so called mild cognitive impairments, that are serious enough to be noticed by the individuals experiencing them or to other people but, at the same time, not severe enough to interfere with daily life or independent function, further delaying the possibility of correct diagnosis and therapeutic approach.

This work integrates the studies on TSPO ligands introducing new synthetic compounds of the same family of DPA-714 and their preliminary biological evaluation, together with that of two more classes of molecules, the chemically related sb series, and the Raj series. Some of the compounds showed both high affinity towards the receptor and promising pregnenolone induction in rat cells, with respect to controls and to the reference compound PK11195, leaving the door open for further investigations to be performed on human astrocytes and SH-SY5Y neuroblastoma cells, as already mentioned, to additionally test their potential as anti-inflammatory and neuroprotective agents.

Concerning the second line of this project, namely the design of a conjugate to be studied as a diagnostic/therapeutic agent (in summary, a theranostic tool), we synthesized two compounds, differentiated only by the spacer length. The compound with the shorter PEG chain showed good affinity results, when tested for its binding ability, and even the labeling trials with ¹¹¹In gave back promising results.

The next labeling step with ⁶⁸Ga, that gave back a remarkable preliminary result, was

CONCLUSIONS

performed thinking about the possibility to successively replace this radionuclide with ^{90}Y , as potential therapeutic agent. In fact, the ^{68}Ga and ^{90}Y radiochemical behavior is quite the same, but ^{68}Ga is much more simple and safe to handle during the trials.

Obviously, the possibility to perform *in vivo* tests (analyzed, for instance, by the micro-PET/SPECT/CT instrument in Careggi) will be the further needful stage to evaluate crucial parameters as the biodistribution and bioavailability.

As for the compound with the longer PEG chain, we would have thought very preliminary, depending on the results of binding test, to a possible use as diagnostic/therapeutic agent, to be carried by the lymphatic system for the identification of metastatic cells, directly correlated with cancer staging and malignancy. Another hypothesis could be to exploit the ability, given by the longer PEG, to have an extended permanence in the body, together with the low immunogenicity, and the deriving benefits for therapeutic purposes.

To end, seems really significant to point out how crucial is today the need to have available specific PET tracers especially for the recognition of Alzheimer's disease, whose approved diagnosis is currently entrusted only to a *post mortem* examination. The research, in this topic, has focused particularly on the evaluation of neuritic plaques, but this choice is showing many limitations. As an instance, in 2011 the FDA approved a new PET scanning radiopharmaceutical compound, Amyvid™ (^{18}F -Florbetapir injection), acquired by Eli Lilly and Company. This radiotracer is indicated for brain imaging with PET for the assessment of the neuritic plaque beta amyloid density in patients with cognitive dysfunction, under evaluation for Alzheimer's disease. In particular, a negative Amyvid™ scan indicates sparse or absence of neuritic plaques and is inconsistent with a neuropathological diagnosis of Alzheimer's disease when performing the analysis. Anyway, even if a positive scan indicates the presence of moderate to frequent amyloid beta plaques, it is not credited for the Alzheimer's disease diagnosis and cannot discriminate between this disease and others cognitive disorders. In addition, the safety and efficacy of Amyvid™ have not been tested neither for the prediction of development of other neurological diseases, such as dementias, nor for the monitoring of the responses to therapies. In this context, the choice to target the TSPO receptor, which is known to be a highly sensitive biomarker of even slight alterations of neuronal physiological state, seems the most promising for a future perspective of early and safe diagnosis of several widespread neurological diseases.

6. EXPERIMENTAL

6.1 Data analysis

6.1.1 Chemical data

¹H-NMR spectra for characterization of synthesized products have been recorded on a Bruker Avance (400 MHz) apparatus or on a Varian Gemini (200 MHz) apparatus using the hydrogenated residue of the deuterated solvents CDCl₃ (d = 7.26 ppm) or CD₃COCD₃ (d=3.31 ppm) for ¹H-NMR. Chemical shifts are reported in ppm (parts per million) downfield from TMS. Multiplicities are reported as s (singlet), d (doublet), t (triplet), q (quadruplet), m (multiplet) and b (broad).

Melting points have been determined with a Gallenkamp apparatus and were uncorrected.

The purity of samples was assessed by means of TLC, performed on Merck silica gel plates F 254. Silica gel (Merck Grade 9385, 230-400 mesh) was used for flash chromatography column.

UPLC/ESI-MS analysis have been performed on a Waters Symmetry 300 Å C18 reverse-phase column (100 mm x 2.1 mm, ID 3.5 μ), 0.60 ml/min flux. MS grade CH₃CN and TFA were purchased from Sigma-Aldrich. The selected gradient was 50700506, with solvent A (H₂O milliQ and 0.1% of TFA) and solvent B (CH₃CN 84% and 0.1% of TFA); injected volume: 10 μl.

Purification was performed by means of HPLC/ESI-MS system, Waters Symmetry 200 Å C18 reverse-phase column (250 mm x 4.6 mm, ID 5 μ), 1 ml/min flux. The selected gradient was 407030, with solvent A (H₂O milliQ and 0.1% of TFA) and solvent B (CH₃CN 84% and 0.1% of TFA).

6.1.2 Biological data

The pregnenolone assay was performed by means of IBL Pregnenolone ELISA 96 Best/determ. kit.

Absorbance values have been recorded at 450 nm on a Perkin Elmer Victor2 Wallac, 1420 Multilabel Counter.

6.1.3 Radiochemical data

- ^{111}In .

^{111}In chloride Mallinckrodt, solution 370 MBq/ml (time of arrival). For compound labeling 100 μl were collected (0.0215 nM), with an activity at the time of calibration of 37 MBq, 1mCi.

Ratio compound: ^{111}In = $10.2/0.0215 = 476:1$.

Ammonium acetate buffer 0.2 M, pH 4-5:

- 3.0833 g of ammonium acetate (Baker cat. 0390, MW 77.0825) were made up to the volume of 200 ml with milli q water;

-1.59 ml of ammonium hydroxide 30-33% (Sigma Aldrich cat. 05002, MA 35.05, d = 0.88) were made up to a volume of 200 ml with milli q water, to a 2 M solution;

- 2.29 ml of glacial acetic acid (Carlo erba cat. 401392, MW 60.05, d = 1.049) were made up to a volume of 200 ml with milli q water to a 0.2 M solution.

Sodium acetate buffer 0.1 M, pH 5.5:

- 820.35 mg of anhydrous sodium acetate (Carlo Erba cat. 478166, MW 82.035) were dissolved in 100 ml milli q water to obtain a solution 0.1 M;

- 0.572 ml of acetic acid (Merck cat. 1.00063) were made up to a volume of 100 ml with milli q water to a 0.1 M solution.

To obtain a pH value of 5.5, 84.5 ml of alkaline solution were mixed with 15.5 ml of acid solution.

Hepes buffer 0.1 M, pH 5.5:

- 2.383 g of Hepes (acid, MW 238.3 pKa 7.55 at 20 °C) were made up to a volume of 100 ml with milli q water;

- 400 mg of sodium hydroxide (Carlo Erba cat. 480507, MW 40) were made up to a volume of 100 ml with milli q water to a solution 0.1 M.

To obtain a pH value of 5.5, 99 ml of acid solution were mixed with 0.8802 ml of alkaline solution.

Quality control were performed on TLC and HPLC.

Whatman CHR chromatography paper (eluent: ammonium acetate 10%/CH₃OH (1:1));

ITLC-SG chromatography paper (eluent: trisodium citrate 0.1 M in HCl 0.2 M).

HPLC reverse-phase analytic column Alltima C18, 5 μ , 4.6 x 250 mm + pre-column Alltima C18, 5 μ , 4.6 x 7.5 mm, Grace Davison Discovery Sciences. Solvent A (H₂O

Experimental

milliQ and 0.1% of TFA) and solvent B (CH₃CN 84% and 0.1% of TFA). The selected gradient was 58020. Injected volume: 20 µl.

- ⁶⁸Ga.

We can not report the whole procedure in details, as we performed this test with protocols developed at the IEO. We briefly indicate below the principal instrumentation and reagents.

The labeling was performed in the synthesis module CEB 2R HE, Radiopharma, which includes a ⁶⁸Ge/⁶⁸Ga generator.

During the synthesis were used sodium acetate buffer 1 M, pH 4.5, physiological saline and EtOH 50%.

Quality control were performed on HPLC-UV and flow scintillation analyzer.

HPLC reverse-phase analytic column Alltima C18, 5 µ, 4.6 x 200 mm, Grace Davison Discovery Sciences. Solvent A (H₂O milliQ and 0.1% of TFA) and solvent B (CH₃CN 84% and 0.1% of TFA). The selected gradient was 58020. Injected volume: 10 µl.

Flow scintillation analyzer, Radiomatic 150RT PerkinElmer.

6.2 Chemistry of PBR 136 analogues

3-(4-methoxyphenyl)-3-oxopropanal (1)

To a solution of NaH (60% dispersion in mineral oil, 83 mM, MW 24.00) in anhydrous toluene (70 mL), stirred at room temperature, was added drop wise a solution of 1-(4-methoxyphenyl)ethanone (83 mM, MW 150.17) and ethyl formate (45 mM, MW 74.08) in anhydrous toluene. From the addition on, the flask is placed in ice bath checking the temperature, that has to remain under 65 °C. The reaction was carried out for 6 h.

At the end, the final product was obtained as a light yellow solid (90% yield) and, after filtration with diisopropyl ether, dried under vacuum. ¹H NMR (CDCl₃, 400 MHz) δ: 3.68 (d, 2H, C=OCH₂C=O), 3.85 (s, 3H, OCH₃), 7.12 (d, 2H, Ph), 7.85 (d, 2H, Ph), 9.74 (t, 1H, O=CH).

5-(4-methoxyphenyl)isoxazole (2)

A solution of NH₂OH hydrochloride (80mM, MW 69.49) in EtOH (40 ml) was stirred at room temperature. To promote the solubility, demineralized water was dribbled in the flask. After the almost complete solubilization, compound 1 (75 mM, MW 178.18) was added and the solution was heated to reflux for 2 h.

Experimental

At the end of the reaction, the suspension obtained was filtered and the liquid phase was collected and evaporated under vacuum, to achieve the final product as a white, pearly solid (85% yield).

^1H NMR (CDCl_3 , 400 MHz) δ : 3.88 (s, 3H, OCH_3), 6.42 (s, 1H, $\text{O}-\text{C}=\text{CH}$), 7.01 (d, 2H, Ph), 7.75 (d, 2H, Ph), 8.27 (s, 1H, $\text{CH}=\text{N}$).

3-(4-methoxyphenyl)-3-oxopropanenitrile (3)

MeOH (30 ml) was stirred in a flask, at room temperature, and Na metal (2 eq., MW 22.99) was added gradually until complete dissolution. Then, 2 (1 eq., MW 175.18) was added to the solution and the whole was heated to reflux for 5 h. The resulting solution was reduced in volume under vacuum, some drops of water were added and a filtration occurred, to separate some solids residues. After, concentrated HCl was dropped in the solution until complete acidification of pH. At this time was clear the formation of a solid bulk of a slightly yellow color. The bulk was dried and crystallized from EtOH.

The final product was achieved as a needle-shaped solid of clear brown color (80%).

^1H NMR (CDCl_3 , 400 MHz) δ : 3.68 (s, 2H, CH_2-CN), 3.89 (s, 3H, OCH_3), 7.06 (d, 2H, Ph), 7.78 (d, 2H, Ph).

3-cyano-N,N-diethyl-4-(4-methoxyphenyl)-4-oxobutanamide (4)

To a solution of 3 (5.71 mM, MW 175.18) and 2-chloro-N,N-diethylacetamide (5.71 mM, MW 149.62, d 1.089 g/ml) in 80% EtOH (40 ml), NaOH (5.71 mM, MW 40.00) and KI (17.1 mM, MW 166.00) were added. The mixture was irradiated in an Explorer 48, CEM microwave system reactor at 80 °C for 40 min. When completed, the mixture was filtered and extracted with CH_2Cl_2 . The residue was concentrated and purified with flash chromatography on silica gel (Hexane/Ethyl acetate = 50/50, V:V) to afford 4 (70% yield) as a brown oil.

^1H -NMR (CDCl_3 , 400 MHz) δ : 1.11 (t, 3H, $\text{N}(\text{CH}_2\text{CH}_3)$), 1.29 (t, 3H, $\text{N}(\text{CH}_2\text{CH}_3)$), 2.97 (dd, 1H, CH_2), 2.73 (dd, 1H, CH_2), 3.40 (q, 2H, $\text{N}(\text{CH}_2\text{CH}_3)$), 3.52 (q, 2H, $\text{N}(\text{CH}_2\text{CH}_3)$), 3.91 (s, 3H, OCH_3), 5.00 (m, 1H, CH), 7.00 (d, 2H, Ph), 8.05 (d, 2H, Ph).

2-(3-amino-5-(4-methoxyphenyl)-1H-pyrazol-4-yl)-N,N-diethylacetamide (5)

To a solution of 4 (3.95 mM, MW 316.35) in EtOH (18 ml) were added to hydrate hydrazine (3.95 mM, MW of the anhydrous basis 32.05) and AcOH (0.13 ml, MW 60.05). The mixture was irradiated at 90 °C for 40 min in the CEM Explorer 48. When

Experimental

completed, the residue was washed with saturated aqueous Na_2CO_3 (50 ml) and extracted with CH_2Cl_2 (x3). The organic layer was then collected and concentrated under vacuum. Purification of the residue by flash chromatography on silica gel ($\text{CH}_2\text{Cl}_2/\text{MeOH} = 100/0 - 90/10, \text{V:V}$) afforded 5 as yellow crystals (42% yield).

$^1\text{H-NMR}$ (CDCl_3 , 400 MHz) δ : 0.86 (t, 3H, $\text{N}(\text{CH}_2\text{CH}_3)$), 1.03 (t, 3H, $\text{N}(\text{CH}_2\text{CH}_3)$), 2.99 (q, 2H, $\text{N}(\text{CH}_2\text{CH}_3)$), 3.26 (q, 2H, $\text{N}(\text{CH}_2\text{CH}_3)$), 3.45 (s, 2H, $\text{CH}_2\text{C}=\text{O}$), 3.77 (s, 3H, OCH_3), 5.71 (s, 2H, NH_2), 6.85 (d, 2H, Ph), 7.27 (d, 2H, Ph).

***N,N*-diethyl-2-(2-(4-methoxyphenyl)-5,7-dimethylpyrazolo[1,5-*a*]pyrimidin-3-yl)acetamide (6)**

To a solution of 5 (1.65 mM, MW 302.37) in EtOH (8.0 ml) was added 2,4-pentanedione (1.65 mM, MW 100.12, d 0.980 g/ml). The mixture was irradiated with Explorer 48 at 160 °C for 30 min. Following the reaction, the residue was purified by flash chromatography ($\text{CH}_2\text{Cl}_2/\text{MeOH} = 100/0 - 90/10, \text{V:V}$) to afford 6 (80% yield) as brown crystals.

$^1\text{H-NMR}$ (CDCl_3 , 400 MHz) δ : 1.13 (t, 3H, $\text{N}(\text{CH}_2\text{CH}_3)$), 1.22 (t, 3H, $\text{N}(\text{CH}_2\text{CH}_3)$), 2.57 (s, 3H, CH_3), 2.76 (s, 3H, CH_3), 3.42 (q, 2H, $\text{N}(\text{CH}_2\text{CH}_3)$), 3.52 (q, 2H, $\text{N}(\text{CH}_2\text{CH}_3)$), 3.85 (s, 3H, OCH_3), 3.96 (s, 2H, $\text{CH}_2\text{C}=\text{O}$), 6.53 (s, 1H, CH), 6.99 (d, 2H, Ph), 7.78 (d, 2H, Ph).

***N,N*-diethyl-2-(2-(4-methoxyphenyl)-5,7-bis(trifluoromethyl)pyrazolo[1,5-*a*]pyrimidin-3-yl)acetamide (6F)**

Same procedure as above, using DMF (2.5 ml, instead of EtOH), hexafluoroacetylacetone instead of 2,4-pentanedione (MW 208.06, d 1.47 g/ml) and irradiating at 130 °C and 300 W, for three times in power cycle modality. The solution was reduced in volume under vacuum, added of some demineralized water and extracted with EtOAc (10 ml x 3). The residue was purified by flash chromatography on silica gel ($\text{CH}_2\text{Cl}_2/\text{MeOH} = 100/0 - 90/10, \text{V:V}$) and the final product afforded as bright yellow crystals (70% yield).

$^1\text{H-NMR}$ (CDCl_3 , 400 MHz) δ : 1.71 (t, 3H, $\text{N}(\text{CH}_2\text{CH}_3)$), 1.34 (t, 3H, $\text{N}(\text{CH}_2\text{CH}_3)$), 3.46 (q, 2H, $\text{N}(\text{CH}_2\text{CH}_3)$), 3.61 (q, 2H, $\text{N}(\text{CH}_2\text{CH}_3)$), 3.89 (s, 3H, OCH_3), 4.06 (s, 2H, $\text{CH}_2\text{C}=\text{O}$), 7.04 (d, 2H, Ph), 7.39 (s, 1H, CH), 7.89 (d, 2H, Ph).

N,N-diethyl-2-(2-(4-hydroxyphenyl)-5,7-dimethylpyrazolo[1,5-a]pyrimidin-3-yl)acetamide (7)

A solution of 6 (1.5 mM, MW 366.46) in aqueous HBr (48%, MW 80.91, d 1.49 g/ml) was heated to reflux and left overnight. When completed, the mixture was washed with saturated aqueous NaHCO₃ and extracted with EtOAc (10 ml x 3). The final product was purified by flash chromatography on silica gel (CH₂Cl₂/MeOH = 100/0 – 90/10, V:V) to afford 7 (65% yield) as white crystals.

¹H-NMR (CDCl₃, 400 MHz) δ: 1.13 (t, 3H, N(CH₂CH₃)), 1.22 (t, 3H, N(CH₂CH₃)), 2.57 (s, 3H, CH₃), 2.76 (s, 3H, CH₃), 3.42 (q, 2H, N(CH₂CH₃)), 3.52 (q, 2H, N(CH₂CH₃)), 3.85 (s, 3H, OCH₃), 3.96 (s, 2H, CH₂C=O), 6.53 (s, 1H, CH), 7.03 (d, 2H, Ph), 7.82 (d, 2H, Ph).

N,N-diethyl-2-(2-(4-hydroxyphenyl)-5,7-bis(trifluoromethyl)pyrazolo[1,5-a]pyrimidin-3-yl)acetamide (7F)

Same procedure as above, using 6F instead of 6 (MW 474.40). The final product, purified with flash chromatography on silica gel (CH₂Cl₂/MeOH = 100/0 – 90/10, V:V) was afforded as deep yellow crystals.

¹H-NMR (CDCl₃, 400 MHz) δ: 1.71 (t, 3H, N(CH₂CH₃)), 1.34 (t, 3H, N(CH₂CH₃)), 3.46 (q, 2H, N(CH₂CH₃)), 3.61 (q, 2H, N(CH₂CH₃)), 3.89 (s, 3H, OCH₃), 4.06 (s, 2H, CH₂C=O), 6.98 (d, 2H, Ph), 7.27 (s, 1H, CH), 7.78 (d, 2H, Ph).

6.2.1 General procedure for the synthesis of compounds 8-9; 8F-12F

To a solution of TEA (1.5 eq.) in CH₂Cl₂ (10 ml) dried on molecular sieves, under N₂ atmosphere, the suitable 2-substituted-pyrazolo[1,5-a]pyrimidin-3-yl)acetamide (1 eq.) was added with the proper acid chloride (1.5 eq.). Reaction was stirred over night at room temperature. When finished, the suspension was filtered and the filtrate was concentrated and purified by flash chromatography on silica gel (Tol/EtOAc = 100/0-80/20, V:V), to obtain the corresponding ester.

4-(3-(2-(diethylamino)ethyl)-5,7-dimethylpyrazolo[1,5-a]pyrimidin-2-yl)phenyl benzoate (8)

This compound was obtained from 7 (0.1 mM, MW 352.43), benzoyl chloride (0.15 mM, MW 140.57, d 1.21 g/ml) and TEA (0.15 mM, MW 101.19, d 0.728 g/ml) as light brown crystals (50% yield).

Experimental

¹H-NMR (CDCl₃, 400 MHz) δ: 1.13 (t, 3H, N(CH₂CH₃)), 1.24 (t, 3H, N(CH₂CH₃)), 2.50 (s, 3H, CH₃), 2.73 (s, 3H, CH₃), 3.46 (q, 2H, N(CH₂CH₃)), 3.61 (q, 2H, N(CH₂CH₃)), 3.85 (s, 3H, OCH₃), 7.10 (s, 1H, CH), 7.30 (d, 2H, Ph), 7.52 (t, 2H, Bz), 7.65 (t, 1H, Bz), 7.99 (d, 2H, Ph), 8.13 (d, 2H, Bz).

4-(3-(2-(diethylamino)-2-oxoethyl)-5,7-dimethylpyrazolo[1,5-a]pyrimidin-2-yl)phenyl 4-methylbenzenesulfonate (9)

This compound was obtained from 7 (0.2 mM, MW 352.43), 4-methylbenzenesulfonyl chloride (0.25 mM, MW 190.65) and TEA (0.25 mM, MW 101.19, d 0.728 g/ml) as bright yellow crystals (40% yield).

¹H-NMR (CDCl₃, 400 MHz) δ: 1.12 (t, 3H, N(CH₂CH₃)), 1.22 (t, 3H, N(CH₂CH₃)), 2.36 (s, 3H, CH₃), 2.48 (s, 3H, CH₃), 2.70 (s, 3H, CH₃), 3.44 (q, 2H, N(CH₂CH₃)), 3.60 (q, 2H, N(CH₂CH₃)), 4.01 (s, 2H, CH₂C=O), 7.28 (s, 1H, CH), 7.38 (t, 2H, Ph), 7.43 (d, 2H, Tol), 8.03 (d, 2H, Ph), 8.26 (d, 2H, Tol).

4-(3-(2-(diethylamino)ethyl)-5,7-bis(trifluoromethyl)pyrazolo[1,5-a]pyrimidin-2-yl)phenyl benzoate (8F)

This compound was obtained from 7F (0.1 mM, MW 460.37), benzoyl chloride (0.15 mM, MW 140.57, d 1.21 g/ml) and TEA (0.15 mM, MW 101.19, d 0.728 g/ml) as yellow crystals (40% yield).

¹H-NMR (CDCl₃, 400 MHz) δ: 1.18 (t, 3H, N(CH₂CH₃)), 1.37 (t, 3H, N(CH₂CH₃)), 3.46 (q, 2H, N(CH₂CH₃)), 3.60 (q, 2H, N(CH₂CH₃)), 4.08 (s, 2H, CH₂C=O), 7.37 (d, 2H, Ph), 7.44 (s, 1H, CH), 7.56 (t, 2H, Bz), 7.68 (t, 1H, Bz), 8.01 (d, 2H, Ph), 8.27 (d, 2H, Bz).

4-(3-(2-(diethylamino)ethyl)-5,7-bis(trifluoromethyl)pyrazolo[1,5-a]pyrimidin-2-yl)phenyl 4-methylbenzenesulfonate (9F)

This compound was obtained from 7F (0.1 mM, MW 460.37), 4-methylbenzenesulfonyl chloride (0.15 mM, MW 190.65) and TEA (0.15 mM, MW 101.19, d 0.728 g/ml) as deep brown crystals (35% yield).

¹H-NMR (CDCl₃, 200 MHz) δ: 1.09 (t, 3H, N(CH₂CH₃)), 1.29 (t, 3H, N(CH₂CH₃)), 2.46 (s, 3H, CH₃), 3.37 (q, 2H, N(CH₂CH₃)), 3.49 (q, 2H, N(CH₂CH₃)), 3.99 (s, 2H, CH₂C=O), 7.11 (d, 2H, Ph), 7.31 (s, 1H, CH), 7.37 (d, 2H, Tol), 7.73 (d, 2H, Ph), 7.86 (d, 2H, Tol).

4-(3-(2-(diethylamino)ethyl)-5,7-bis(trifluoromethyl)pyrazolo[1,5-*a*]pyrimidin-2-yl)phenyl 4-fluorobenzoate (10F)

This compound was obtained from 7F (0.1 mM, MW 460.37), 4-fluorobenzoyl chloride (0.15 mM, MW 158.56, d 1.342 g/ml) and TEA (0.15 mM, MW 101.19, d 0.728 g/ml) as bright yellow crystals (32% yield).

¹H-NMR (CDCl₃, 400 MHz) δ: 1.16 (t, 3H, N(CH₂CH₃)), 1.47 (t, 3H, N(CH₂CH₃)), 3.46 (q, 2H, N(CH₂CH₃)), 3.60 (q, 2H, N(CH₂CH₃)), 4.07 (s, 2H, CH₂C=O), 7.23 (t, 2H, FBz), 7.38 (d, 2H, Ph), 7.44 (s, 1H, CH), 8.02 (d, 2H, Ph), 8.27 (dd, 2H, FBz).

4-(3-(2-(diethylamino)ethyl)-5,7-bis(trifluoromethyl)pyrazolo[1,5-*a*]pyrimidin-2-yl)phenyl 2-fluorobenzoate (11F)

This compound was obtained from 7F (0.3 mM, MW 460.37), 2-fluorobenzoyl chloride (0.45 mM, MW 158.56, 1.328 g/ml) and TEA (0.45 mM, MW 101.19, d 0.728 g/ml) as bright yellow crystals (30% yield).

¹H-NMR (CDCl₃, 200 MHz) δ: 1.18 (t, 3H, N(CH₂CH₃)), 1.35 (t, 3H, N(CH₂CH₃)), 3.46 (q, 2H, N(CH₂CH₃)), 3.60 (q, 2H, N(CH₂CH₃)), 4.07 (s, 2H, CH₂C=O), 7.28 (s, 1H, CH), 7.39 (d, 2H, Ph), 7.41 (m, 2H, FBz), 7.56 (m, 1H, FBz), 8.01 (d, 2H, Ph), 8.18 (m, 1H, FBz).

4-(3-(2-(diethylamino)ethyl)-5,7-bis(trifluoromethyl)pyrazolo[1,5-*a*]pyrimidin-2-yl)phenyl furan-2-carboxylate (12F)

This compound was obtained from 7F (0.1 mM, MW 460.37), 2-furoyl chloride (0.15 mM, MW 130.53, d 1.324 g/ml) and TEA (0.15 mM, MW 101.19, d 0.728 g/ml) as light brown crystals (32% yield).

¹H-NMR (CDCl₃, 400 MHz) δ: 1.17 (t, 3H, N(CH₂CH₃)), 1.36 (t, 3H, N(CH₂CH₃)), 3.44 (q, 4H, N(CH₂CH₃)), 3.58 (q, 4H, N(CH₂CH₃)), 4.07 (s, 2H, CH₂C=O), 6.64 (m, 1H, Fur), 7.28 (s, 1H, CH), 7.36 (d, 2H, Ph), 7.44 (m, 1H, Fur), 7.27 (m, 1H, Fur), 8.00 (d, 2H, Ph).

6.3 General procedure for DPA ether analogues (Prof. Michael Kassiou, University of Sydney, Australia)

Commercial methyl 4-hydroxybenzoate (I) was quantitatively protected as its isopropyl ether and treated with conjugate base of CH₃CN, to obtain cyanoacetophenone (II). Subsequently, cyanoacetophenone was deprotonated to the corresponding enolate,

Experimental

following with treatment with excess of N,N-diethylbromoacetamide, to give crude (III). The latter product was condensed with hydrate hydrazine, to yield aminopyrazole (IV); a subsequent condensation of IV with 2,4-pentanedione generated the pyrazolopyrimidine core (V). Cleavage of the isopropyl ether with aluminum chloride afforded common phenolic precursor.

Starting from V, with a mild heating in the presence of the appropriate alkyl bromide and K_2CO_3 the alkylation of phenolic OH provide the DPA analogues.

6.4 Membrane preparation and binding assay

For binding studies, mitochondria were prepared from kidneys of male Wistar rats. Kidneys were homogenized in 20 volumes of ice-cold 50 mM Tris/HCl, pH 7.4, 0.32 M sucrose, 1 mM EDTA (buffer A), containing protease inhibitors (160 μ g/ml benzamidine, 200 μ g/ml bacitracine and 20 μ g/ml soybean trypsin inhibitor) and centrifuged for 10 min at 600 g at 4°C. The resulting supernatant was centrifuged for 10 min at 10,000 g at 4°C. The pellet was then suspended, homogenized in 20 volumes of ice-cold 50 mM Tris/HCl, pH 7.4 (buffer B) and centrifuged for 10 min at 10,000 g at 4°C. The crude mitochondrial pellet was frozen at -20°C until the time of assay or incubated with 0.6 nM [3 H]PK11195 in buffer B, with a range of concentrations of the tested compounds (from 0.1 nM to 10 μ M) in a total volume of 0.5 ml for 90 min at 4°C.

The incubation was stopped by dilution to 5 ml with ice-cold buffer B, immediately followed by rapid filtration through glass fiber Whatman GF/C filters. The filters were then washed two times with 5 ml of buffer B and the amount of radioactivity retained on the filters was determined by Packard 1600 TR liquid scintillation counter at 66% efficiency. Non specific binding was estimated in the presence of unlabeled 1 μ M PK11195. All experiments were performed in triplicate.

For the active compounds, the IC_{50} values were determined and K_i values were derived according to the equation of Cheng and Prusoff. Protein concentration was estimated by the method of Lowry *et al.*, with bovine serum as standard.

6.5 Cell culture

Rat glioma C6 cells were cultured in Dulbecco's Modified Eagle Medium, supplemented with 10% FBS, 1% L-glutamine, 1% Penstrep.

Cultures were maintained in a humidified atmosphere of CO₂/air (5% and 95%, respectively) at 37 °C.

6.6 Steroids biosynthesis

C6 cells were seeded in 96 well plates at a density of $\sim 1 \times 10^4$ cells/well in a final volume of 60 μ l.

The cells were washed three times with a simple salts medium consisting of 140 mM NaCl, 5 mM KCl, 1.8 mM CaCl₂, 1 mM MgSO₄, 10 mM glucose, 10 mM HEPES/NaOH, pH 7.4, plus 0.1% BSA. During experiments, cells were incubated with this simple salts medium in CO₂/air (5%/95%) incubator at 37°C. In order to measure pregnenolone secreted into the medium, its further metabolism was blocked by addition of 25 μ M Trilostane (2a, 4a, 5a, 17b-4,5epoxy-17-hydroxy-3-oxoandrostane-2-carbonitrile) and 10 μ M SU10603 (1, 2, 3, 4-tetrahydro-4-oxo-7-chloro-2-naphthylpyridine), inhibitors of 3 β -hydroxysteroid dehydrogenase and 17 α -hydroxylase, respectively, to the simple salts medium. Trilostane and SU10603 were gifts from Dr. D. Zister (University of Dublin, Dublin, Ireland) and Novartis Farma (Varese, Italy), respectively.

The addition of the novel compounds (Raj 210, 211, 292, 297, 299, 300, 301, 304) and of PK11195 to the C6 cells was made by complete change of the simple salts medium to the medium containing 40 μ M concentration of the different compounds above mentioned.

The secreted pregnenolone in cell medium was measured with an enzyme immunoassay (IBL Pregnenolone ELISA kit).

Briefly, cell salt medium was retained and centrifuged at 1500 g for 10 min and used for quantitative determination of pregnenolone. 100 μ l/well of the working solution of pregnenolone-HRP and 300 (x3) μ l/well of wash buffer were prepared. 50 μ l of each calibrator, control and specimen sample were pipetted into the correspondingly labeled wells in duplicate for the first two and in triplicate for the others. 100 μ l of the conjugate working solution were pipetted into each well and the plate was incubated for 1 h on a plate shaker (at approximately 200 rpm) at room temperature. At the end of incubation, the wells were washed 3 times with wash buffer and, after have properly dried the plate, 150 μ l of TMB substrate were pipetted into each well at timed intervals. The plate was once again incubated on the shaker at room temperature for 10-15 min, or until

Experimental

Calibrator A attains dark blue color. At this time, 50 μ l of stopping solution were injected into each well at the same timed intervals registered while pipetting TMB. The plate was read on a micro well plate at 450 nm within 20 min after addition of the stopping solution.

Cross-reactivity with other steroids is typically less than 1% and cross-reactivity with progesterone is 6% (IBL, Hamburg, Germany). The sensitivity of the assay was 0.05 ng/ml.

6.7 Chemistry of PBR 127-DOTA conjugates

***tert*-butyl (2-(2-(2-hydroxyethoxy)ethoxy)ethyl)carbamate (a)**

In a flask containing CH_2Cl_2 (8 mL), 2-(2-(2-aminoethoxy)ethoxy)ethanol (1 mM, MW 149.19) was dissolved, and Boc anhydride (1 mM, MW 218.25) and DIPEA (1 mM, 101.19, d 0.742 g/ml) were added. The reaction was stirred at room temperature over night. Once completed, the solution was evaporated, the residue solubilized with some demineralized water and extract with EtOAc (10 mL x 3). The organic layer was collected and dried under vacuum, to achieve the final product (92% yield) as a transparent gel.

$^1\text{H-NMR}$ (CDCl_3 , 200 MHz) δ : 1.37 (s, 9H, $\text{OC}(\text{CH}_3)_3$), 3.22 (t, 2H, CH_2NH), 3.46 (t, 2H, CH_2OH), 3.53-3.58 (m, 6H, $\text{CH}_2\text{CH}_2\text{O}$), 3.66 (t, 2H, $\text{OCH}_2\text{CH}_2\text{NH}$).

2,2-dimethyl-4-oxo-3,8,11-trioxa-5-azatridecan-13-yl 4-methylbenzenesulfonate (b)

A solution of **a** (0.92 mM, MW 249.30) in CH_2Cl_2 (5 ml) dried on molecular sieves, under N_2 atmosphere, was stirred at room temperature. TEA (1 mM, MW 101.19, d 0.728 g/ml) was added to the solution and then tosyl chloride (0.92 mM, MW 190.65). The reaction was carried out overnight. When finished demineralized water (2 x 5 ml) was poured in the flask, to wash out the unreacted chloride. Then the bulk in the flask was solubilized with the smallest amount of CH_2Cl_2 , transferred in a falcon and precipitated with cold Et_2O (7 ml). After 30 min at -4°C , the flacon was centrifuged (3,000 rpm, 4 min), and the supernatant was collected. After repeating this procedure for two times, the whole volume of Et_2O was evaporated under vacuum, to achieve the final product, **b**, as a transparent gel (83% yield).

$^1\text{H-NMR}$ (CDCl_3 , 200 MHz) δ : 1.37 (s, 9H, $\text{OC}(\text{CH}_3)_3$), 2.37 (CH_3Ph), 3.22 (t, 2H,

Experimental

CH₂NH), 3.53-3.58 (m, 6H, CH₂CH₂O), 3.72 (t, 2H, CH₂OS), 3.79 (t, 2H, OCH₂CH₂NH), 7.48 (d, 2H, Ph), 7.76 (d, 2H, Ph).

tert-butyl (2-(2-(2-(4-(3-(2-(diethylamino)-2-oxoethyl)-5,7-bis(trifluoromethyl)pyrazolo[1,5-a]pyrimidin-2-yl)phenoxy)ethoxy)ethoxy)ethyl)carbamate (c)

To a solution of 7F (0.7 mM, MW 460.37) in DMF (2 mL), were added K₂CO₃ (1.4 mM, MW 138.21) and **b** (0.76 mM, MW 403.49). The reaction was stirred at 85 °C (± 5 °C) overnight. When finished, demineralized water (2 ml) was dropped into the flask and the solution extracted with EtOAc (3 x 2 mL). The organic layers were collected and dried over Na₂SO₄, then filtered and evaporated until complete exsiccation.

The final product, **c**, was achieved as a yellow semi-solid bulk (68% yield).

¹H-NMR (CDCl₃, 400 MHz) δ: 1.17 (t, 3H, N(CH₂CH₃)), 1.34 (t, 3H, N(CH₂CH₃)), 1.47 (s, 9H, OC(CH₃)₃), 3.35 (t, 2H, CH₂NH), 3.49 (dt, 4H, CH₂O), 3.57 (q, 2H, N(CH₂CH₃), 3.67 (q, 2H, N(CH₂CH₃)₂), 3.85 (t, 2H, CH₂OPh), 3.88 (s, 4H, CH₂CH₂O), 4.05 (s, 2H, CH₂C=O), 7.02 (d, 2H, Ph), 7.39 (s, 1H, CH), 7.87 (d, 2H, Ph).

2-(2-(4-(2-(2-(2-aminoethoxy)ethoxy)ethoxy)phenyl)-5,7-bis(trifluoromethyl)pyrazolo[1,5-a]pyrimidin-3-yl)-N,N-diethylacetamide (d)

Compound **c** (0.47 mM, MW 691.66) was dissolved in CH₂Cl₂ (5 ml) and 30% TFA (1.5 ml, MW 114.02, d 1.49 g/ml) was added. The solution was stirred at room temperature for 3 h. The reaction was then evaporated to dryness and the residue was solubilized once again with the same percentage of CH₂Cl₂ and TFA. After 2 more h, the volume was evaporated, and the residue partitioned between a saturated aqueous solution of K₂CO₃ (2 ml) and CH₂Cl₂ (2 ml); the organic phase was collected and evaporated to give the final product **d** (80% yield).

¹H-NMR (CDCl₃, 400 MHz) δ: 1.17 (t, 3H, N(CH₂CH₃)), 1.27 (t, 3H, N(CH₂CH₃)), 3.35 (t, 2H, CH₂NH), 3.46 (dt, 4H, CH₂O), 3.59 (q, 2H, N(CH₂CH₃), 3.61 (q, 2H, N(CH₂CH₃)₂), 3.69 (m, 4H; 2H-N(CH₂CH₃); 2H-CH₂OPh), 3.89 (s, 4H, CH₂CH₂O), 4.08 (s, 2H, CH₂C=O), 7.03 (d, 2H, Ph), 7.04 (s, 1H, CH), 7.81 (d, 2H, Ph).

tri-tert-butyl 2,2',2''-(10-(2-((2-(2-(2-(4-(3-(2-(diethylamino)-2-oxoethyl)-5,7-bis(trifluoromethyl)pyrazolo[1,5-a]pyrimidin-2-yl)phenoxy)ethoxy)ethoxy)ethyl)amino)-2-oxoethyl)-1,4,7,10-

Experimental

tetraazacyclododecane-1,4,7-triyl)triacetate (e)

DOTA (tBu)₃ (0.4 mM, MW 572.73) was dissolved in DMF (4 ml), with HATU (0.4 mM, MW 380.23) and NMM (0.04 ml, MW 101.15, d 0.92 g/ml). Then, compound **d** (0.38 mM, MW 591.55) was added and the solution was stirred at room temperature over night. When finished, demineralized water (2 ml) was poured into the flask, and the solution extract with CH₂Cl₂. The organic phase was collected, dried over Na₂SO₄, filtered and reduced in volume, and cold Et₂O (7 ml) was added drop wise until the formation of a precipitate. After centrifugation (3,000 rpm, 4 min), the supernatant was evaporated to reach the final product **e** (72% yield).

¹H-NMR (CDCl₃, 400 MHz) δ: 1.10 (t, 3H, N(CH₂CH₃)), 1.17 (t, 3H, N(CH₂CH₃)), 1.44 (s, 27H, t(Bu)), 2.79 (s, 16H, CH₂CH₂ DOTA), 3.42-3.69 (m, 14H; 8H-CH₂C=O DOTA; 4H-N(CH₂CH₃)₂; 2H-CH₂NH), 3.78 (t, 4H, CH₂CH₂O), 3.86 (s, 4H, CH₂CH₂O), 4.02 (s, 2H, CH₂C=O), 4.18 (t, 2H, CH₂OPh), 7.01 (d, 2H, Ph), 7.36 (s, 1H, CH), 7.80 (d, 2H, Ph).

2,2',2''-(10-(2-((2-(2-(2-(4-(3-(2-(diethylamino)-2-oxoethyl)-5,7-bis(trifluoromethyl)pyrazolo[1,5-a]pyrimidin-2-yl)phenoxy)ethoxy)ethoxy)ethyl)amino)-2-oxoethyl)-1,4,7,10-tetraazacyclododecane-1,4,7-triyl)triacetic acid (f)

To a solution of **e** (0.015 mM, MW 1,161.30) in CH₂Cl₂ (4 ml), TFA (0.17 ml, MW 114.02, d 1.49 g/ml) was added slowly and the solution was stirred at room temperature for 1 h. After that, the CH₂Cl₂ was evaporated and fresh TFA was added in the flask, stirring overnight. The latter procedure was repeated twice. When completed, the volume of the solution was reduced and cold Et₂O (7 ml) was added slowly, until the formation of a yellow precipitate. After centrifugation (3,000 rpm, 4 min) and removal of the supernatant, the final product **f** was achieved as deep yellow solid, after two washing with Et₂O and exsiccation.

¹H-NMR (CD₃)₂CO, 400 MHz) δ: 1.10 (t, 6H, N(CH₂CH₃)₂), 2.05 (s, 16H, CH₂CH₂ DOTA), 3.41-3.81 (m, 22H; 8H-CH₂C=O DOTA; 4H-N(CH₂CH₃)₂; 4H-CH₂CH₂O; 2H-CH₂NH; 4-CH₂CH₂O), 4.15 (s, 2H, CH₂C=O), 4.26 (t, 2H, CH₂OPh), 7.14 (d, 2H, Ph), 7.85 (s, 1H, CH), 7.92 (d, 2H, Ph).

UPLC/ESI-MS: m/z 977 M⁺; 978 [M + 1], 489 [(M + 2H)/2]⁺.

Experimental

The crude was purified on 200 Å C18 reverse-phase column, gradient 407030 (see indication before).

6.8 Membrane preparation and binding assay

See directions above (par. 6.4).

6.9 Labeling procedure of compound f (Department of Nuclear Medicine, Azienda Ospedaliera di Careggi, Florence).

¹¹¹In.

A solution of **f** (2 mg/ml) in CH₃CN/H₂O (10:90, 50 µl CH₃CN + 450 µl milli q water) was prepared, aliquoted and, a part from the fraction immediately used aliquoted and stored at -20 °C.

HPLC-UV of the compounds was performed, to define the t_R (11.35 min), both on an aliquot of the **f** solution maintained at +4 °C for 24, on an aliquot defrosted after 24 h at -20 °C and on an aliquot defrosted after 24 h at -20 °C and subsequently incubated at 90 °C for 20 min, to validate the temperature-related stability.

A TLC on ¹¹¹InCl was performed too, to determine its t_R (~ 0.9 min).

During the first labeling trial, the solution 2 mg/ml of compound **f** was diluted to a solution of 1 mg/ml, with ammonium acetate buffer 0.2 M, pH 4-5. 10 µl of this solution (1.02 mM) were collected with 100 µl of ammonium acetate buffer 0.2 M, gentisic acid (10 µg/900 µl) 90 µl and ¹¹¹In chloride, and the mixture (final volume of 200 µl) was incubated for 20' at 90°C.

When completed, quality control was performed to asses the radiochemical purity, by means of TLC and HPLC (analytic specs above). Measurement of the pH gave back a value of 5.

The TLC radiochemical purity shown 3 peaks: t_R ~ 0, ascribable to ¹¹¹In labeled compound **f** (32.7%); t_R ~ 0.4, unidentified (21.0%); t_R ~ 0.9, ascribable to unlabeled ¹¹¹In (46.2%).

The HPLC radiochemical purity highlighted the presence of several peaks, the main of which attributable to unlabeled ¹¹¹In (36.92%, t_R 3.19 min) and to ¹¹¹In labeled compound **f** (18.68%, t_R 11.31 min). Five more peaks were displayed, with t_R between 4.24 and 10.2 min, accounting for the 44.39% of the total residual activity.

Experimental

After the quality control tests, the mixture was purified on Sep Pak light C18 column (previously conditioned with EtOH 5 ml and milli q water 15 ml). Once charged the sample, the C18 was dried with pressurized air; after that, the C18 was washed twice with milli q water and dried with pressurized air; finally, 0.5 ml EtOH was flowed through before the last drying with pressurized air.

On the elute phase, with a measured activity of 150 μCi (labeling yield of 21%), new quality control tests were done. The TLC analysis shown the lack of unlabeled ^{111}In peak ($t_{\text{R}} \sim 0.9$) and the presence of the peak with of the ^{111}In labeled compound **f** (72.1%, $t_{\text{R}} \sim 0$) and of a wide band at $t_{\text{R}} \sim 0.2$ (27.8%). The HPLC results confirmed the absence of unlabeled ^{111}In and the presence of a remarkable peak (t_{R} 11.34 min) due to the ^{111}In labeled compound **f**, together with the presence of three more peaks (t_{R} 4.19, 8.33 and 10.07 min, with percentage value, respectively, of 8.87, 21.62, 10.92).

At the end of this procedure, the resulting purified solution was dried for 5 min at 90 °C under a flow of helium, then resuspended in 200 μl of saline solution (NaCl 0.9%) and analyzed one more time for the radiochemical purity, with a final value of about 73.8% of the whole residual activity ascribable to ^{111}In labeled compound **f** deriving from TLC and of 51.56% from HPLC.

The same procedure already described was use for six more labeling trial, varying the temperature and duration of reaction, in one case exchanging the ammonium acetate with a Hepes buffer and, in four cases, not adding gentisic acid to the mixture. Best results were achieved at 60 °C for 30 min, in ammonium acetate buffer and with no gentisic acid added: in this case, the TLC radiochemical purity had a value of about 77.3% and the HPLC radiochemical purity a value of 75.9%.

Reaction mixture labeling trial 1:

- ammonium acetate buffer 0.2 M (100 μl);
- compound **f** 1 mg/ml (10 μl);
- gentisic acid 10 mg/900 μl (90 μl);
- ^{111}In chloride (100 μl).

Stirred at 90 °C for 20 min. Labeling yield: 21%; radiochemical purity by HPLC: 57.7%; radiochemical purity by TLC 72.1%.

Experimental

Reaction mixture labeling trial 2:

- ammonium acetate buffer 0.2 M (200 µl);
- compound **f** 1 mg/ml (20 µl);
- gentisic acid 10 mg/900 µl (180 µl);
- ¹¹¹In chloride (200 µl).

Stirred at 90 °C for 20 min. Labeling yield: 19%; radiochemical purity by HPLC: 31.4%; radiochemical purity by TLC 67.3%.

Reaction mixture labeling trial 3:

- ammonium acetate buffer 0.2 M (100 µl);
- compound **f** 1 mg/ml (10 µl);
- gentisic acid 10 mg/900 µl (90 µl);
- ¹¹¹In chloride (50 µl).

Stirred at 45 °C for 40 min. Labeling yield: 12%; radiochemical purity by HPLC: 27.7%; radiochemical purity by TLC 54.4%.

Reaction mixture labeling trial 4:

- ammonium acetate buffer 0.2 M (200 µl);
- compound **f** 0.1 mg/ml (10 µl);
- ¹¹¹In chloride (50 µl).

Stirred at 60 °C for 30 min. Labeling yield: 22%; radiochemical purity by HPLC: 75.9%; radiochemical purity by TLC 77.3%.

Reaction mixture labeling trial 5:

- Hepes buffer 0.1 M (250 µl);
- compound **f** 0.1 mg/ml (10 µl);
- ¹¹¹In chloride (50 µl).

Stirred at 60 °C for 30 min. Labeling yield: 13%; radiochemical purity by HPLC: 51.9%; radiochemical purity by TLC 70.8%.

Reaction mixture labeling trial 6:

- ammonium acetate buffer 0.2 M (250 µl);
- compound **f** 0.1 mg/ml (10 µl);
- ¹¹¹In chloride (50 µl).

Experimental

Stirred at 65 °C for 60 min. Labeling yield: 1.75%; radiochemical purity by HPLC: 27.0%; radiochemical purity by TLC 52.7%.

Reaction mixture labeling trial 7:

- ammonium acetate buffer 0.2 M (250 µl);
- compound **f** 0.1 mg/ml (10 µl);
- ¹¹¹In chloride (100 µl).

Stirred at 70 °C for 30 min. Labeling yield: 16%; radiochemical purity by HPLC: 54.7%; radiochemical purity by TLC 78.2%.

6.10 General procedure for the labeling of compound **f with ⁶⁸Ga (IEO, European Institute of Oncology, Milan)**

A solution of **f** (2 mg/ml) in CH₃CN/H₂O (10:90, 50 µl CH₃CN + 450 µl milli q water) was aliquoted.

HPLC-UV (220 nm and 280 nm) of the compounds was performed, to define the t_R (12.67 min).

10 µl of the solution were diluted with 30 µl of H₂O, and then 40 µl of this second solution were collected in the reaction vessel of the synthesis module, together with 200 µl of sodium acetate buffer 1 M and 1 ml of physiological saline. The vessel was preheated at 95 °C. When the activity measured in the generator was enough (near 35/37 mCi, that is about 12 pM of ⁶⁸Ga), the ⁶⁸Ga was eluted with diluted HCl, and the flow was poured into the vessel (final volume of about 4 ml). Then, the temperature was increased to 100 °C and the solution was left to react for 8 min. After that, the solution was pumped out of the vessel through a C18 Sep-Pak Cartridge, and washed once with physiological saline, to remove the free ⁶⁸Ga, and then with 1 ml of EtOH 50%, to elute the labeled compound together with the other products originated during the reaction.

The EtOH eluted phase was diluted with 1 ml of physiological saline, for a final volume of 2 ml. The activity measured in 1.5 ml of this solution was 4.3 mCi.

Labeling yield: 30%; radiochemical purity by HPLC: 56%.

7. REFERENCES

1. Baulieu E.E.: "Steroid hormone regulation of the brain". Fuxe K. Gustafsson J.A. editors. Oxford: Pergamon; 1981. pp- 3-14.
2. Corpéchet C. *et al*: "Characterization and measurement of dehydroepiandrosterone sulfate in rat brain". Proc. Natl. Acad. Sci. U.S.A; 1981. 78(8): 4704-4707.
3. Baulieu E.E. and Robel P: "Dehydroepiandrosterone (DHEA) and dehydroepiandrosterone sulfate (DHEAS) as neuroactive neurosteroids". Proc. Natl. Acad. Sci. U.S.A; 1998. Vol. 95: 4089-4091.
4. Zwain I.H. and Yen S.S: "Neurosteroidogenesis in astrocytes, oligodendrocytes, and neurons of cerebral cortex of rat brain". Endocrinol; 1999. 140: 3843-3852.
5. Baulieu E.E. and Robel P: "Neurosteroids: a new brain function?". J. Steroid Biochem. Mol. Biol; 1990. 37(3): 395-403.
6. Koenig H.L. *et al*: "Progesterone synthesis and myelin formation by Schwann cells". Science; 1995. 268: 1500-1503.
7. Corpéchet C. *et al*: "Pregnenolone and its sulfate ester in the rat brain". Brain Res; 1983. 270(81): 119-125.
8. Do Rego J.L. *et al*: "Neurosteroid biosynthesis: enzymatic pathways and neuroendocrine regulation by neurotransmitters and neuropeptides". Front. Neuroendocrinol; 2009. 30(3): 259-301.
9. Mensah-Nyagan A.G. *et al*: "Neurosteroids: expression of steroidogenic enzymes and regulation of steroid biosynthesis in the central nervous system". Pharmacol. Rev; 1999. 51(1): 63-81.
10. Stoffel-Wagner *et al*: "Expression of 5 α -reductase and 3 α -hydroxysteroid oxidoreductase in the hippocampus of patients with chronic temporal lobe epilepsy". Epilepsia; 2000. 41(2): 140-147.
11. Agís-Balboa R.C. *et al*: "Characterization of brain neurons that express enzymes mediating neurosteroids biosynthesis". Proc. Natl. Acad. Sci. U.S.A; 2006. 103(39): 14602-14607.
12. Corpéchet C. *et al*: "Neurosteroids: 3 α -hydroxy-5 α -pregnan-20-one and its precursor in the brain, plasma and steroidogenic glands of male and female rats". Endocrinol; 1993. 133(3): 1003-1009.
13. Reddy D.S: "Pharmacology of endogenous neuroactive steroids". Crit. Rev.

References

- Neurobiol; 2003. 15(3-4): 197-234.
14. Olsen R.W. and Tobin A.J: "Molecular biology of GABA_A receptors". the FASEB J; 1990. 4(5): 1469-1480.
 15. Schofield P.R. *et al*: "Sequence and functional expression of the GABA_A receptor shows a ligand-gated receptor super-family". Nature; 1987. 328(6127): 221-227.
 16. Mamalaki C. *et al*: "The GABA_A/benzodiazepine receptor is a heterotetramer of homologous alpha and beta subunits". The EMBO J; 1987. 6(3): 561-565.
 17. Zhang S.J. and Jackson M.B: "GABA_A receptor activation and the excitability of nerve terminals in the rat posterior pituitary". J Physiol; 1995. 483(3): 583-595.
 18. Majewska M.D: "Neurosteroids: endogenous bimodal modulators of the GABA_A receptors. Mechanism of action and physiological significance". Prog. Neurobiol; 1992. 38(4): 379-395.
 19. Reddy D.S. and Rogawski M.A: "Stress-induced deoxycorticosterone-derived neurosteroids modulate GABA_A receptor function and seizure susceptibility". J. Neurosci; 2002. 22(9): 3795-3805.
 20. Akk G. *et al*: "The influence of the membrane on neurosteroid actions at GABA_A receptors". Psychoneuroendocrinol; 2009. 34(1): S59-66.
 21. Hosie A.M. *et al*: "Conserved site for neurosteroid modulation of GABA_A receptors". Neuropharmacol; 2009. 56(1): 149-154.
 22. Twyman R.E. and MacDonald R.L: "Neurosteroid regulation of GABA_A receptor single-channel kinetic properties of mouse spinal cord neurons in culture". J. Physiol; 1992. 456: 215-245.
 23. Lambert J.J. *et al*: "Neurosteroids and GABA_A receptor function". Trends Pharmacol. Sci; 1995. 16(9): 295-303.
 24. Rupprecht R. *et al*: "Progesterone receptor-mediated effects of neuroactive steroids". Neuron; 1993. 11(3): 523-530.
 25. Joëls M: "Steroid hormones and excitability in the mammalian brain". Front. Neuroendocrinol; 1997. 18(1): 2-48.
 26. Rupprecht R. *et al*: "Steroid receptor-mediated effects of neuroactive steroids: characterization of structure-activity relationship". Eur. J. Pharmacol; 1996. 303(3): 227-234.
 27. Reddy D.S. *et al*: "Anticonvulsant activity of progesterone and neurosteroids in progesterone receptor knockout mice". J. Pharmacol. Exp. Ther; 2004. 310(1): 230-239.

References

28. Herzog A.G: “Progesterone therapy in women with epilepsy: a 3-year follow up”. *Neurology*; 1999. 52(9): 1917-1918.
29. Reddy D.S. and Rogawski: “Neurosteroid replacement therapy for catamenial epilepsy”. *Neurother*; 2009. 6(2): 392-401.
30. Purdy R.H. *et al*: “Stress-induced elevation of gamma-aminobutyric acid type A receptor-active steroids in the rat brain”. *Proc. Natl. Acad. Sci. U.S.A*; 1991. 88(10): 4553-4557.
31. Khisti R.T. *et al*: “Antidepressant-like effect of the neurosteroid 3alpha-hydroxy-5alpha-pregnan-20-one in mice forced swim test”. *Pharmacol. Biochem. Behav*; 2000. 67(1): 137-143.
32. Uzunov D.P. *et al*: “Fluoxetine-elicited changes in brain neurosteroid content measured by negative ion mass fragmentography”. *Proc. Natl. Acad. Sci. U.S.A*; 1996. 93(22): 12599-12604.
33. Velísková J. and Moshé S.L: “Sexual dimorphism and developmental regulation of substantia nigra function”. *Ann. Neurol*; 2001. 50(5): 596-601.
34. Papadopoulos V. *et al*: “Translocator protein (18 kDa): new nomenclature for the peripheral-type benzodiazepine receptor based on its structure and molecular function”. *Trends Pharmacol. Sci*; 2006. 27(8): 402-409.
35. Papadopoulos V. *et al*: “The peripheral-type benzodiazepine receptor is functionally linked to Leydig cell steroidogenesis”. *J. Biol. Chem*; 1990. 265(7): 3772-3779.
36. Yeliseev A.A. and Kaplan S: “TspO of *Rhodobacter sphaeroides*. A structural and functional model of the mammalian peripheral benzodiazepine receptor”. *J. Biol. Chem*; 2000. 275(8): 5657-5667.
37. Fan J. *et al*: “Structural and functional evolution of the translocator protein (18 kDa)”. *Curr. Mol. Med*; 2012. 12(4): 369-386.
38. Papadopoulos V. *et al*: “Peripheral benzodiazepine receptor in cholesterol transport and steroidogenesis”. *Steroids*; 1997. 62: 21-28.
39. Lacapere J.J and Papadopoulos V: “Peripheral-type benzodiazepine receptor: structure and function of a cholesterol-binding protein in steroid and bile acid biosynthesis”. *Steroids*; 2003. 68: 569-585.
40. Veenman L. *et al*: “Channel-like functions of the 18-kDa translocator protein (TSPO): regulation of apoptosis and steroidogenesis as part of the host-defense response”. *Curr. Pharm. Des*; 2007. 13(23): 2385-2405.

References

41. Miller W.L: "Steroidogenic acute regulatory protein (StAR), a novel mitochondrial cholesterol transporter". *Biochim. Biophys. Acta*; 2007. 1771(6): 663-676.
42. Liu J. *et al*: "Protein-protein interactions mediate mitochondrial cholesterol transport and steroid biosynthesis". *J. Biol. Chem*; 2006. 281(50): 38879-38893.
43. Soustiel J.F. *et al*: "The effect of oxygenation level on cerebral post-traumatic apoptosis is modulate by the 18-kDa translocator protein (also known as peripheral-type benzodiazepine receptor) in a rat model of cortical contusion". *Neuropathol. Appl. Neurobiol*; 2008. 34(4): 412-423.
44. Veenman L. and Gavish M: "The role of 18-kDa mitochondrial translocator protein (TSPO) in programmed cell death, and effects of steroids on TSPO expression". *Curr. Mol. Med*; 2012. 12(4): 398-412.
45. Veenman L. *et al*: "Potential involvement of FOF1-ATP(synth)ase and reactive oxygen species in apoptosis induction by the antineoplastic agent erucylphosphohomocholine in glioblastoma cell lines: a mechanism for induction of apoptosis via the 18 kDa mitochondrial translocator protein". *Apoptosis*; 2010. 15(7): 753-768.
46. Zeno S. *et al*: "The 18 kDa mitochondrial translocator protein (TSPO) prevents accumulation of protoporphyrin IX. Involvement of reactive oxygen species (ROS). *Curr. Mol. Med*; 2012. 12(4): 494-501.
47. Delavoie F. *et al*: "*In vivo* and *in vitro* peripheral-type benzodiazepine receptor polymerization: functional significance in drug ligand and cholesterol binding". *Biochem*; 2003. 42: 4506-4519.
48. Yeliseev A.A. and Kaplan S: "A sensory transducer homologous to the mammalian peripheral-type benzodiazepine receptor regulates photosynthetic membrane complex formation in *Rhodobacter sphaeroides*".
49. Korkhov V.M. *et al*: "Three-dimensional structure of TspO by electron cryomicroscopy of helical crystals". *Structure*; 2010. 18(6): 677-687.
50. Marangos P.J. *et al*: "Characterization of peripheral-type benzodiazepine binding sites in brain using [3H]Ro5-4864". *Mol. Pharmacol*; 1982. 22(1): 26-32.
51. File S.E. and Pellow S: "Ro5-4864, a ligand for benzodiazepine micro molar and peripheral binding sites: antagonism and enhancement of behavioral effects". *Psychopharmacol*; 1983. 80(2): 166-170.
52. Le Fur G. *et al*: "Differentiation between two ligands for peripheral benzodiazepine

References

- binding sites, [3H]Ro5-4864 and [3H]PK11195, by thermodynamic studies". *Life Sci*; 1983. 33(5): 449-457.
53. Le Fur G. *et al*: "Peripheral benzodiazepine binding sites: effects of PK11195, 1-(2-chlorophenyl)-N-methyl-(1-methylpropyl)-3 isoquinolinecarboxamide. *In vivo* studies". *Life Sci*; 1983. 32(16): 1849-1856.
54. Casellas P. *et al*: "Peripheral benzodiazepine receptors and mitochondrial function". *Neurochem. Intern*; 2002. 40: 475-486.
55. Sakai M. *et al*: "Translocator protein (18 kDa) mediates the pro-growth effects of diazepam on Ehrlich tumorr cells *in vivo*". *Eur. J. Pharmacol*; 2010. 626: 131-138.
56. Kreisl W.C. *et al*: "Comparison of [¹¹C]-(R)-PK11195 and [¹¹C]PBR28, two radioligands for translocator protein (18 kDa) in human and monkey: implications for positron emission tomographic imaging of this inflammation biomarker". *NeuroImage*; 2010. 49: 2924-2932.
57. Epand R.F. *et al*: "Induction of raft-like domains by a myristoylated NAP-22 peptide and its Tyr mutant". *FEBS J*; 2005. 272(7): 1792-1803.
58. Xie H.Q. *et al*: "Targeting acetylcholinesterase to membrane rafts: a function mediated by the proline-rich membrane anchor (PRiMA) in neurons". *J. Biol. Chem*; 2010. 285(15): 11537-11546.
59. Li H. and Papadopoulos V: "Peripheral-type benzodiazepine receptor function in cholesterol transport. Identification of a putative cholesterol recognition/interaction amino acid sequence and consensus pattern". *Endocrinol*; 1998. 139(12): 4991-4997.
60. Rupprecht R. *et al*: "Translocator protein (18kDa) (TSPO) as a therapeutic target for neurological and psychiatric disorders". *Nat. Rev. Drug Disc*; 2010. 9: 971-988.
61. Bessler H. *et al*: "Immunomodulatory effect of peripheral benzodiazepine receptor ligands on human mononuclear cells". *J. Neuroimmunol*; 1992. 38: 19-25.
62. Sanger N. *et al*: "Cell cycle-related expression and ligand binding of peripheral benzodiazepine receptor in human breast cancer cell lines". *Eur. J. Cancer*; 2000. 36: 2157-2163.
63. Mendonça-Torres M.C. and Roberts S.S: "The translocator protein (TSPO) ligand PK11195 induces apoptosis and cell cycle arrest and sensitizes to chemotherapy treatment in pre- and post-relapse neuroblastoma cell lines". *Canc. Biol. Ther*; 2013. 14(4): 319-326.
64. Veenman L. *et al*: "Channel-like functions of the 18kDa translocator protein

References

- (TSPO): regulation of apoptosis and steroidogenesis as part of the host-defense response". *Curr. Pharm. Des*; 2007. 13: 2385-2405.
65. Scarf A.M. and Kassiou M: "The translocator protein". *J. Nucl. Med*; 2011. 52: 677-680.
66. Batarseh A. and Papadopoulos V: "Regulation of translocator protein 18 kDa (TSPO) expression in health and disease states". *Mol. Cell Endocrinol*; 2010. 327: 1-12.
67. Maaser K. *et al*: "Up-regulation of the peripheral benzodiazepine receptor during human colorectal carcinogenesis and tumor spread". *Clin. Cancer Res*; 2005. 11: 1751-1756.
68. Cagnin A. *et al*: "*In vivo* measurement of activated microglia in dementia". *Lancet*; 2001. 358: 461-467.
69. Gulyás B. *et al*: "A comparative autoradiography study in post mortem whole hemisphere human brain slices taken from Alzheimer patients and age-matched controls using two radiolabelled DAA1106 analogues with high affinity to the peripheral benzodiazepine receptor (PBR) system". *Neurochem. Int*; 2009. 54(1): 28-36.
70. Pavese N. *et al*: "Microglial activation correlates with severity in Huntington disease: a clinical and PET study". *Neurology*; 2006. 66(11): 1638-1643.
71. Gerhard A. *et al*: "In vivo imaging of microglial activation with [¹¹C](R)-PK11195 PET in idiopathic Parkinson's disease". *Neurobiol. Dis*; 2006. 21(2): 404-412.
72. Turner M.R. *et al*: "Evidence of widespread cerebral microglial activation in amyotrophic lateral sclerosis: an [¹¹C](R)-PK11195 positron emission tomography study". *Neurobiol. Dis*; 2004. 15(3): 601-609.
73. Cagnin A. *et al*: "*In vivo* detection of microglial activation in frontotemporal dementia". *Ann. Neurol*; 2004. 56: 894-897.
74. Carmel I. *et al*: "Peripheral-type benzodiazepine receptors in the regulation of proliferation of MCF-7 human breast carcinoma cell line. *Biochem. Pharmacol*; 1999. 58: 273-278.
75. Galiègue S. *et al*: "Immunohistochemical assessment of the peripheral benzodiazepine receptor in breast cancer and its relationship with survival". *Clin. Cancer Res*; 2004. 10: 2058-2064.
76. Katz Y. *et al*: "Increased density of peripheral benzodiazepine-binding sites in ovarian carcinomas as compared with benign ovarian tumors and normal ovaries". *Clin. Sci. (Lond.)*; 1990. 78(2): 155-158.

References

77. Han Z. *et al*: “Expression of peripheral benzodiazepine receptor (PBR) in human tumors: relationship to breast, colorectal, and prostate tumor progression”. *J. Recept. Signal Transduct. Res*; 2003. 23: 225-238.
78. Veenman L. *et al*: “Peripheral-type benzodiazepine receptor density and *in vitro* tumorigenicity of glioma cell lines”. *Biochem. Pharmacol*; 2004. 68: 689-698.
79. Vlodavsky E. *et al*: “Immunohistochemical expression of peripheral benzodiazepine receptors in human astrocytomas and its correlation with grade of malignancy, proliferation, apoptosis and survival”. *J. Neurooncol*; 2007. 81: 1-7.
80. Demierre M.F. *et al*: “Statins and cancer prevention”. *Nat. Rev. Canc*; 2005. 5: 930-942.
81. Chen M.K. *et al*: “Peripheral benzodiazepine receptor imaging in CNS demyelination: functional implications of anatomical and cellular localization”. *Brain*; 2004. 127: 1397-1392.
82. Guilarte T.R. *et al*: “Enhanced expression of peripheral benzodiazepine receptors in trimethyltin-exposed rat brain: a biomarker of neurotoxicity”. *Neurotoxicol*; 1995. 16(3): 441-450.
83. Lacor P. *et al*: “Enhanced expression of the peripheral benzodiazepine receptor (PBR) and its endogenous ligand octadecaneuropeptide (ODN) in the regenerating adult rat sciatic nerve”. *Neurosci. Lett*; 1996. 220(1): 61-65.
84. Mills C.D. *et al*: “Role of the peripheral benzodiazepine receptor in sensory neuron regeneration”. *Mol. Cell Neurosci*; 2005. 30(2): 228-237.
85. Rone M.B. *et al*: “Cholesterol transport in steroid biosynthesis: role of protein-protein interactions and implications in disease states”. *Biochim. Biophys. Acta*; 2009. 1791(7): 646-658.
86. Irwin R.W. *et al*: “Neuroregenerative mechanisms of allopregnanolone in Alzheimer’s disease”. *Front. Endocrinol. (Lausanne)*; 2012. Volume 2, article 117.
87. Mirzaton A. *et al*: “Injury-induced regulation of steroidogenic gene expression in the cerebellum”. *J. Neurotrauma*; 2010. 27(10): 1875-1882.
88. Rampon C. *et al*: “Translocator protein (18kDa) is involved in primitive erythropoiesis in zebrafish”. *The FASEB J*; 2009. 3(12): 4181-4192.
89. Benavides J. *et al*: “Labelling of “peripheral-type” benzodiazepine binding sites in the rat brain by using [3H]PK11195, an isoquinoline carboxamide derivative: kinetic studies and autoradiographic localization”. *J. Neurochem*; 1983. 41(6): 1744-1750.

References

90. Anzini M. *et al*: "Mapping and fitting the peripheral benzodiazepine receptor binding site by carboxamide derivatives. Comparison of different approaches to quantitative ligand-receptor interaction modeling". *J. Med. Chem*; 2001. 44(8): 1134-1150.
91. Okubo T. *et al*: "Design, synthesis and structure-activity relationships of aryloxyanilide derivatives as novel peripheral benzodiazepine receptor ligands". *Bioorg. Med. Chem*; 2004. 12: 423-438.
92. Berson A. *et al*: "Toxicity of alpidem, a peripheral benzodiazepine receptor ligand, but not zolpidem, in rat hepatocytes: role of mitochondrial permeability transition and metabolic activation". *J. Pharmacol. Exp. Ther*; 2001. 299(2): 793-800.
93. Tebib S. *et al*: "The active analogue approach applied to the pharmacophore identification of benzodiazepine receptor ligands". *J. Comput.-Aided Mol. Des*; 1987. 1: 153-170.
94. Trapani G. *et al*: "Novel 2-phenylimidazo[1,2-*a*]pyridine derivatives as potent and selective ligands for peripheral benzodiazepine receptors. Synthesis, binding affinity, and *in vivo* studies". *J. Med. Chem*; 1999. 42: 3934-3941.
95. Cinone N. *et al*: "Development of a unique 3d interaction model of endogenous and synthetic peripheral benzodiazepine receptor ligands". *J. Comput.-Aided Mol. Des*; 2000. 14: 753-768.
96. Selleri S. *et al*: "2-Arylpyrazolo[1,5-*a*]pyrimidin-3-ylacetamides. New potent and selective peripheral benzodiazepine receptor ligands". *Bioorg. Med. Chem*; 2001. 9: 2661-2671.
97. Selleri S. *et al*: "Insight into 2-phenylpyrazolo[1,5-*a*]pyrimidin-3-ylacetamides as peripheral benzodiazepine receptor ligands: synthesis, biological evaluation and 3D-QSAR investigation". *Bioorg. Med. Chem*; 2005. 13: 4821-4834.
98. Batra S. *et al*: "Characterization of peripheral benzodiazepine receptors in rat prostatic adenocarcinoma". *Prostate*; 1994. 24: 269-278.
99. Nagler R. *et al*: "Oral cancer, cigarette smoke and mitochondrial 18 kDa translocator protein (TSPO) - *in vitro*, *in vivo*, salivary analysis". *Biochim. Biophys. Acta*; 2010. 1802(5): 454-461.
100. Venturini I. *et al*: "Up-regulation of peripheral benzodiazepine receptor system in hepatocellular carcinoma". *Life Sci*; 1998. 63(14): 1269-1280.
101. Charbonneau P. *et al*: "Peripheral-type benzodiazepine receptors in the living heart

References

- characterized by positron emission tomography". *Circulation*; 1986. 73(3): 476-483.
102. Junck L. *et al*: "PET imaging of human gliomas with ligands for the peripheral benzodiazepine binding site". *Ann. Neurol*; 1989. 26(6): 752-758.
103. Hashimoto K. *et al*: "Synthesis and evaluation of ^{11}C -PK11195 for *in vivo* study of peripheral-type benzodiazepine receptors using positron emission tomography". *Ann. Nucl. Med*; 1989. 3(2): 63-71.
104. Maeda J. *et al*: "Novel peripheral benzodiazepine receptor ligand [^{11}C]DAA1106 for PET: an imaging tool for glial cells in the brain. *Synapse*; 2004. 52(4): 283-291.
105. Zhang M.R. *et al*: "[^{18}F]FMDAA1106 and [^{18}F]FEDAA1106: two positron-emitter labeled ligands for peripheral benzodiazepine receptor (PBR). *Bioorg. Med. Chem. Lett*; 2003. 13(2): 201-204.
106. Kam L: "N- [^{18}F]Fluoroacetyl-N-(2,5-dimethoxybenzyl)-2-phenoxyaniline". *Mol. Imag. and Cont. Agent Database, NLM, NIH*; 2007.
107. Buck J.R. *et al*: "Quantitative, preclinical PET of translocator protein expression in glioma using ^{18}F -N-fluoroacetyl-N-(2,5-dimethoxybenzyl)-2-phenoxyaniline". *J. Nucl. Med*; 2011. 52(1): 107-114.
108. Imaizumi M. *et al*: "PET imaging with [^{11}C]PBR28 can localize and quantify upregulated peripheral benzodiazepine receptors associated with cerebral ischemia in rat". *Neurosci. Lett*; 2007. 411(3): 200-205.
109. James M.L. *et al*: "Synthesis and *in vivo* evaluation of a novel peripheral benzodiazepine receptor PET radioligand". *Bioorg. Med. Chem*; 2005. 13(22): 6188-6194.
110. Boutin H. *et al*: " ^{11}C -DPA-713: a novel peripheral benzodiazepine receptor PET ligand for *in vivo* imaging of neuroinflammation". *J. Nucl. Med*; 2007. 48(4): 573-581.
111. James M.L. *et al*: "DPA-714, a new translocator protein-specific ligand: synthesis, radiofluorination, and pharmacologic characterization". *J. Nucl. Med*; 2008. 49: 814-822.
112. Chauveau F. *et al*: "Comparative evaluation of the translocator protein radioligands ^{11}C -DPA-713, ^{18}F -DPA-714, and ^{11}C -PK11195 in a rat model of acute neuroinflammation". *J. Nucl. Med*; 2009. 50(3): 468-476.
113. Medran Navarrete V. *et al*: "Synthesis of a new [^{18}F]Fluoropropyl pyrazolo[1,5-*a*]pyrimidine acetamide for tracing the TSPO 18 kDa by positron emission tomography". <http://seco49.wifeo.com/documents/abstractbook3>.

References

114. Cerutti E. *et al*: “Synthesis and characterization of an MRI Gd-based probe designed to target the translocator protein”. *Magn. Reson. Chem*; 2013. 51(2): 116-122.
115. Daugherty D. *et al*: “A TSPO ligand is protective in a mouse model of multiple sclerosis”. *EMBO Mol. Med*; 2013. 5(6): 891-903.
116. Tang D. *et al*: “Microwave-assisted organic synthesis of a high-affinity pyrazolo-pyrimidinyl TSPO ligand”. *Tetrahed. Lett*; 2010. 51(35): 4595-4598.
117. Vallabhajosula S. *et al*: “Pharmacokinetics and biodistribution of ¹¹¹In- and ¹⁷⁷Lu-labeled J591 antibody specific for prostate-specific membrane antigen: prediction of ⁹⁰Y-J591 radiation dosimetry based on ¹¹¹In or ¹⁷⁷Lu?”. *J. Nucl. Med*; 2005. 46(4): 634-641.
118. Heppeler A. *et al*: “Radiometal-labelled macrocyclic chelator-derivatised somatostatin analogue with superb tumor-targeting properties and potential for receptor mediated internal radiotherapy”. *Chem. A Europ. J*; 1999. 5: 1016-1023.
119. Velikyan I. *et al*: “Preparation and evaluation of ⁶⁸Ga-DOTA-hEGF for visualization of EGFR expression in malignant tumors”. *J. Nucl. Med*; 2005. 46(11): 1881-1888.